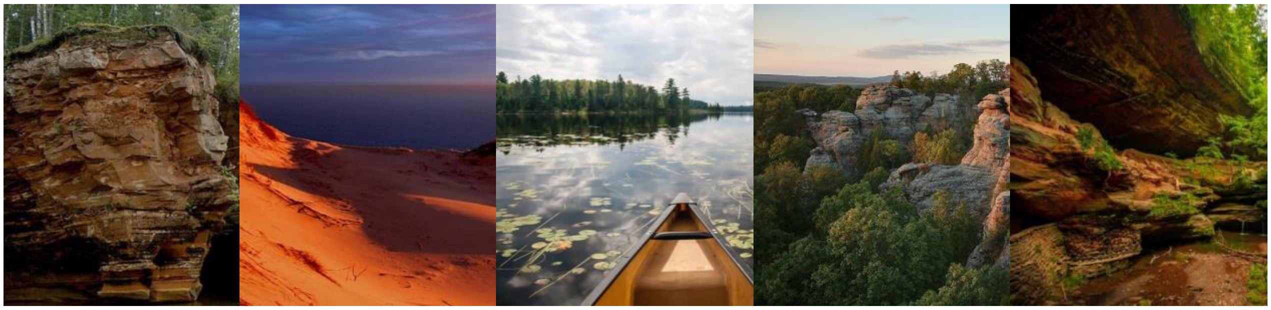

Weather Research Forecast 2016 Meteorological Model Simulation and Evaluation

Technical Support Document

Prepared by:

Tsengel Nergui and **Zac Adelman**

Lake Michigan Air Directors Consortium

Wusheng Ji

Wisconsin Department of Natural Resources

June 22,2022

.

This page is intentionally left blank

.

Contents

FIGURES ... 3

TABLES ... 4

1 EXECUTIVE SUMMARY ... 5

1 INTRODUCTION ... 7

2 WRF MODEL CONFIGURATION ... 8

2.1 WRF MODEL VERSION ... 8
2.2 HORIZONTAL MODELING DOMAIN ... 8
2.3 VERTICAL LAYER STRUCTURE ... 10
2.4 TOPOGRAPHY AND LAND USE DATA ... 11
2.5 ATMOSPHERIC DATA INPUTS ... 11
2.6 DIFFUSION OPTIONS ... 11
2.7 LATERAL BOUNDARY CONDITIONS ... 11
2.8 TOP AND BOTTOM BOUNDARY CONDITIONS ... 12
2.9 SEA SURFACE TEMPERATURE INPUTS ... 12
2.10 FDDA DATA ASSIMILATION ... 12
2.11 SOIL TEMPERATURE AND MOISTURE DATA ... 13
2.12 WRF PHYSICS ... 13
2.13 MODEL SIMULATION DETAILS ... 15

3 WRF MODEL PERFORMANCE EVALUATION ... 16

3.1 MODEL PERFORMANCE EVALUATION APPROACH ... 17
3.2 SYNOPTIC SCALE MODEL PERFORMANCE ... 19
3.3 REGIONAL SCALE MODEL PERFORMANCE ... 24

4 WRF PERFORMANCE EVALUATION FOR LAKE BREEZE EVENTS ... 36

4.1 IDENTIFYING LAKE BREEZE DAYS ... 37
4.2 SATELLITE IMAGERY ANALYSIS ... 40
4.3 OBSERVED AND MODELED WIND FIELDS NEAR LAKE MICHIGAN AND LAKE ERIE ... 42
4.4 CART ANALYSIS FOR LAKE BREEZE EVENTS ... 44
4.5 LAKE BREEZE PERFORMANCE SUMMARY ... 56

5 CONCLUSIONS AND FUTURE WOK ... 58

5.1 CUMULATIVE ASSESSMENT FOR THE 2016 WRF MODEL ESTIMATES ... 58
5.2 LESSON LEARNED AND FUTURE WORK ... 59

REFERENCES ... 61

APPENDIX A: ADDITIONAL MATERIALS ... 64

A.1 CONUS 12 WRF MPE PLOTS ... 65
A.2 LAKE BREEZE ANALYSIS PLOTS ... 81

.

Figures

Figure 1. LADCO WRF 12/4/1.33-km domains 9
Figure 2. Multi-Jurisdictional Organizations in the Continental U.S. 16
Figure 3. Comparison of surface weather maps at 7:00 am EST with modeled outputs at 12:00 pm UTC for May 18, 2016 20
Figure 4. Comparison of surface weather maps at 7:00 am EST with modeled outputs at 12:00 pm UTC for June 13, 2016 20
Figure 5. Comparison of surface weather maps at 7:00 am EST with modeled outputs at 12:00 pm UTC for July 16, 2016 21
Figure 6. Comparison of surface weather maps at 7:00 am EST with modeled outputs at 12:00 pm UTC for August 3, 2016 21
Figure 7. Comparison of model surface fields at 12km and 4km grid resolutions in Midwest for May 18, 2016 22
Figure 8. Comparison of model surface fields at 12km and 4km grid resolutions in Midwest for June 13, 2016 22
Figure 9. Comparison of model surface fields at 12km and 4km grid resolutions in Midwest for July 19, 2016 23
Figure 10. Comparison of model surface fields at 12km and 4km grid resolutions in Midwest for August 3, 2016 23
Figure 11. Mean Absolute Errors and Biases for Temperature in the 4km Domain, Summer 2016 29
Figure 12. Mean absolute errors and biases for specific humidity in the 4km domain, Summer 2016 30
Figure 13. Mean absolute errors and biases for wind speed in the 4km domain, Summer 2016 31
Figure 14. Mean absolute errors and biases for wind direction in the 4km domain, Summer 2016 32
Figure 15. Mean absolute errors and biases for air temperature (a), specific humidity (b), wind speed (c) and wind direction (d) in the 1.33km domains, summer (JJA) 2016 34
Figure 16. METAR stations on shoreline of Lake Michigan (left) and Lake Erie (right). The stations are elevated less than 200 m a.s.l and located south of the 44°N latitude 36
Figure 17. Lake breeze front viewed by VIIRS satellite true color imagery (left), radar reflective imagery (middle), and surface wind field in the Great Lakes simulated by the GFS model are shown for July 16, 2016, 2-4pm 39
Figure 18. May 18, 2016 (1400 CST) satellite imagery and modeled PBL height and wind vectors 40
Figure 19. July 16, 2016 (1400 CST) satellite imagery and modeled PBL height and wind vectors 41
Figure 20. August 3, 2016 (1400 CST) satellite imagery and modeled PBL height and wind vectors 41
Figure 21. VIIRS true color imagery (left), observed (middle) and 1.33 km WRF (right) surface winds at 4:00 pm CDT on June 3, 2016 over Lake Michigan 43
Figure 22. VIIRS true color imagery (left), observed (middle) and 1.33 km WRF (right) surface winds at 4:00 pm CDT on July 31, 2016 over Lake Michigan 44
Figure 23. Meteorological conditions classified during the lake breeze periods at western shoreline (KRAC station on the top) and eastern shoreline (KMKG station on the bottom) of Lake Michigan during 12-16 local standard time. Graduated red and blue colored tree nodes indicate strength of predicted probability of the lake breeze events and offshore flows. 46
Figure 24. MAEs for temperature, specific humidity, wind speed and direction at METAR stations in Lake Michigan shore. 49
Figure 25. MBs for temperature, specific humidity, wind speed and direction at METAR stations in Lake Michigan shore 50
Figure 26. Meteorological conditions classified during the lake breeze periods at KBKL and KERI stations in the south shore of Lake Erie in 2016. Graduated red and blue colored tree nodes indicate strength of predicted probability of the lake breeze events and offshore flow and non-lake breeze days, respectively. 52
Figure 27. Mean absolute errors (top) and mean biases (bottom) for temperature, specific humidity, wind speed and direction at METAR stations in the south shore of Lake Erie 55
Figure 28. Mean Absolute Errors and Biases for Temperature, the 12 km Domain, Winter 2016 65
Figure 29. Mean Absolute Errors and Biases for Temperature, the 12 km Domain, Spring 2016 66
Figure 30. Mean Absolute Errors and Biases for Temperature, the 12 km Domain, Summer 2016 67
Figure 31. Mean Absolute Errors and Biases for Temperature, the 12 km Domain, Fall 2016 68
Figure 32. Mean Absolute Errors and Biases for Specific Humidity, the 12 km Domain, Winter 2016 69

.

Figure 33. Mean Absolute Errors and Biases for Specific Humidity, the 12 km Domain, Spring 2016 70
Figure 34. Mean absolute errors and biases for Specific Humidity, the 12 km Domain, Summer 2016 71
Figure 35. Mean Absolute Errors and Biases for Specific Humidity, the 12 km Domain, Fall 2016 72
Figure 36. Mean Absolute Errors and Biases for Wind Speed, the 12 km Domain, Winter 2016 73
Figure 37. Mean Absolute Errors and Biases for Wind Speed, the 12 km Domain, Spring 2016 74
Figure 38. Mean Absolute Errors and Biases for Wind Speed, the 12 km Domain, Summer 2016 75
Figure 39. Mean Absolute Errors and Biases for Wind Speed, the 12 km Domain, Fall 2016 76
Figure 40. Mean Absolute Errors and Biases for Wind Direction, the 12 km Domain, Winter 2016 77
Figure 41. Mean Absolute Errors and Biases for Wind Direction, the 12 km Domain, Spring 2016 78
Figure 42. Mean Absolute Errors and Biases for Wind Direction, the 12 km Domain, Summer 2016 79
Figure 43. Mean Absolute Errors and Biases for Wind Direction in the 12US2 Domain, Fall 2016 80
Figure 44. Observed (top) and 1.33 km WRF (bottom) surface wind barbs in the western shore of Lake Michigan, 10:00am - 7:00pm CDT on June 3, 2016 81
Figure 45. Observed (top) and 1.33 km WRF (bottom) surface winds in the eastern shore of Lake Michigan, 10:00am - 7:00pm CDT on July 31, 2016 82
Figure 46. Observed (top) and 1.33 km WRF (bottom) surface winds surface winds in Lake Erie, 10:00am and 1:00pm CDT on August 9, 2016 83
Figure 47. Observed (top) and 1.33 km WRF (bottom) surface winds in Lake Erie, 4:00pm and 7:00pm CDT on August 9, 2016 84

Tables

Table 1. Projection and grid parameters for the LADCO 2016 WRF modeling domains 9
Table 2. LADCO WRF vertical layer structure 10
Table 3. LADCO 2016 WRF Physics and Other Options 14
Table 4. Meteorological model performance benchmarks for simple and complex conditions 18
Table 5. 2016 seasonal average 12-km WRF model performance for entire 12US2 domain 26
Table 6. 2016 seasonal average 12-km WRF model performance for the LADCO states 27
Table 7. 2016 seasonal average 4-km WRF model performance for entire LADCO4 domain 28
Table 8. 2016 summer season (JJA) 4-km WRF model performance for the LADCO states 33
Table 9. 2016 seasonal average 1.33-km WRF model performance statistics 35
Table 10. 2016 summer season (JJA) WRF model performance for common locations in the three LADCO WRF modeling domains 35
Table 11. Classified meteorological conditions for lake breeze events in Lake Michigan basin during 12-16 CST, summer of 2016 47
Table 12. Average WRF model performance summary for lake breeze and non-lake breeze days along the shoreline of Lake Michigan 48
Table 13. Average WRF model performance summary by model grid resolution for the lake breeze events in the shoreline of Lake Michigan 49
Table 14. Typical meteorological conditions during lake breeze in the south shore of Lake Erie, summer of 2016 53
Table 15. Model performance summary for lake breeze and non-lake breeze events in the south shore of Lake Erie 54
Table 16. Model performance summary by model grid resolution for the lake breeze events in the south shoreline of Lake Erie 54

1 Executive Summary

The Lake Michigan Air Directors Consortium (LADCO) prepared this technical report on a 2016 Weather Research Forecast (WRF) model simulation to support 2016-based regulatory planning modeling for O_3, $PM_{2.5}$, regional haze and visibility assessments. This report details the WRF modeling inputs and configuration, modeling procedures, model evaluation methodology, and model performance analysis results. LADCO used the WRF version 3.9.1.1 model (Advanced Research WRF dynamic core WRF-ARW) to simulate meteorology on 12-km, 4-km, and 1.33-km domains focused on the Great Lakes Basin for the year 2016. The physics options for the LADCO WRF simulation were based on the best performing configuration identified through a collaboration with University of Wisconsin researchers through a NASA Health and Air Quality (HAQ) program grant-funded project.

LADCO conducted qualitative and quantitative analysis to assess operational performance of the 2016 WRF modeling. Particular focus of this analysis is on the LADCO region. For the 4-km domains, the WRF performance is evaluated by state; and for the 1.33 domains the performance is evaluated for the entire domain. LADCO compared modeled surface pressure, precipitation, and wind vectors against observations by season and for high-concentration ozone episodic events. We also performed a detailed analysis of the model during lake breeze events at the shoreline monitors of Lake Michigan and Lake Erie.

LADCO found that the 12-km and 4-km WRF simulations adequately captured the observed meso- and synoptic-scale processes during high-concentration ozone periods. The LADCO WRF 2016 output fields represent a reasonable approximation of the actual meteorology that occurred in 2016. While the WRF performance statistics for the 12-km grid resolution simulation are within the acceptable performance benchmarks, the simulation has a cold and dry bias in the summer across much of the Eastern U.S. For the 4-km WRF simulation all of the summer season metrics, with the exception of wind direction error, fall within the simple terrain model performance benchmarks; the wind direction error falls within the complex terrain benchmark. The 1.33 km WRF simulations had very good model performance with low errors for all variables and biases near zero. Both errors and biases for temperature and specific humidity at the 12-km grid resolution are reduced by about 20% at the 4-km resolution. Model performance remains about the same for the wind speed and direction when going from 12-km to 4-km resolution. There was not an appreciative improvement in model performance for the analyzed variables between the 4-km and 1.33-km resolution simulations.

Analysis of WRF performance at shoreline monitors during lake breeze events showed that the model successfully reproduced the surface conditions. LADCO developed a CART statistical model using data from selected surface stations on the shorelines of Lake Michigan and Lake Erie for predicting lake-breeze days. The CART lake breeze model prediction accuracies were 92% for Lake Michigan and 82% for Lake Erie, on average. LADCO used the CART model to determine the typical meteorological conditions and indicators for lake-breeze days along the shores of Lake Michigan and Lake Erie. The model identified wind direction and 2-m temperature as the top two variables for explaining lake breeze vs. non-lake breeze events in the Lake Michigan shore, while 2-m temperature, wind speed, and specific humidity were the variables most associated with the lake breeze along the south shore of Lake Erie. WRF performed well predicting temperature, moisture, and winds at the shoreline monitors of both lakes during lake breeze events. The WRF model errors and biases are within the WRF performance benchmarks for temperature, specific humidity and wind speed, and less than 30-degree errors for wind direction. The model performance is slightly degraded on the lake-breeze days compared to the non-lake breeze days on shoreline of Lake Michigan, while opposite is true on the south shore of Lake Erie. The errors and biases for lake breeze days were slightly improved at finer grids in Lake Michigan and Lake Erie shore.

1 Introduction

The Lake Michigan Air Directors Consortium (LADCO) used the Weather Research and Forecasting (WRF) model (Advanced Research WRF dynamic core WRF-ARW; Skamarock et al, 2008) to simulate meteorology in the Great Lakes Basin for the year 2016. WRF is a next-generation mesoscale numerical weather prediction system designed to serve both operational forecasting and atmospheric research needs. WRF contains separate modules to compute different physical processes such as surface energy budgets and soil interactions, turbulence, cloud microphysics, and atmospheric radiation. LADCO used the WRF Preprocessing System (WPS) to generate the initial and boundary conditions used by WRF, based on topographic datasets, land use information, and larger-scale atmospheric and oceanic models.

This report describes an application and performance evaluation of WRF version 4.9.1.1 to simulate 2016 meteorology on 12-km, 4-km, and 1.33-km domains focused on the Great Lakes Basin. This report describes the meteorology model configuration and input data (Section 2) used for the simulation; the model performance evaluation approach and results (Section 3); model performance for simulating lake breeze events (Section 4); and conclusions and future work (Section 5).

2 WRF Model Configuration

This section describes the software configuration for the LADCO 2016 WRF simulation, including the version of the model, horizontal and vertical domain structures, input data sources, physical parameterization options and application methodology. LADCO designed the 2016 WRF simulation to estimate regional to continental scale meteorology to support emissions and air quality modeling applications for the Great Lakes region. The physics options for the LADCO WRF simulation were based on the best performing WRF configuration identified through a collaboration with University of Wisconsin researchers through a NASA Health and Air Quality (HAQ) program grant-funded project (A Satellite Constrained Meteorological Modeling Platform for LADCO States SIP Development).

2.1 WRF Model Version

LADCO used the publicly available version of WRF version 3.9.1.1. The WPS preprocessor programs used to develop model inputs included GEOGRID, UNGRIB, and METGRID.

2.2 Horizontal Modeling Domain

LADCO simulated meteorology with WRF for four one-way nested domains that are based on the standard Lambert Conformal Conic (LCC) projection centered on the continental U.S.:

- USEPA 12US2 (d01): 12-km continental U.S. domain
- LADCO4 (d02): 4-km Great Lakes regional domain that contains all of the LADCO states, and parts of the adjacent states and Canada
- LADCO1.33west (d03): 1.33-km domain that focuses on coastal sites around Lake Michigan
- LADCO1.33east (d04): 1.33-km domain that includes the region from Detroit, Michigan south to the Ohio River Valley

Figure 1 illustrates the WRF modeling domain extents and coverage and Table 1 shows the map projection and parameters for the WRF modeling domains. The LCC projection has a grid center at 40^{o}N, -97^{o}W with true latitudes of 33^o and 45^o. The outer 12-km domain (d01) has 472 columns and 312 rows, selected to be consistent with the existing U.S. EPA 12US2 modeling domain[1]. The 4-km domain (d02) has 445 columns and 421 rows with an offset from the d01 grid origin of 206 columns and 110 rows. The Lake Michigan 1.33-km domain (d03) has 301 columns and 493 rows with an offset from the 4-km grid origin of 186 columns and 144 rows. The Michigan/Ohio 1.33-km domain (d04) has 328 columns and 493 rows with an offsets from the 4-km grid origin of 290 columns and 84 rows.

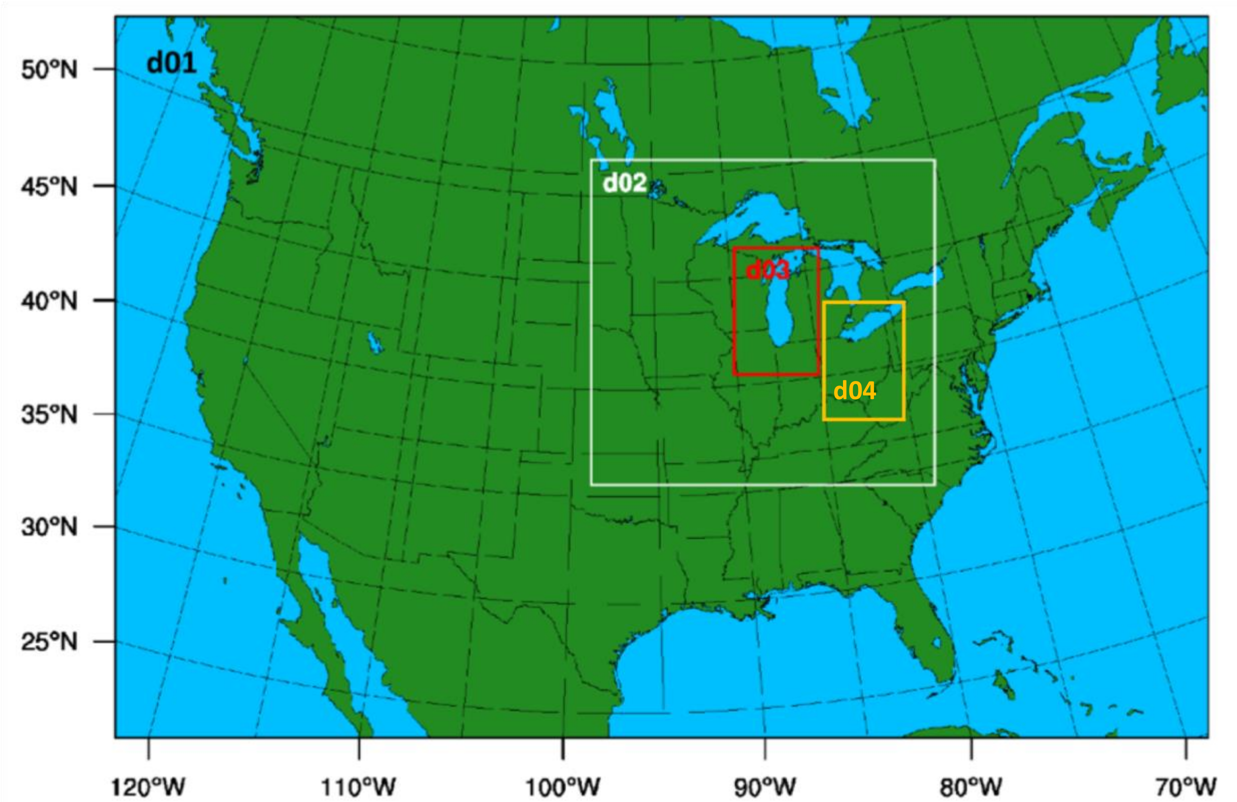

Figure 1. LADCO WRF 12/4/1.33-km domains

Table 1. Projection and grid parameters for the LADCO 2016 WRF modeling domains

Parameter	Value
Projection	Lambert-Conformal
1st True Latitude	33 degrees N
2nd True Latitude	45 degrees N
Central Longitude	-97 degrees W
Central Latitude	40 degrees N
d01 X,Y origin offset	-2412 km, -1620 km
d02 X,Y origin offset	-132 km, -420 km

[1] https://www.epa.gov/sites/default/files/2020-10/documents/met_model_performance-2016_wrf.pdf

d03 km X,Y origin offset	576 km, 84 km
d04 km X,Y origin offset	1008 km, 108 km

2.3 Vertical Layer Structure

LADCO configured the WRF model to use a terrain-following sigma coordinate system defined by pressure levels from the surface up to 50 hPa with a total of 36 vertical layer interfaces. Table 2 tabulates the LADCO WRF vertical model layer structure.

Table 2. LADCO WRF vertical layer structure

WRF Layer	Height (m)	Pressure (Pa)	Sigma	Thickness (m)
36	17,556	5,000	0.000	2,776
35	14,780	9,750	0.050	1,958
34	12,822	14,500	0.100	1,540
33	11,282	19,250	0.150	1,280
32	10,002	24,000	0.200	1,101
31	8,901	28,750	0.250	969
30	7,932	33,500	0.300	868
29	7,064	38,250	0.350	789
28	6,275	43,000	0.400	722
27	5,553	47,750	0.450	668
26	4,885	52,500	0.500	621
25	4,264	57,250	0.550	581
24	3,683	62,000	0.600	547
23	3,136	66,750	0.650	517
22	2,619	71,500	0.700	393
21	2,226	75,300	0.740	285
20	1,941	78,150	0.770	276
19	1,665	81,000	0.800	180
18	1,485	82,900	0.820	177
17	1,308	84,800	0.840	174
16	1,134	86,700	0.860	170
15	964	88,600	0.880	167
14	797	90,500	0.900	83
13	714	91,450	0.910	82
12	632	92,400	0.920	81
11	551	93,350	0.930	81
10	470	94,300	0.940	80
9	390	95,250	0.950	79
8	311	96,200	0.960	79
7	232	97,150	0.970	78
6	154	98,100	0.980	39
5	115	98,575	0.985	38
4	77	99,050	0.990	39
3	38	99,525	0.995	19
2	19	99,763	0.9975	19

1	0	100,000	1.000	0

2.4 Topography and Land Use Data

LADCO developed the topographic information for WRF using standard WRF terrain databases. We based all domain simulations on nine second (~300 m) resolution topography data; the landuse and land cover data were based on the 2011 National Land Cover Database. The NLCD is a 40-category, 30-meter resolution dataset of land-cover for the continental U.S.

2.5 Atmospheric Data Inputs

WRF relies on meteorological fields from other models or reanalysis (blend of model and observations) to provide initial and boundary conditions (IC/BC) and input fields for the four-dimensional data assimilation (FDDA). FDDA refers to the nudging of the WRF simulation toward observed analyses to control model drift so that the WRF meteorological fields better represent actual historical conditions.

The LADCO WRF simulation used 0.25-degree resolution GFS (Grid 4) datasets available from the National Climatic Data Center (NCDC) National Operational Model Archive and Distribution System (NOMADS) server[2] for IC/BC and FDDA.

2.6 Diffusion Options

Horizontal Smagorinsky first-order closure with sixth-order numerical diffusion and suppressed up-gradient diffusion.

2.7 Lateral Boundary Conditions

Lateral boundary conditions were specified from the GFS initialization dataset on the 12 km CONUS domain with continuous updates nested from the 12 km domain to the 4 km domain and continuous updates nested from the 4 km domain to the 1.33 km domains.

[2] https://nomads.ncep.noaa.gov/

2.8 Top and Bottom Boundary Conditions

The top boundary condition was selected as an implicit Rayleigh dampening for the vertical velocity. Consistent with the model application for non-idealized cases, the bottom boundary condition was selected as physical, not free-slip.

2.9 Sea Surface Temperature Inputs

The 1 km sea surface temperature (SST) from the Group for High Resolution Sea Surface Temperatures (GHRSST)[3] used for the 12-km domain simulation. The daily SST fields were ingested from the GHRSST datasets into the WRF model surface boundary files by utilizing the WRF Preprocessing System. Daily Great Lake surface temperatures fields with a horizontal resolution of ~1.3 km, were obtained from the Great Lakes Surface Environmental Analysis (GLSEA4) produced at the NOAA Great Lakes Environmental Research Laboratory (Schwab 1992). We used to constrain SST over the Great Lakes in the 4-km and 1.33-km domain simulations.

2.10 FDDA Data Assimilation

LADCO constrained the WRF model solution using a combination of analysis and surface observation nudging, i.e., FDDA. We ran the WRF model with a combination of GFS analysis and observational data for all domains. For the GFS grid nudging we used analysis nudging coefficients of $0.3x10^{-4}$ s^{-1} for horizontal winds and temperature, and a coefficient of $1.0x10^{-5}$ s^{-1} for water vapor mixing ratio. We only applied the analysis nudging above the planetary boundary layer[5]. We used LDAD Mesonet, METAR, RAOB, and profiler data for observational nudging at the surface in all domains. We applied a nudging coefficient of $0.3x10^{-4}$ s^{-1} for horizontal winds and temperature and a nudging coefficient of $1.0x10^{-5}$ s^{-1} for water vapor mixing ratio for the surface observational nudging.

---

[3] Stammer, D., F.J. Wentz, and C.L. Gentemann (2003). Validation of Microwave Sea Surface Temperature Measurements for Climate Purposes. J. Climate, 16, 73-87. Available at: https://data.nodc.noaa.gov/ghrsst/L4/GLOB/JPL/MUR/

[4] https://coastwatch.glerl.noaa.gov/glsea/

[5] Otte, T.L.(2008). The impact of nudging in the meteorological model for retrospective air quality simulations. Part II: Evaluating collocated meteorological and air quality observations. Journal of Applied Meteorology and Climatology, 47(7): 1868-1887.

2.11 Soil Temperature and Moisture Data

Previous studies (Case et al. 2008; Case et al. 2011) concluded that estimates from the NASA Land Information System (LIS) led to an improvement in the timing and evolution of a sea-breeze circulation due to corrected surface sensible heating from the LIS soil temperature and moisture integration in WRF modeling. In addition, the LIS data integration produced a more accurate diurnal range in 2-m temperatures. The LIS soil information reduced nighttime warm bias and minimized daytime cold bias. A primary conclusion from these studies is that the LIS soil initialization data (particularly the soil moisture fields) modulated surface heating rates and subsequent sensible weather elements such as lake or sea-breeze development and mesoscale convective processes in finer grid WRF modeling.

LADCO incorporated soil temperature and humidity estimates from the NASA Short-term Prediction Research and Transition (SPoRT) Center[6] LIS into the 4km WRF simulation. The value added by the LIS data on the 4-km modeling propagated into the 1.33-km grid solutions through the WRF initialization and boundary fields. The NASA SPoRT team prepared LIS soil information at 0.03-deg resolution (~3 km) over the continental U.S. for use in the LADCO 4-km WRF Midwest domain. To incorporate SpoRT LIS soil temperature and moisture fields into WRF, LADCO followed an established procedure provided by NASA SPoRT involving the WPS tools UNGRIB and METGRID for domains d03 and d04. The WRF model only reads the initial soil information (from wrfinput_d0* files) at the first timestep, and then calculates soil variables internally. Thus, to ensure the LIS soil information was used on a daily basis in WRF simulation, we used two scripts: one to run real.exe to generate daily initial conditions (wrfinput_d0* files) that contains LIS soil information at 00Z as suggested by Case et al. (2011), and one to overwrite the TSLB and SMOIS variables in the WRF daily restart files (wrfrst_d0*) with those from the daily wrfinput files at the first soil layer of the model.

2.12 WRF Physics

The NASA HAQ WRF sensitivity modeling experiments by the University of Wisconsin found that at finer grid resolutions in the LADCO region WRF configured with the YSU PBL (Hong et al. 2006),

[6] https://weather.msfc.nasa.gov/sport/case_studies/lis_CONUS.html

Noah LSM (Chen and Dudhia, 2001; Ek et al. 2003), and Thompson microphysics (Thompson et al. 2008, 2016) schemes outperforms the EPA's latest continental U.S. configuration with the Morrison microphysics (Morrison et al. 2005), ACM2 PBL (Pleim 2007) parameterization schemes, and the Kain-Fritsch cumulus scheme (Kain 2004). The choice of this particular set of schemes is rooted from previous studies showing that they performed well during the warm season across the United States (e.g., Harkey and Holloway 2013; Cintineo et al. 2014; Griffin et al. 2021). The YSU PBL scheme is a first-order, nonlocal closure scheme that allows nonlocal mixing with explicit entrainment processes at the top of the PBL (Hong et al. 2006; Hong 2010). The Noah LSM is a community model that has been widely used within the weather and climate modeling communities (Campbell et al. 2019). It contains four soil layers (0-10, 10-40, 40-100, and 100-200 cm depth) along with vegetation canopy, soil drainage, and runoff estimates, which help improve WRF simulation accuracy through improved land surface processes such as hydrological processes and surface heat fluxes when moving towards higher model resolutions (e.g., Sutton et al. 2006; Case et al. 2008). The optimized WRF model physics options for the Great Lakes and central Midwest U.S. used in the LADCO 2016 WRF simulations are shown in Table 3.

Table 3. LADCO 2016 WRF Physics and Other Options

WRF Treatment	Option Selected	Notes
Microphysics	Thompson Scheme	mp_physics=8
Longwave Radiation	RRTMG	ra_lw_physics=4; Rapid Radiative Transfer Model (RRTM) for GCMs includes random cloud overlap and improved efficiency over RRTM.
Shortwave Radiation	RRTMG	rw_ww_physics=4; Same as above, but for shortwave radiation.
Land Surface Model (LSM)	Unified Noah land-surface model MM5 Monin-Obukhov scheme surface layer	sf_surface_physics=2 sf_sfclay_physics=1
Planetary Boundary Layer (PBL) scheme	YSU	bl_pbl_physics=1
Cumulus parameterization	Kain-Fritsch in the 12-km and 4-km domains with moisture-advection based trigger. None in the 1.33-km domain	cu_physics=1 and trigger_option=2; 1.33-km can explicitly simulate cumulus convection so parameterization not needed.

WRF Treatment	Option Selected	Notes
Analysis Nudging	Aloft nudging applied to winds, temperature and moisture in all domains	Only nudging above the planetary boundary layer
Observational Nudging	Surface nudging applied to winds, temperature and moisture in all domains	
Initialization (initial and boundary conditions)	GFS Grid 4 (0.25 degree)	

2.13 Model Simulation Details

LADCO simulated meteorology with WRFv3.9.1.1 for the four nested domains over the U.S. on the Amazon Web Services (AWS) Elastic Compute Cloud using 96 CPUs (8 nodes and 12 CPUs per node) for 15.5 day periods. Each 15.5 day simulation block was initialized with the 0.25 degree GFS (Grid 4) dataset at 12Z with a 60 second integration time step. We output the WRF model results every 60 minutes and output files were split at 12 hour intervals. LADCO excluded the first twelve hours of spin-up from each 15.5-day block before evaluating the WRF results and using the data for air quality modeling. LADCO simulated WRF from December 15, 2015 through January 1, 2017 for the 12-km CONUS domain (d01), and from March 15, 2016 through October 1, 2016 and for the nested domains (d02 through d04).

3 WRF Model Performance Evaluation

LADCO conducted qualitative and quantitative analysis to assess operational performance of the 2016 WRF modeling. For the 12-km domain modeling, which covers the entire continental U.S. and parts of Canada and Mexico, we used state groups by Multi-Jurisdictional Organization (MJO) to evaluate model performance. MJOs are regional air quality planning organizations that provide a forum for neighboring states to collaborate on regional air pollution mitigation strategies (Figure 2). Particular focus of this analysis is on the LADCO region. For the 4-km domains, the WRF performance is evaluated by state; and for the 1.33 domain the performance is evaluated for the entire domain.

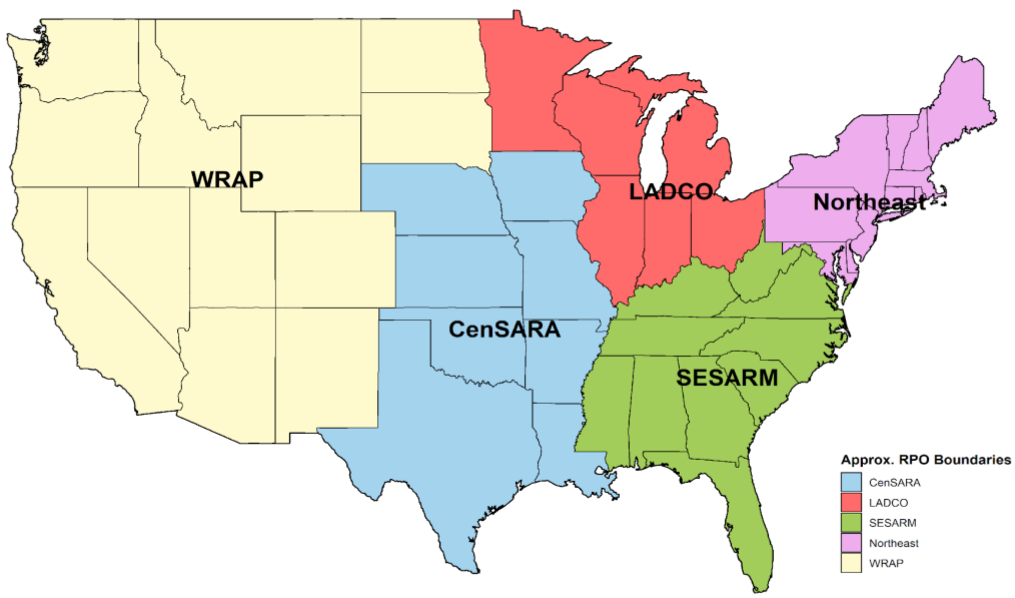

Figure 2. Multi-Jurisdictional Organizations in the Continental U.S.

LADCO compared modeled surface pressure, precipitation, and wind vectors against observation-based weather maps for high ozone episodic events. We also performed a detailed analysis of the lake breeze at the shoreline monitors. The lake breeze is a significant dynamical feature in the region that drives some of the highest observed surface ozone concentrations. Correctly simulating the dynamics, timing, and spatial extent of the lake breeze with WRF is important because an accurate simulation of these events is required to simulate lake breeze-driven ozone in the downstream air quality model. This chapter details the model performance evaluation (MPE) approach used by LADCO to understand the skill of the 2016 WRF simulation.

3.1 Model Performance Evaluation Approach

LADCO conducted qualitative and quantitative analysis to assess operational performance of the 2016 WRF modeling. The quantitative model performance evaluation of WRF using surface meteorological measurements are performed using the Atmospheric Model Evaluation Tool (AMET)[7] version 1.4. AMET calculates statistical performance metrics such as bias, error, and correlation for surface winds, temperature, and mixing ratio and can produce time series of predicted and observed meteorological variables and diurnal performance statistics.

3.1.1 Observational Data for Model Evaluation

The National Oceanic and Atmospheric Administration (NOAA) Earth System Research Laboratory (ESRL) Meteorological Assimilation Data Ingest System (MADIS) data were used to evaluate 2-m temperature, 2-m water vapor mixing ratio, and 10-m wind speed and wind direction estimates for each simulation domain and month. LADCO evaluated the WRF model hourly outputs against observed surface temperature, specific humidity, and wind fields from the METAR network. The quantitative model performance evaluation of WRF using surface meteorological measurements are performed based on collocated hourly observed and model values for grid cells in which monitors are located using the AMET tool, and summary plots and tables were created using the statistical software R version 4.1.3.

3.1.2 Benchmarks for Meteorological Model Performance

LADCO used a number of performance benchmarks to evaluate the performance of the WRF 2016 simulation. Emery et al. (2001) derived and proposed a set of performance “benchmarks” for typical meteorological conditions for good performing meteorological simulations used in contemporary air quality model applications. These performance benchmarks were based upon the evaluation of about 30 MM5 and RAMS meteorological simulations of limited duration (multi-day episodes) in support of air quality modeling study applications performed over several

[7] http://www.cmascenter.org

years. The benchmarks were based on ozone model applications for cities in the eastern and Midwestern U.S. and Texas that were primarily simple (flat) terrain and simple (stationary high-pressure and stagnant) meteorological conditions. More recently these benchmarks have been used in annual meteorological modeling studies that include areas with complex terrain and more complicated meteorological conditions; therefore, they must be viewed as being applied as guidelines and not bright-line numbers. That is, the purpose of these benchmarks is not to give a passing or failing grade to any one particular meteorological model application, but rather to put the modeling results into the proper context of other models and meteorological data sets. Recognizing that these simple conditions benchmarks may not be appropriate for more complex conditions, McNally (2009) analyzed multiple annual runs that included complex terrain conditions and suggested an alternative set of benchmarks for temperature, namely a guideline of within ±1.0 K for bias and 3.0 K for error. As part of the Western Regional Air Partnership (WRAP) meteorological modeling of the western United States, including the Rocky Mountain Region as well as the complex conditions in Alaska, Kemball-Cook et al. (2005) proposed model performance benchmarks for complex conditions. Based on these reviews, we have adopted "simple" and "complex" model performance benchmarks for surface temperature, mixing ratio, and winds (
Table 4).

Table 4. Meteorological model performance benchmarks for simple and complex conditions

Parameter	Simple	Complex
Temperature Bias	≤ ±0.5 K	≤ ±2.0 K
Temperature Error	≤ 2.0 K	≤ 3.5 K
Mixing Ratio Bias	≤ ±1.0 g/kg	NA
Mixing Ratio Error	≤ 2.0 g/kg	NA
Wind Speed Bias	≤ ±0.5 m/s	≤ ±1.5 m/s
Wind Speed RMSE	≤ 2.0 m/s	≤ 2.5 m/s
Wind Direction Bias	≤ ±10 degrees	NA
Wind Direction Error	≤ 30 degrees	≤ 55 degrees

.

The equations for bias, error, and root mean square error (RMSE) are given below.

Mean Bias (Bias) = $\frac{1}{N}\sum_{i=1}^{N}(P_i - O_i)$

Mean Absolute Gross Error (Error) = $\frac{1}{N}\sum_{i=1}^{N}|P_i - O_i|$

Root Mean Square Error (RMSE) = $\left[\frac{1}{N}\sum_{i=1}^{N}(P_i - O_i)^2\right]^{1/2}$

The following sections will present model performance results and discussion for each grid resolution.

3.2 Synoptic Scale Model Performance

LADCO compared modeled surface pressure, precipitation and divergence winds with observation-based weather maps for days in 2016 during which conditions in the Great Lakes region were conducive to high concentrations of ground-level ozone. Figure 3 through Figure 10 show the comparisons of the weather map and the model outputs for May 18, June 13, July 16 and August 3, 2016. The National Centers for Environmental Prediction (NCEP), Hydrometeorological Prediction Center, National Weather Service[8] surface weather maps show the surface pressure isobars as solid lines in 4 mbar intervals and is annotated with centers of high- and low-pressure systems. Surface temperature isotherms are shown as dashed blue lines in 10 ^{o}C intervals. The maps show fronts in blue or red, and precipitation areas in green. LADCO created model-based surface maps using the 12 km and 4km WRF outputs of the surface pressure, precipitation and divergence winds to indicate fronts and pressure system centers.

The comparisons of the NCEP and WRF surface maps show that WRF simulates well the extent and location of the high-pressure and low-pressure systems, cold fronts, trough lines, and precipitation in the contiguous U.S. (Figure 3 through Figure 6). WRF captures the locations of

[8] https://www.wpc.ncep.noaa.gov/dailywxmap/explaination.html

the high-pressure systems in the Midwest reasonably well at both 12 km and 4-km resolution, but the model tends to underestimate surface pressure levels by 10 hPa in the earlier morning (7:00 am EST). This performance deficit is partially explained by the difficulty in simulating the unstable atmospheric conditions around sunrise.

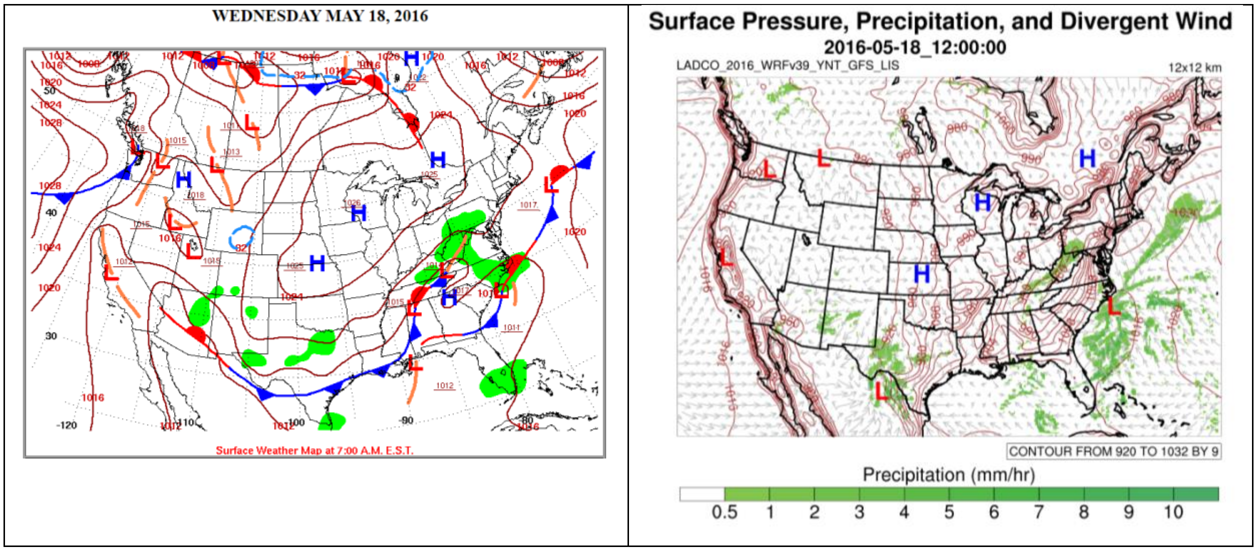

Figure 3. Comparison of surface weather maps at 7:00 am EST with modeled outputs at 12:00 pm UTC for May 18, 2016

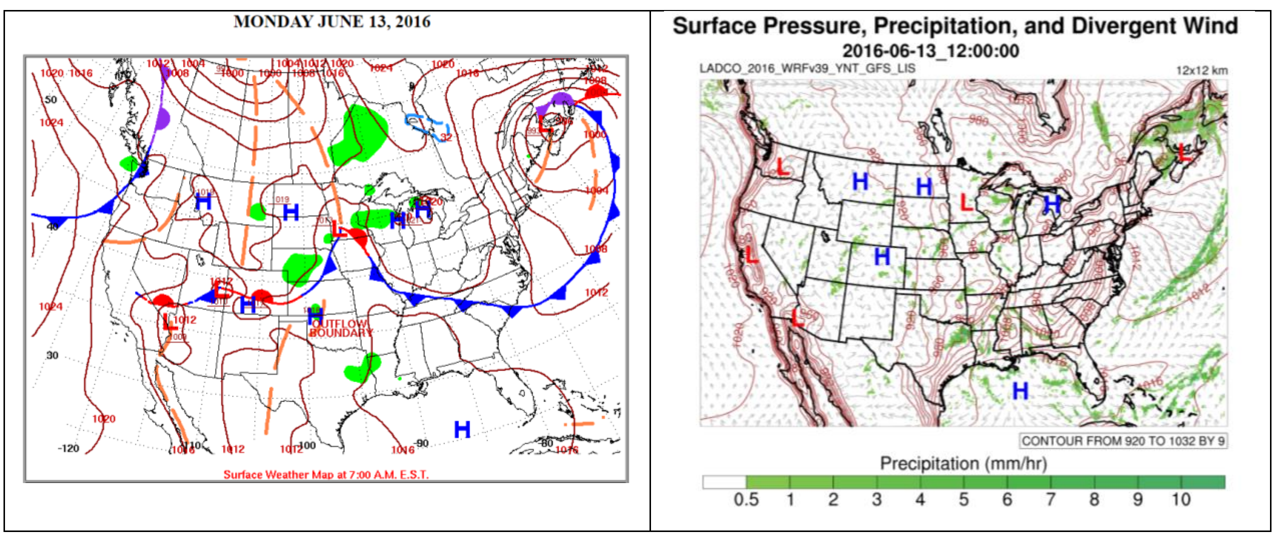

Figure 4. Comparison of surface weather maps at 7:00 am EST with modeled outputs at 12:00 pm UTC for June 13, 2016

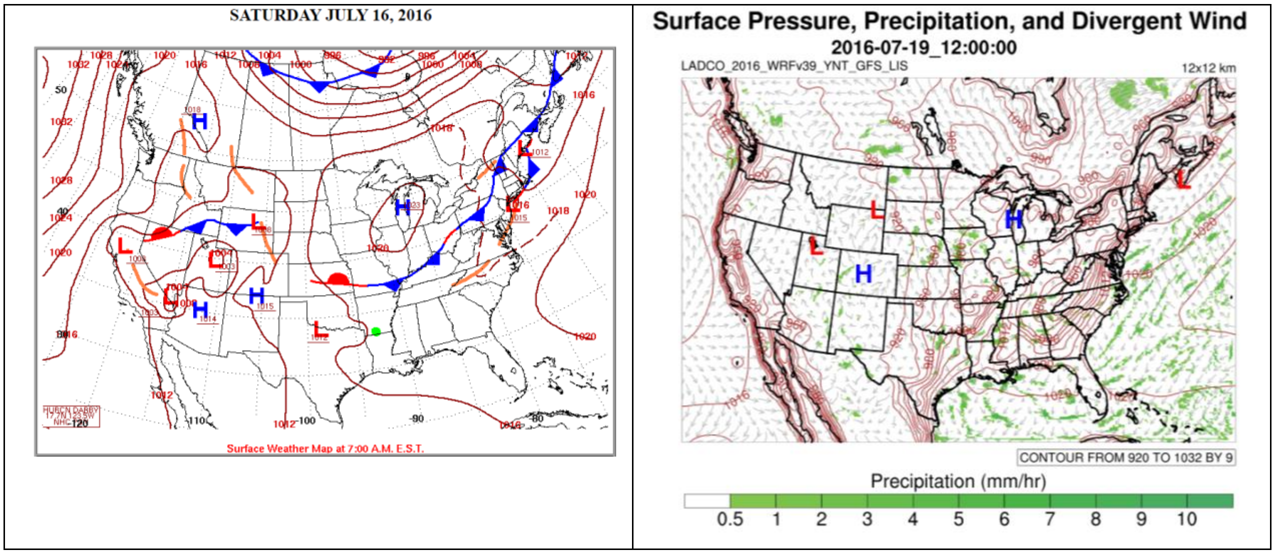

Figure 5. Comparison of surface weather maps at 7:00 am EST with modeled outputs at 12:00 pm UTC for July 16, 2016

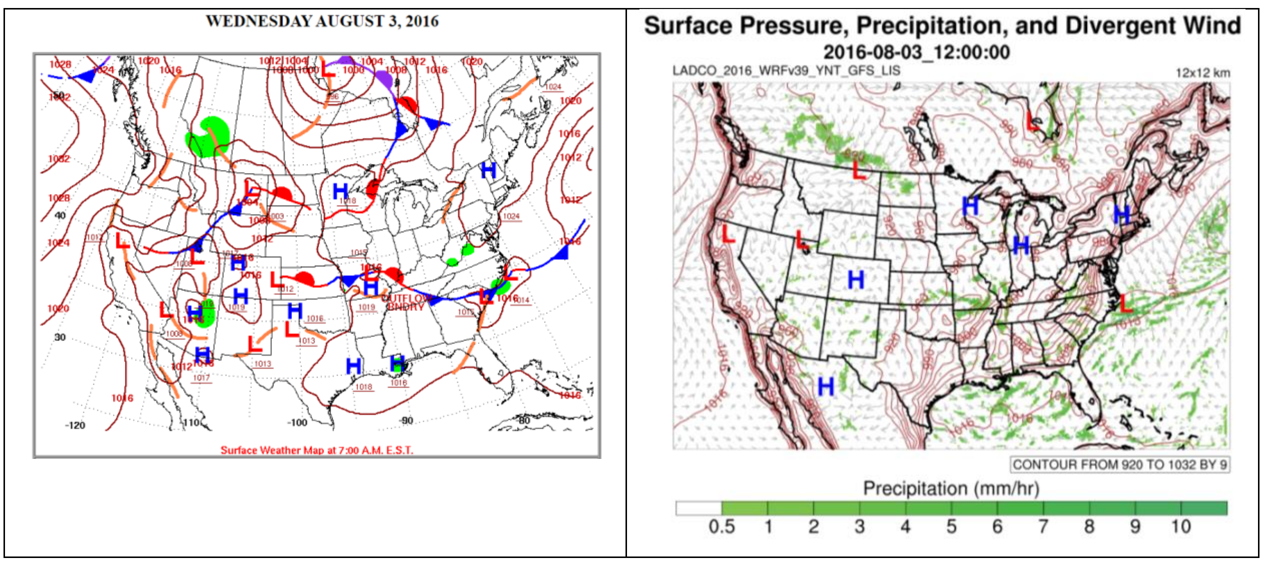

Figure 6. Comparison of surface weather maps at 7:00 am EST with modeled outputs at 12:00 pm UTC for August 3, 2016

Figure 7 through Figure 10 show that the 4-km WRF simulation deepens the surface pressure levels compared to the 12-km simulation. However, little appreciable difference is observed in surface pressure estimates between the two model resolutions despite initializing the 4-km WRF simulation with daily soil moisture and temperature fields with the NASA SpoRT LIS data. We also observed that WRF missed some of the precipitation features in the 4-km domain for these days.

.

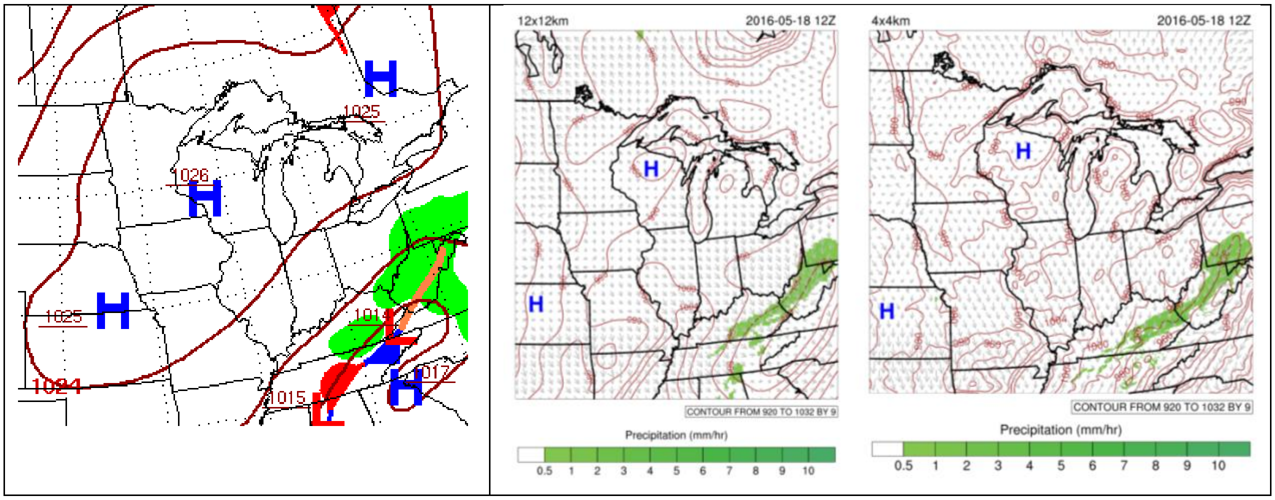

Figure 7. Comparison of model surface fields at 12km and 4km grid resolutions in Midwest for May 18, 2016

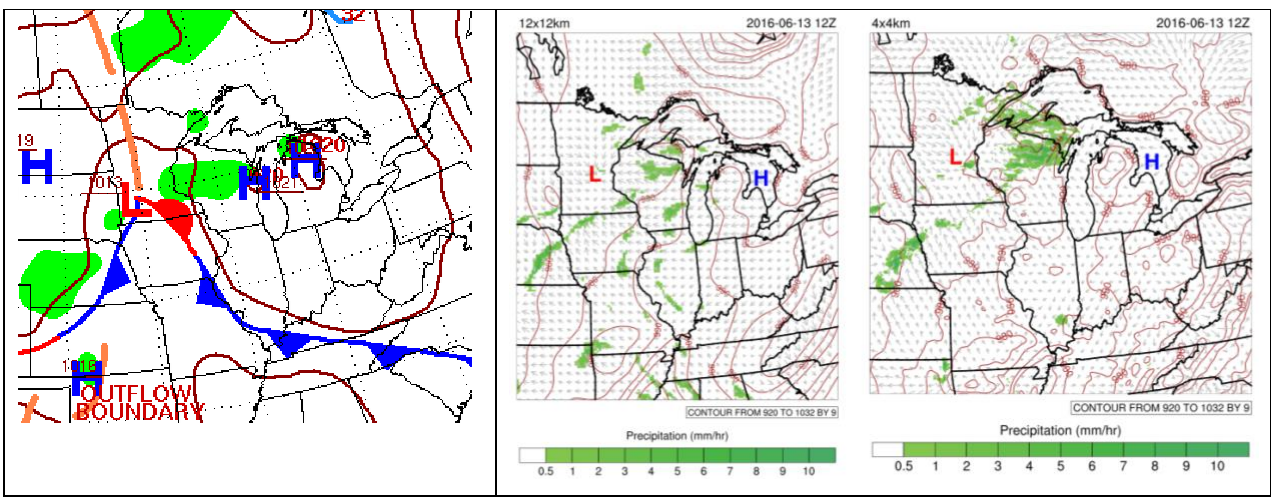

Figure 8. Comparison of model surface fields at 12km and 4km grid resolutions in Midwest for June 13, 2016

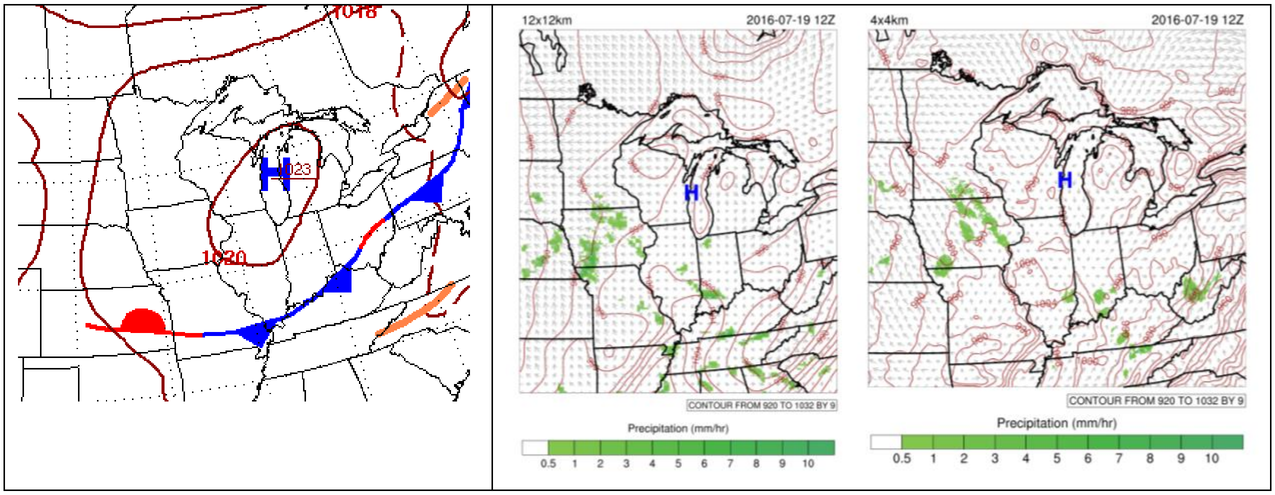

Figure 9. Comparison of model surface fields at 12km and 4km grid resolutions in Midwest for July 19, 2016

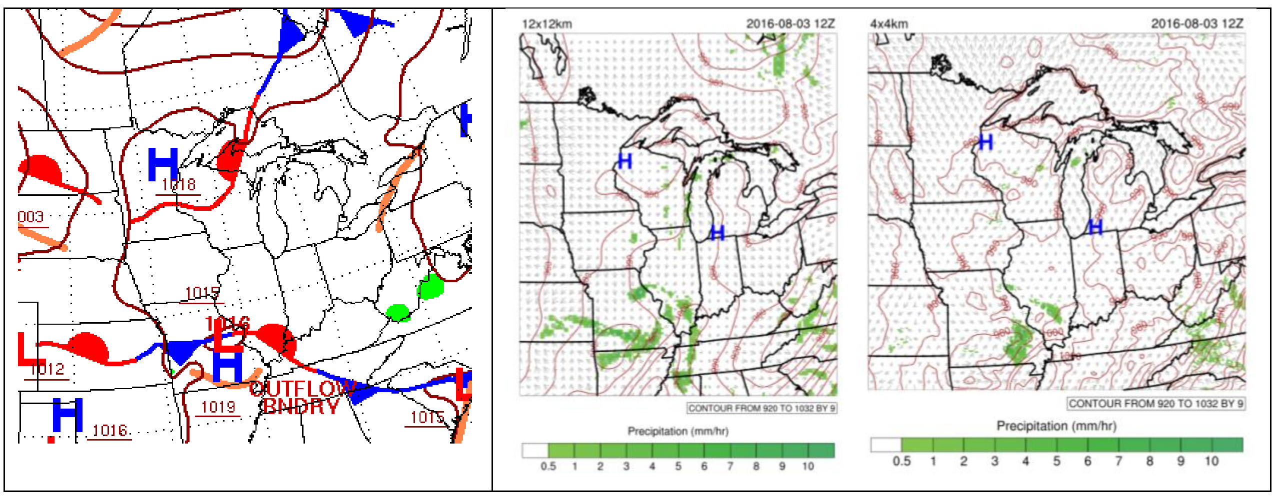

Figure 10. Comparison of model surface fields at 12km and 4km grid resolutions in Midwest for August 3, 2016

Overall, the 12-km and 4-km WRF simulations adequately captured the observed meso- and synoptic-scale processes during these periods. The LADCO WRF 2016 output fields represent a reasonable approximation of the actual meteorology that occurred in 2016.

3.3 Regional Scale Model Performance

The following sections present the LADCO WRF 2016 model performance at surface METAR network monitors for temperature, winds, and specific humidity. Average statistics are provided across the following dimensions for each of the WRF modeling domains:

- CONUS 12-km (d01): by season and monitors in each MJO
- LADCO 4-km (d02): by month and monitors in each state
- LADCO 1.33-km (d03 and d04): by month and monitors in each model domain

The average mean absolute errors (MAE) and mean biases (MB) of the key meteorology variables are derived by averaging all hourly performance statistics for particular months or season across all METAR meteorological stations within the evaluation domain.

3.3.1 CONUS12 WRF Model Performance

Table 5 summarizes the WRF 12-km domain-wide model performance by season. Spatial plots for the WRF model performance at surface sites in the CONUS12 domain for 2-meter temperature, 2-meter specific humidity, 10-meter wind speed, and 10-meter wind direction for each season are shown in Appendix A1.1. These performance plots depict the seasonal model MB (colors) and MAE (circle size) at each monitor simulated by WRF. Figure 28 through Figure 31 show that the LADCO's 12-km WRF simulation has a general cold bias across the domain in all seasons with an annual domain-wide 2-m temperature MB of -0.5 ±0.8 K. The seasonal MAEs for the WRF 2-meter temperature predictions across the MJO regions range from -2.0 to 1.1 K. Overall, temperature estimates are in a good agreement with observations, except for the west, where severe cold biases (<-3.0K) are seen in the mountainous areas.

Figure 32 through Figure 35 summarize the WRF 2-meter specific humidity (i.e., water vapor mixing ratio) performance. The LADCO 2016 12-km WRF simulation has a general dry bias, with MAEs ranging from 0.5-1.7 g/kg depending on region and season. The magnitude and regional variability of MAEs for specific humidity are lower in winter (0.5±0.3 k/kg) compared to the summer (1.7±0.7 k/kg). Specific humidity is generally unbiased in winter across the domain, but is underestimated in summer and fall, with mean biases of -0.5 k/kg in the LADCO region and -1.0 g/kg in the South Central and the Southeast. The model fails to simulate the enhanced spring season water vapor mixing ratio due to convective activity, and the influx of moist air masses in the summer and fall that come into the domain from the Gulf Mexico and travel to the Eastern U.S. In general, WRF performance for water vapor mixing ratio was adequate and within the commonly used benchmark, except for the South Central and the Southeast regions in the summer.

Figure 36 through Figure 39 summarize the 10-meter wind speed performance of the LADCO2016 12-km WRF simulation. Modeled surface wind speeds are in a good agreement with observations throughout the domain and season. Regional average errors (1.1±0.4 m/s) and biases (-0.2±0.7 m/s) are within the benchmark criteria of 2.0 m/s MAE and ±0.5 m/s MB for typical meteorological conditions. Overall, the LADCO 2016 12-km WRF simulation of wind speed is generally unbiased across the MJO regions and seasons.

Figure 40 through Figure 43 summarize the 10-meter wind direction performance of the LADCO 2016 12-km WRF simulation. The WRF wind direction predictions have higher MAEs in the west and relatively lower MAEs in the east. The higher MAEs (30-45 degrees) in the west that persist throughout the year along with the 2-meter temperature MBs are partly explained by the model not accurately resolving the orographic effects in the region. The 12-km WRF wind direction predictions are the best for the LADCO region as compared to other MJO regions. The mean MAE is about 25 degrees in cold seasons and about 30 degrees in warm seasons for the LADCO region. The LADCO 2016 12-km WRF simulation underestimates wind direction up to 40 degrees in the South Central and the Southeast coastal states in winter and fall seasons. These biases are impacted by the LADCO WRF model's inability to accurately simulate the tropical storms that developed in the Atlantic Ocean and passed through the region during these periods. Similar magnitudes of positive bias are seen in the northwest and north side of these regions where WRF did not correctly predict the wind direction. Considering that a number of complex mesoscale weather systems occurred during 2016[9] (National Weather Service, 2016 Weather Review), the LADCO 2016 12-km WRF wind direction estimates are considered reasonable when compared to the complex terrain model performance benchmark of 55 degrees (Kemball-Cook et al., 2005).

[9] 2016 Weather Year-in-Review - Climate Highlights

Overall, the LADCO 2016 WRF simulation for the surface meteorological variables are in a good agreement with observations. The WRF performance statistics for the 12-km grid resolution simulation are within the acceptable performance benchmarks proposed by Emery et al. (2001) and Kemball-Cook et al. (2005) for air quality model applications. It is worth noting that the LADCO 2016 WRF simulation has a cold and dry bias in the summer across much of the Eastern U.S. The model has a dry bias and underestimates wind direction in the South Central and Southeast in fall and winter seasons.

Table 5. 2016 seasonal average 12-km WRF model performance for entire 12US2 domain

Season*	Temp2m (K)		MixingRatio2m (g/kg)		WS10m (m/s)		WD10m (degrees)	
	MAE	MB	MAE	MB	MAE	MB	MAE	MB
Winter (DJF)	1.4	-0.4	0.5	0.0	1.2	0.0	38.0	0.2
Spring (MAM)	1.3	-0.4	0.8	0.0	1.2	-0.2	41.0	1.7
Summer (JJA)	1.4	-0.5	1.7	-0.9	1.1	-0.3	42.4	2.2
Fall (SON)	1.4	-0.5	1.0	-0.5	1.1	-0.1	42.3	-0.4

*Green shading indicates a metric that meets the performance benchmarks for simple conditions, orange for complex conditions, and red for outside of the performance benchmarks

3.3.2 WRF 12-km Performance Summary for the LADCO region

Table 6 summarizes the seasonal LADCO 2016 12-km WRF model performance for the part of the domain covering only the LADCO states. There is relatively similar WRF performance by season in the LADCO region compared to the entire CONUS domain. The LADCO 12-km WRF run for the LADCO region has MAEs of 1.2 K for temperature, about 0.7 g/kg for specific humidify, about 1 m's for wind speed and 30 degree for wind speed. On average, the 12km model run has a slight cool and wet biases in summer and fall, although within the model performance benchmarks. The WRF wind field predictions also have biases and errors that are within the performance benchmarks.

.

Table 6. 2016 seasonal average 12-km WRF model performance for the LADCO states

Season*	Temp2m (K)		MixingRatio2m (g/kg)		WS10m (m/s)		WD10m (degrees)	
	MAE	MB	MAE	MB	MAE	MB	MAE	MB
Winter (DJF)	1.2	-0.6	0.3	0.0	1.1	0.3	20.3	2.1
Spring (MAM)	1.2	-0.5	0.7	0.2	1.1	0.0	32.9	1.2
Summer (JJA)	1.3	-0.7	1.4	-0.7	1.0	-0.1	33.9	2.8
Fall (SON)	1.2	-0.5	0.7	-0.5	1.0	0.2	27.4	0.9

*Green shading indicates a metric that meets the performance benchmarks for simple conditions, orange for complex conditions, and red for outside of the performance benchmarks

3.3.3 Model Performance for the 4-km LADCO Domain

LADCO simulated WRF at a 4-km grid resolution centered on the Great Lakes Basin for April-October, 2016. Summer (June-August) model performances for temperature, specific humidity, wind speed, and wind direction is shown in Figure 11 through Figure 14. The 4-km resolution model performance for the LADCO states is summarized in Table 8. Appendix A shows the model performance statistics for individual sites in each of the LADCO states.

In general, the LADCO 2016 4-km WRF simulation estimated summertime surface temperatures well (MAE = 1.2 ±0.3 K; MB = -0.0±0.7 K) when the performance statistics at stations were averaged across the entire modeling domain. The WRF simulation has a slight warm bias (mean bias = 0.5-1.5 K) in urban areas, such as Chicago, Detroit, Cleveland, Columbus, and Cincinnati. The model has a slight dry bias as seen in the domain-averaged water vapor mixing ratios (MAEs = 1.2 ±0.3 g/kg; MB = -0.2 ±0.7 g/kg). The LADCO 2016 4-km WRF simulation has larger negative biases (dryer) in the southern part of the 4-km modeling domain relative to the rest of the domain (Figure 12).

Figure 13 shows that the summertime modeled surface wind speeds are in good agreement with observations throughout the domain and season. State-specific average errors (1.0±0.1 m/s) and biases (0.1±0.4 m/s) are within model performance benchmarks (Emery et al. 2001). Figure 14 shows that the LADCO 2016 4-km WRF simulation predicts wind direction with slightly higher errors than the benchmark (MAE ≤ 30°). The summertime wind direction errors ranges from 32-40 degrees, with lower errors in the northern part of the 4-km domain and higher errors in the south. Wind direction errors for the 12-km grid vs. 4-km grid domains are comparable. Magnitude and variability of wind speed errors are lesser in summer (1.0±0.1 m/s) than those in spring and fall (1.1±0.2 m/s), which indicates that the Great Lakes create a stagnant, high pressure environment in summer.

Table 7. 2016 seasonal average 4-km WRF model performance for entire LADCO4 domain

Season*	Temp2m (K)		MixingRatio2m (g/kg)		WS10m (m/s)		WD10m (degrees)	
	MAE	MB	MAE	MB	MAE	MB	MAE	MB
Spring (AM)	1.2	-0.1	0.8	0.3	1.1	0.2	35.4	2.1
Summer (JJA)	1.2	-0.2	1.3	-0.4	1.0	0.0	37.1	4.4
Fall (SO)	1.2	0.0	0.8	-0.3	1.1	0.3	35.1	-0.5

*Green shading indicates a metric that meets the performance benchmarks for simple conditions, orange for complex conditions, and red for outside of the performance benchmarks

.

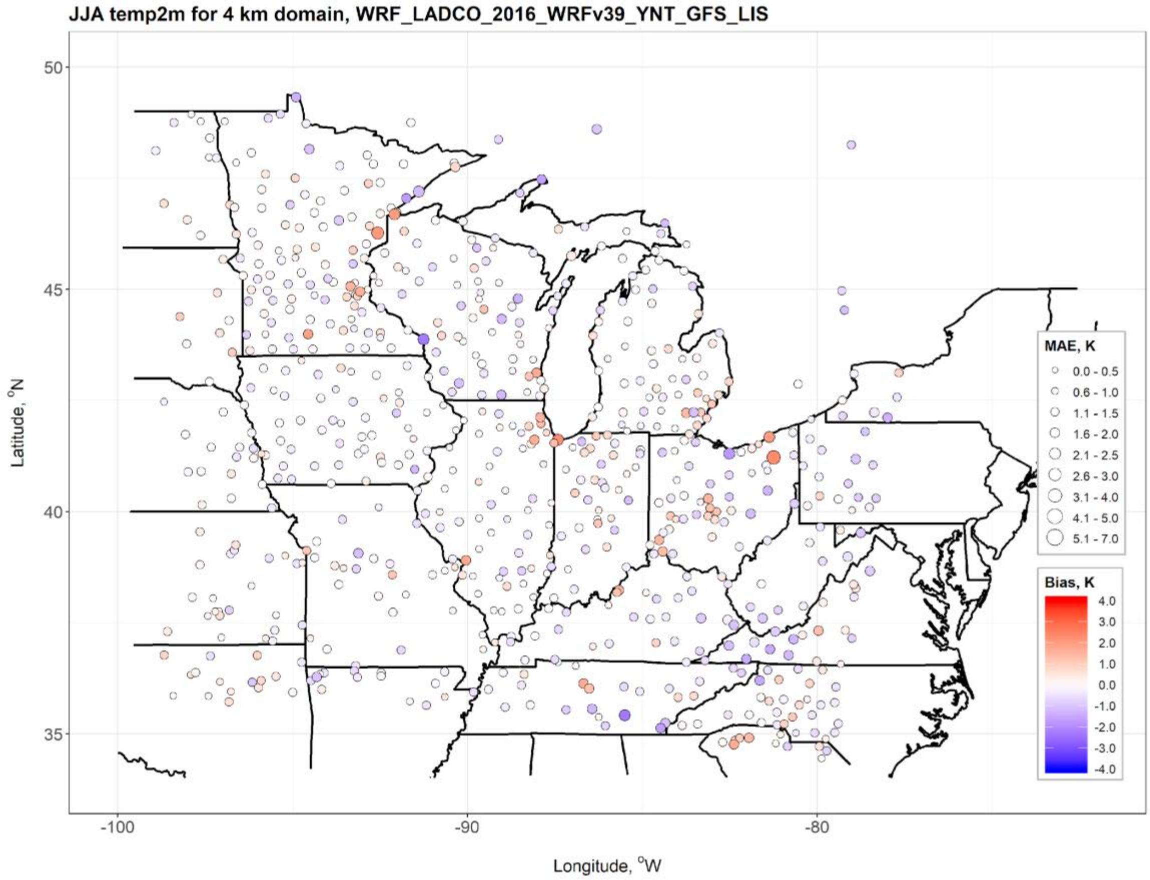

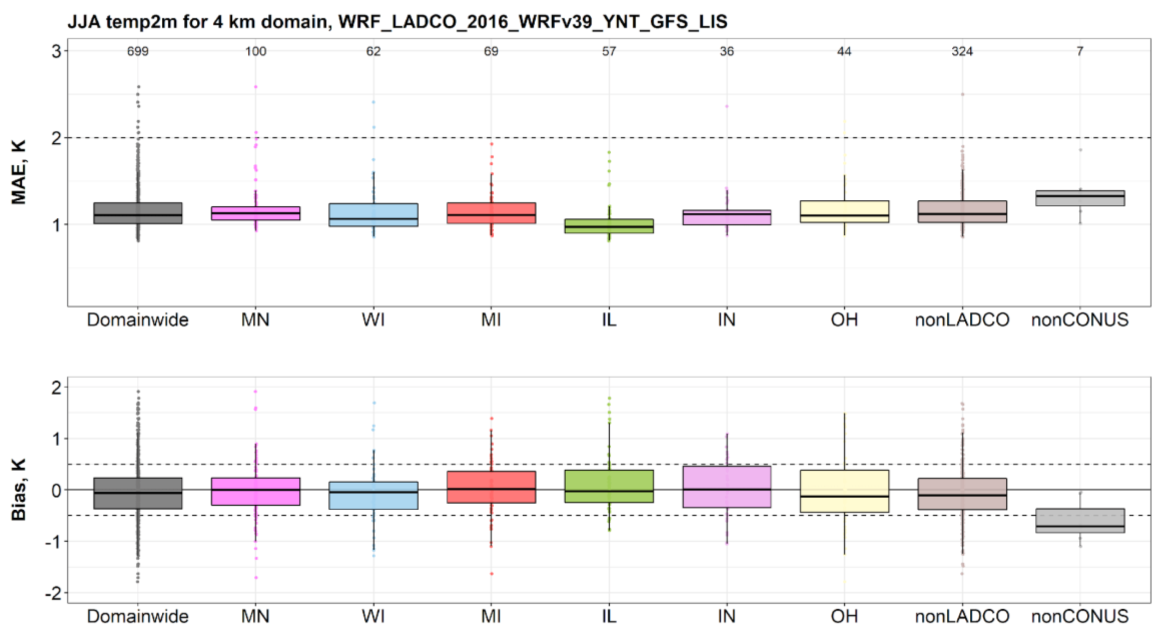

Figure 11. Mean Absolute Errors and Biases for Temperature in the 4km Domain, Summer 2016

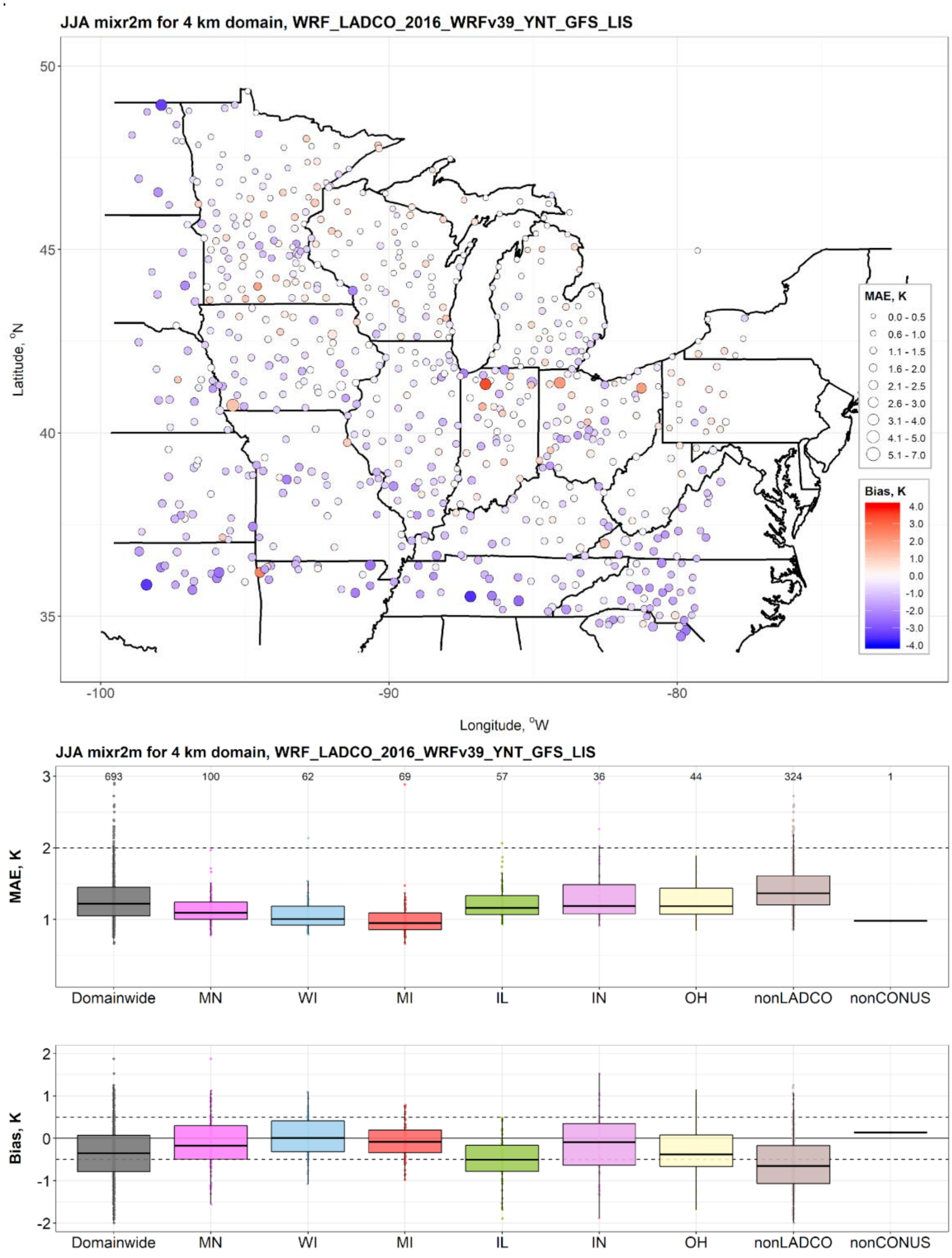

Figure 12. Mean absolute errors and biases for specific humidity in the 4km domain, Summer 2016

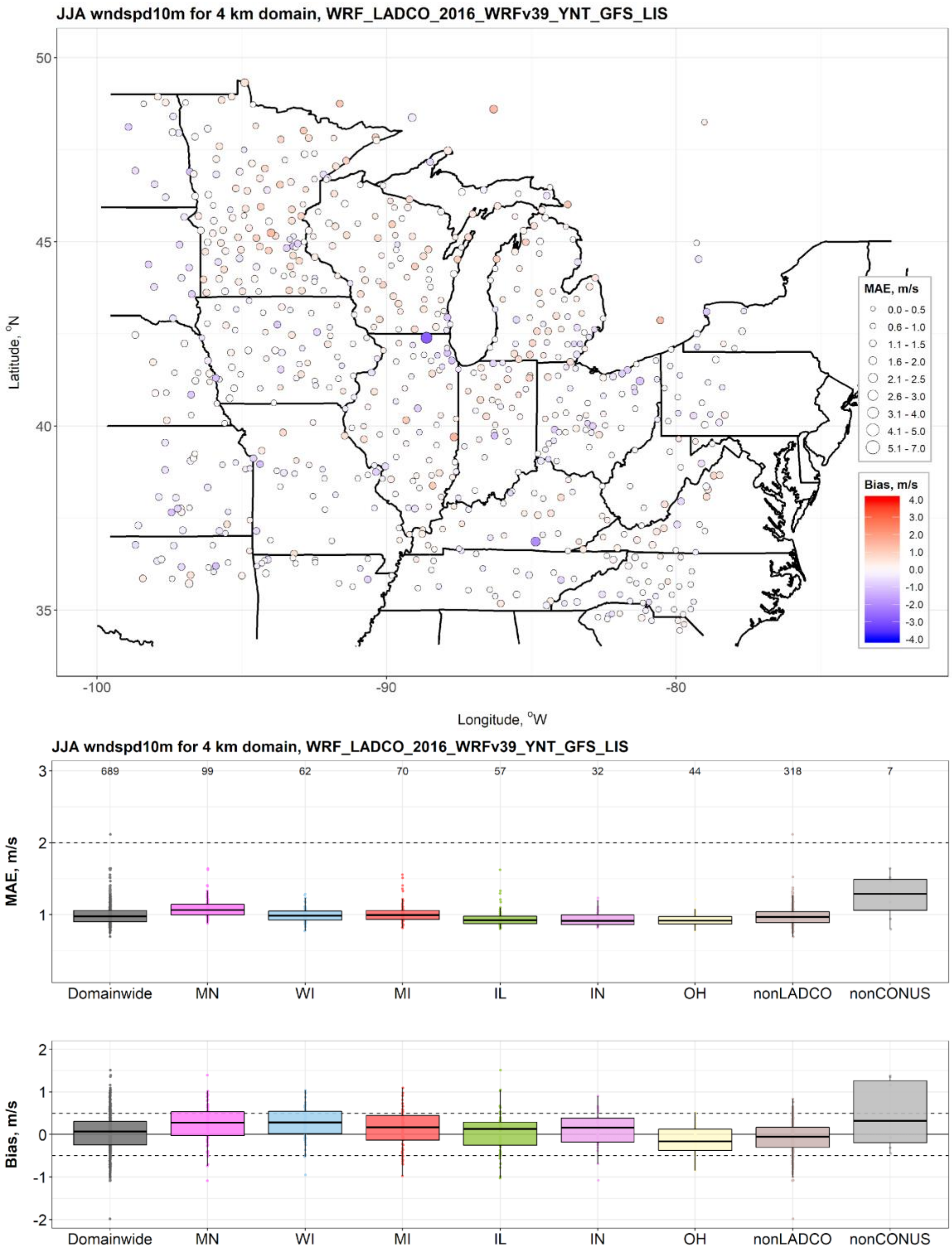

Figure 13. Mean absolute errors and biases for wind speed in the 4km domain, Summer 2016

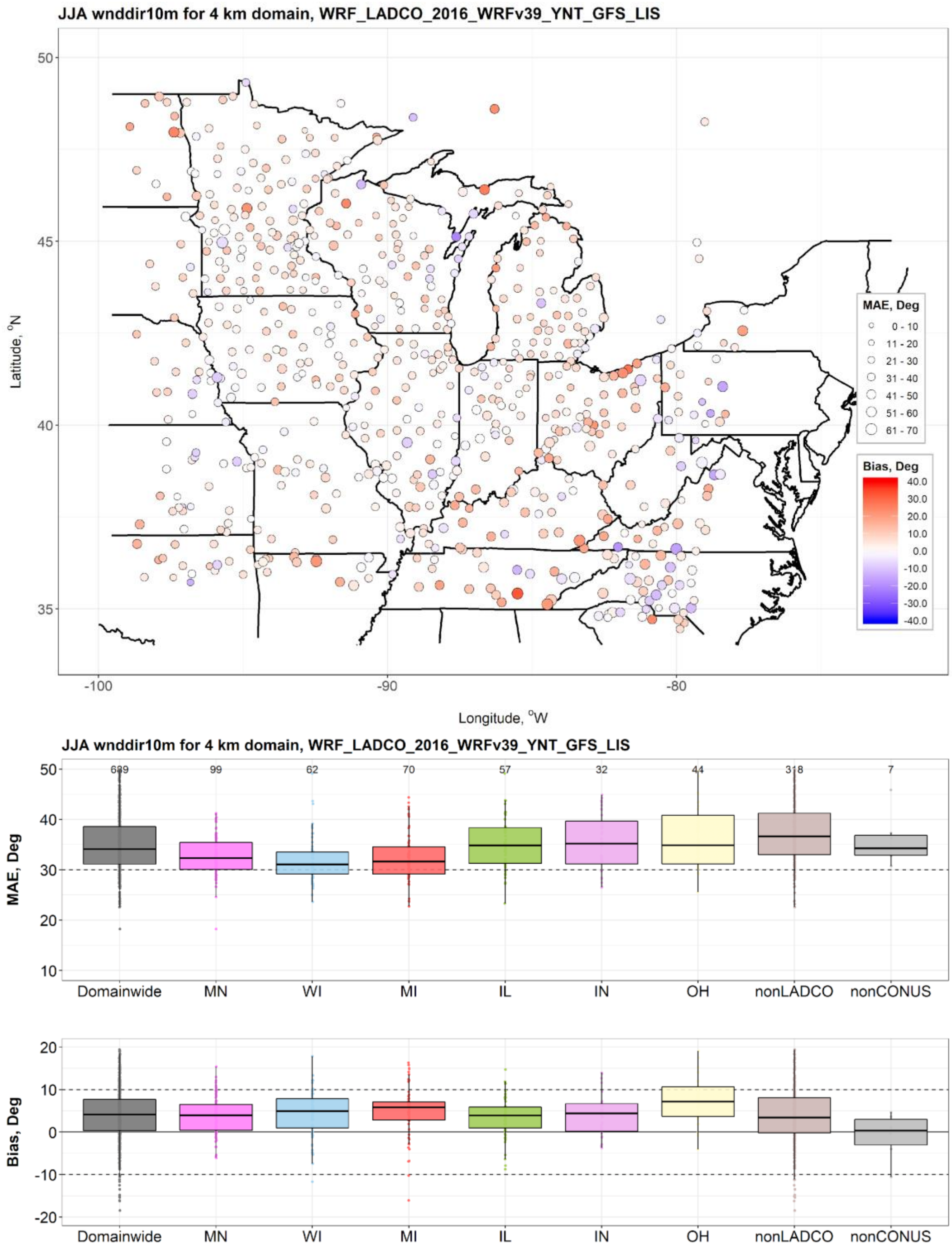

Figure 14. Mean absolute errors and biases for wind direction in the 4km domain, Summer 2016

3.3.4 WRF 4-km Performance Summary for the LADCO states

Table 8 summarizes the summer season model performance for monitor locations in each of the LADCO states. All of the summer season metrics, with the exception of wind direction error, fall within the simple terrain model performance benchmarks; the wind direction error falls within the complex terrain benchmark. The average summer season WRF model temperature and humidity (mixing ratio) performance is slightly improved when calculated for each individual state as compared to the 4-km domain average. The box and whisker plots in Figure 11 and Figure 12 confirm that the model performance deficiencies at the non-LADCO and non-CONUS (Canadian) sites in the 4-km domain skew the domain-wide bias and errors for temperature and humidity. Larger errors in the WRF predictions of wind-direction near the Ohio River valley in the southern part of the 4-km domain contribute to the higher errors in IL, IN, and OH relative to the 4-km domain average.

Table 8. 2016 summer season (JJA) 4-km WRF model performance for the LADCO states

State*	Temp2m (K)		MixingRatio2m (g/kg)		WS10m (m/s)		WD10m (degrees)	
	MAE	MB	MAE	MB	MAE	MB	MAE	MB
IL	1.0	0.1	1.2	-0.5	1.0	0.1	35.3	3.6
IN	1.1	0.1	1.4	-0.1	0.9	0.1	35.4	3.8
MI	1.2	0.0	1.0	0.0	1.0	0.1	34.4	5.5
MN	1.2	0.0	1.1	-0.1	1.1	0.2	33.4	4.0
OH	1.2	0.0	1.3	-0.3	0.9	-0.1	37.5	8.5
WI	1.2	-0.1	1.1	0.0	1.0	0.3	32.0	4.6

*Green shading indicates a metric that meets the performance benchmarks for simple conditions, orange for complex conditions, and red for outside of the performance benchmarks

3.3.5 Model Performance for the 1.33 km domains

LADCO used WRF to simulate meteorology over two 1.33-km domains covering a) Lake Michigan and b) Detroit and the Ohio River Valley for April through September 2016. Figure 15 shows summertime MAE and MB for surface temperature, water vapor, wind speed and wind direction. Table 9 shows that overall, the LADCO 2016 1.33 km WRF simulations are exceptional with the domain-averaged model performance statistics all well below the model performance benchmarks.

The seasonal average statistics are based on 90-100 surface meteorological stations depending on variable and domain. The 2-m temperature MAE was 1.3±0.6°K, the 2-m specific humidity MAE was 1.0±0.8 g/kg, the 10-m wind speed MAE was 1.2±0.7 m/s, and the 10-m wind direction was 34.8°±8.3. The model estimates are mostly unbiased at stations, except for slight overestimation at few stations in both domains.

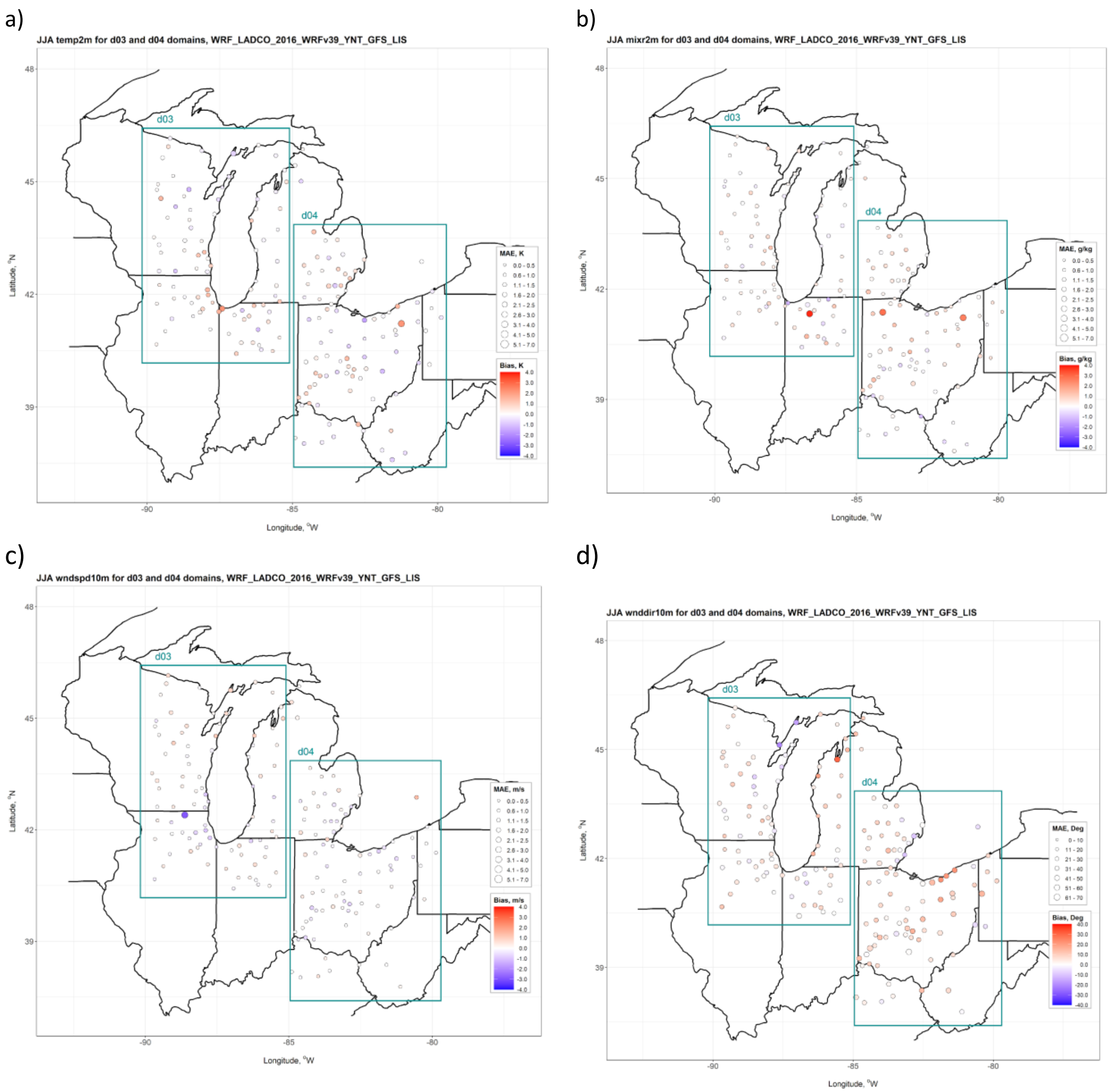

Figure 15. Mean absolute errors and biases for air temperature (a), specific humidity (b), wind speed (c) and wind direction (d) in the 1.33km domains, summer (JJA) 2016

Table 9. 2016 seasonal average 1.33-km WRF model performance statistics

Season*	Temp2m (K)		MixingRatio2m (g/kg)		WS10m (m/s)		WD10m (degrees)	
	MAE	MB	MAE	MB	MAE	MB	MAE	MB
	1.33 km d03: Lake Michigan							
Spring (AM)	1.3	0.0	0.9	0.5	1.3	0.1	34.1	1.1
Summer (JJA)	1.3	0.1	1.2	0.2	1.1	0.1	32.8	3.4
Fall (SO)	1.2	0.0	0.8	0.0	1.2	0.3	31.1	-0.1
	1.33 km d04: Detroit and Ohio River Valley							
Spring (AM)	1.3	-0.2	1.1	0.6	1.2	0.1	37.0	1.7
Summer (JJA)	1.3	0.7	1.3	0.3	1.1	0.0	37.1	5.1
Fall (SO)	1.3	0.0	0.8	-0.1	1.1	0.1	36.9	1.6

*Green shading indicates a metric that meets the performance benchmarks for simple conditions, orange for complex conditions, and red for outside of the performance benchmarks

3.3.6 LADCO 2016 WRF Model Region Scale Performance Summary

We compared the LADCO WRF 2016 summer model performance across domains at the same stations to see how model performance varies by the grid resolution. There are about 170 METAR stations located in the two 1.33 km domains. Table 10 tabulates summer season (JJA) WRF performance at 12-km, 4-km, and 1.3-km grid resolutions. Both errors and biases for temperature and specific humidity at the 12-km grid resolution are reduced by about 20% at the 4-km resolution. Model performance remains about the same for the wind speed and direction when going from 12-km to 4-km resolution. There was not an appreciative improvement in model performance for the analyzed variables between the 4-km and 1.33-km resolution simulations. Although the 1.33-km simulations did not produce a significant performance improvement for summertime overall statistics, the model resolved pretty well local-scale convective processes and had a better performance (specifically, lesser wind direction errors) during the lake breeze afternoon hours, which are discussed in Section 4.

Table 10. 2016 summer season (JJA) WRF model performance for common locations in the three LADCO WRF modeling domains

Domain	Temp2m (K)		MixingRatio2m (g/kg)		WS10m (m/s)		WD10m (degrees)	
	MAE	MB	MAE	MB	MAE	MB	MAE	MB
CONUS 12	1.4	-0.7	1.5	-0.6	1.1	-0.1	34.2	2.8
LADCO 4	1.2	0.1	1.2	-0.1	1.0	0.0	34.2	5.0
LADCO 1.33	1.3	0.1	1.2	0.2	1.1	0.0	34.8	4.4

4 WRF Performance Evaluation for Lake Breeze Events

The highest surface ozone concentrations in the Great Lakes Basin are observed near the shorelines of the lakes. The dynamical features at the land-water interface are well-known to be conducive to ground-level ozone formation. The lake-breeze is a key meteorological phenomenon that is associated with high ozone conditions in the region. This section presents an assessment of the skill of the LADCO 2016 WRF model to simulate the lake breeze, particularly during periods with observed high ozone concentrations.

LADCO used qualitative and quantitative methods to evaluate how well the WRF model simulates lake breeze events that occur on the shorelines of Lake Michigan and Lake Erie. The qualitative evaluation includes comparisons of satellite imagery and observed wind fields with modeled PBL height and wind vectors. Statistical model performance at eleven METAR stations located near the shoreline are used for quantitative evaluation for lake breeze events. The station locations are shown in Figure 16.

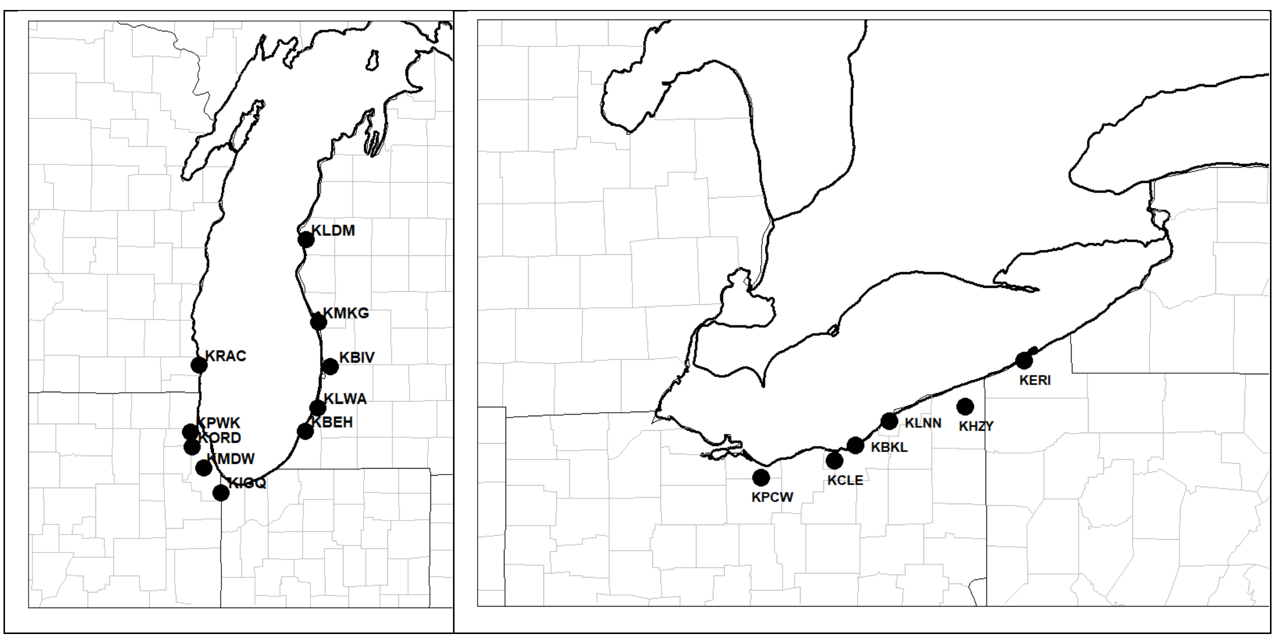

Figure 16. METAR stations on shoreline of Lake Michigan (left) and Lake Erie (right). The stations are elevated less than 200 m a.s.l and located south of the 44^{o}N latitude

.

We used timeseries and CART (Classification and Regression Tree)[10] analyses to identify the conditions at the surface meteorological stations that are associated with the lake breeze. We used the statistical software R version 4.1.3 and the R package rpart[11] for classifying meteorological conditions during the identified lake breeze days. We pruned the CART analysis trees using site-specific complexity parameters to increase the overall accuracy of the model and to minimize cross-validation errors. We then calculated WRF performance statistics, such as mean absolute error and mean bias, using observed and WRF modeled values on the lake breeze days predicted by CART for selected shoreline monitors.

4.1 Identifying Lake Breeze Days

LADCO used the Visible Infrared Imaging Radiometer Suite (VIIRS) Corrected Reflectance and National Doppler Radar daily imagery for May 15 through September 16, 2016 to identify lake breeze days along the south shore of Lake Erie and the eastern and westerns shores of Lake Michigan. Imagery from the VIIRS instrument, which is on the joint NASA/NOAA Suomi National Polar orbiting Partnership (Suomi NPP) satellite, is available through NASA Worldview and the Global Imagery Browse Services (GIBS, https://worldview.earthdata.nasa.gov/). High-resolution reflectivity composite data from national doppler radar stations can also illustrate features of the lake breeze, such as front and outflow boundaries and associated precipitation features near the land-water interface (https://weather.us/radar-us). Table 11 shows the screening results for identifying Lake Michigan lake breeze days in 2016.

Both the VIIRS surface reflectance and radar imagery show fair weather low-to-mid level cumulus cloud fronts that penetrate inland during a lake breeze event. These fronts are associated with rising, warm air masses over land that get replaced by relatively cold air masses originating over the lake during the summer season. The lake breeze can be observed by local changes in lake-to-

[10] L. Breiman, J.H. Friedman, R.A. Olshen, and C.J Stone. Classification and Regression Trees. Wadsworth, Belmont, CA, 1983

[11] https://cran.r-project.org/web/packages/rpart/vignettes/longintro.pdf

land winds. The changes in winds can be indicated by numerical weather modeling results from the GFS/NCEP/ US National Weather Service (https://earth.nullschool.net).

Table 11. Screening of the lake breeze events near the Lake Michigan in 2016

Date	NPP/VIIS Surface Reflectance (https://worldview.earthdata.nasa.gov/)	Doppler Radar Reflectivity Composite (https://weather.us/radar-us)	GFS/NCEP/National Weather Service Surface Wind (https://earth.nullschool.net)
5/17/2016	y	y	y
5/18/2016	y	y	y
5/29/2016	y		
5/30/2016	y	y	y
6/3/2016			y
6/8/2016		no radar data (June 17-28)	y
6/29/2016	y	y	y
6/30/2016	y	y	
7/1/2016	y		y
7/2/2016	y		y
7/3/2016			y
7/4/2016			y
7/5/2016	y		y
7/9/2016	y	y	y
7/16/2016	y	y	y
7/18/2016		y	
7/19/2016	y	y	y
7/26/2016	y	y	
7/27/2016	y	y	
7/28/2016	y	y	
7/31/2016	y		
8/1/2016	y		y
8/2/2016	y	y	y
8/3/2016	y	y	y
8/4/2016			y
8/5/2016			y
8/6/2016	y	y	y
8/10/2016	y	y	y
8/16/2016	y		y

Both the VIIRS and radar imagery indicated that the surface wind convergence zones due to a lake breeze occurred during 21 days[12] in the summer months of 2016 along the shore of Lake Michigan.

As an example, the VIIRS surface reflectance, radar imagery and GFS modeled surface wind field in afternoon of July 16, 2016 are shown in Figure 17. The satellite and radar imageries show a lake breeze front around Lake Michigan and surface wind divergence over the lake, which are typical features of lake breeze events.

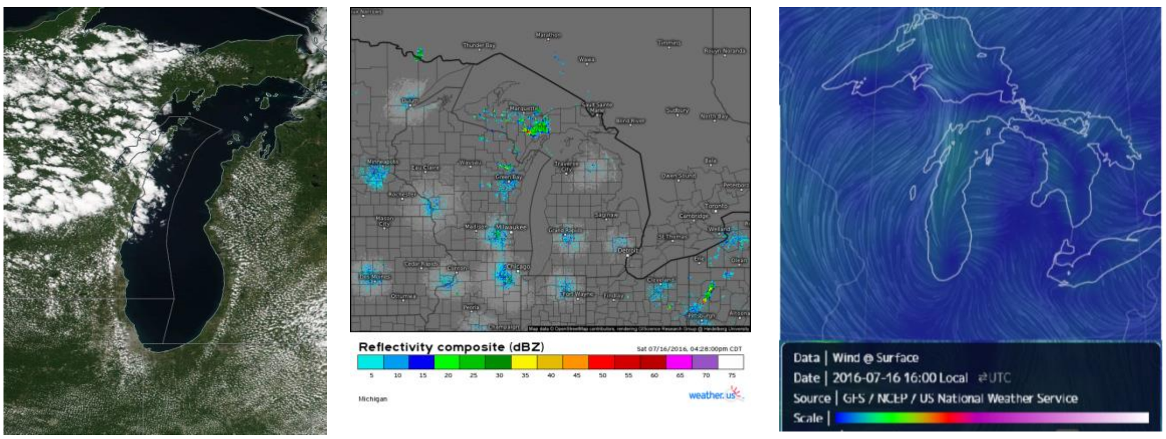

Figure 17. Lake breeze front viewed by VIIRS satellite true color imagery (left), radar reflective imagery (middle), and surface wind field in the Great Lakes simulated by the GFS model are shown for July 16, 2016, 2-4pm

Similarly, we have identified lake breeze days in the shoreline of Lake Erie[13] using lake breeze fonts and associated surface convergence seen by VIIRS satellite true color imagery and the GFS modeled surface wind field.

To verify that the LADCO 2016 WRF modeling reproduced the features of the lake breeze, we looked at simulated images of the predicted surface (10-m) winds, surface (2-m) temperatures,

[12] Satellite data informed lake breeze days in Lake Michigan: 5/17,5/18, 5/30, 6/29,6/30, 7/1,7/2, 7/5, 7/9, 7/16, 7/18, 7/19, 7/26, 7/28, 8/1, 8/2, 8/3, 8/6, 8/10, 8/16

[13] Satellite data informed lake breeze days in Lake Erie shore: 5/18, 5/19, 5/29, 6/21, 6/25, 6/29, 6/30, 7/5, 7/7, 7/19, 7/22, 7/27, 8/1, 8/2, 8/3, 8/4, 8/6, 8/7, 8/8, 8/10, 8/18, 8/22, 8/23, 8/28, 8/29, 8/30, 9/4, 9/5, 9/9, 9/12, 9/19, 9/21, 9/22

and planetary boundary layer (PBL) heights during the morning and afternoon hours on these days. In addition, we used classification and regression tree analysis (CART) to help us identify the meteorological conditions that are most associated with lake breeze days. Descriptions of the lake breeze analysis and results follow.

4.2 Satellite Imagery Analysis

Figure 18 through Figure 20 depict lake breeze fronts that formed around Lake Michigan on May 18, July 16, and August 3, 2016, respectively. The fronts are seen in the satellite true color imagery, and in the WRF modeled planetary boundary layer (PBL) height and wind fields. Figure 3 through Figure 5 show the presence of a high-pressure system in the Midwest on these days. WRF simulated light east or north-easterly winds in the morning hours (before 0900 CST) over Lake Michigan on these days. The simulated winds shifted in the afternoon with divergence over the lake. WRF simulated a lake-to-land breeze with onshore convergence starting around noon that dissipated around 2100 CST. WRF simulated calm and fair-weather conditions on July 16 and Aug 3, 2016, which is the typical condition for forming a lake breeze in afternoon hours.

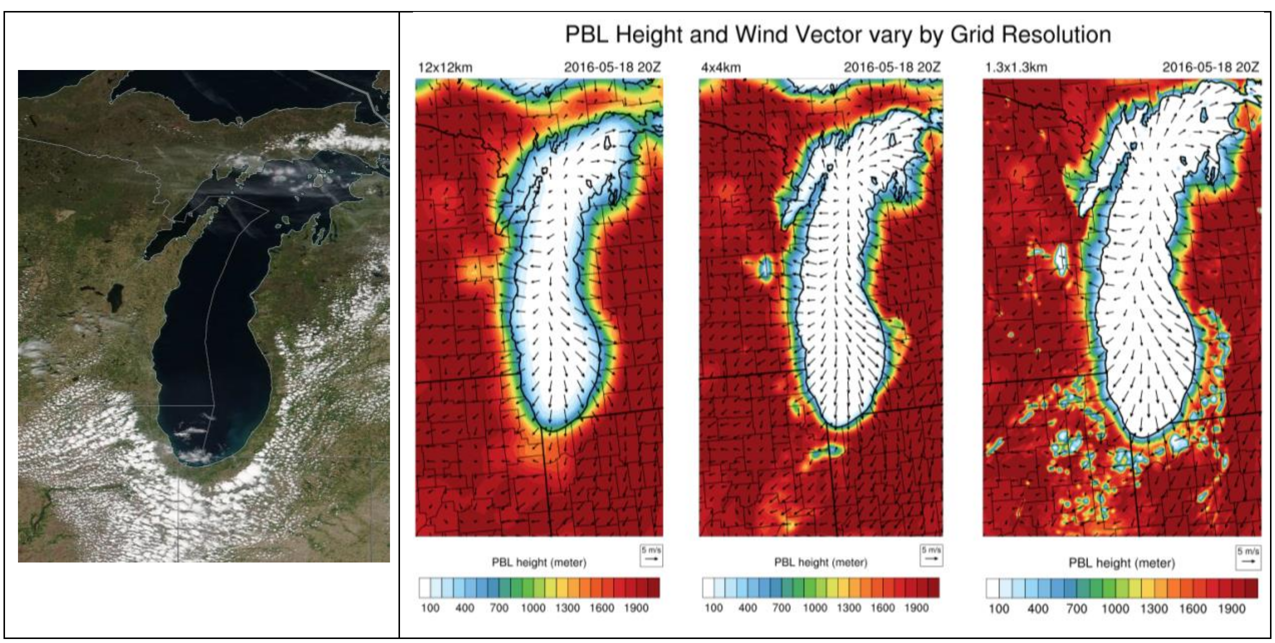

Figure 18. May 18, 2016 (1400 CST) satellite imagery and modeled PBL height and wind vectors

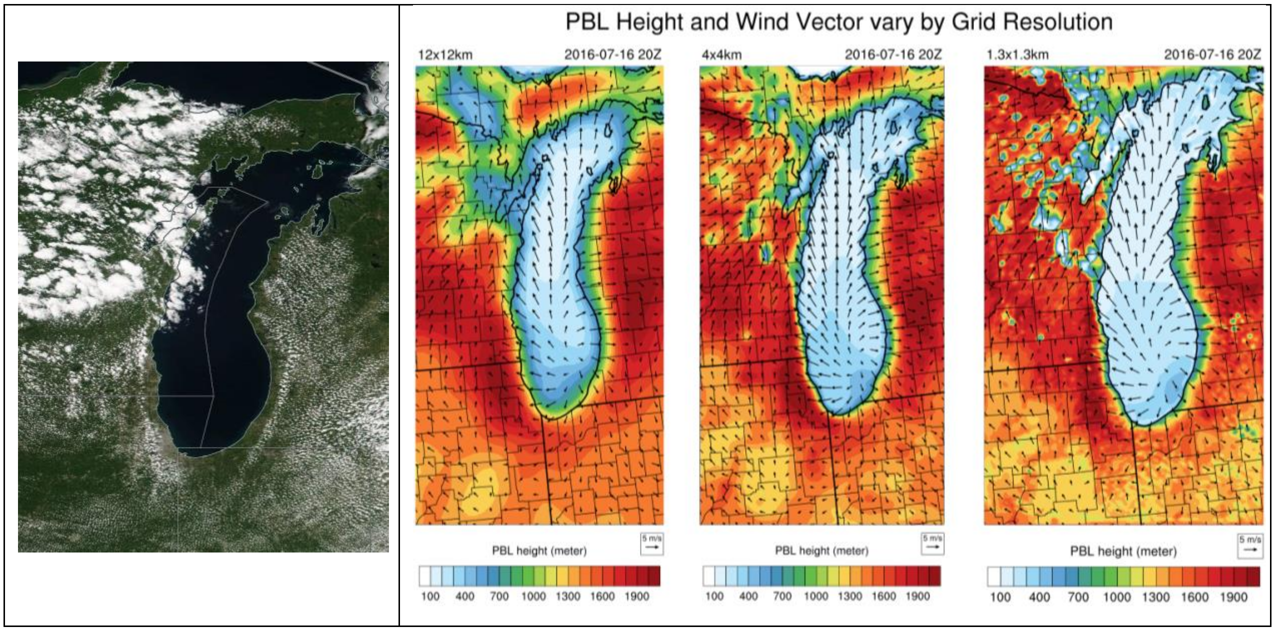

Figure 19. July 16, 2016 (1400 CST) satellite imagery and modeled PBL height and wind vectors

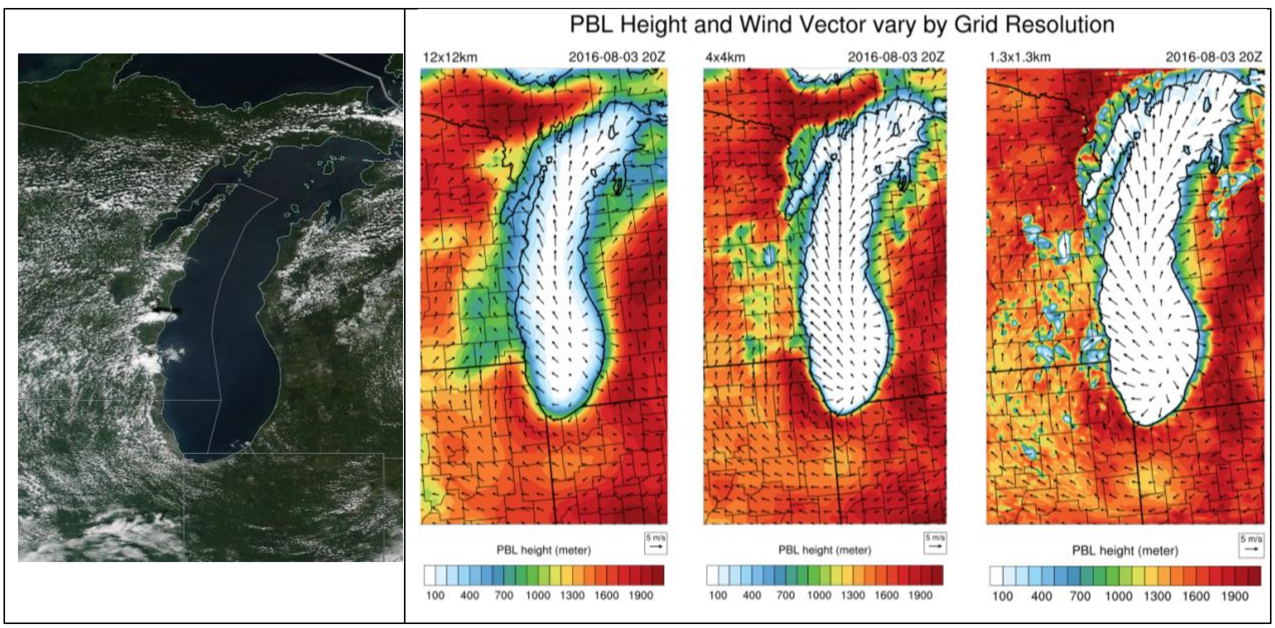

Figure 20. August 3, 2016 (1400 CST) satellite imagery and modeled PBL height and wind vectors

WRF successfully reproduced the surface flow convergence zone inland from the lakeshore, seen as the higher inland PBL heights in the figures above. The finer grid (4 km and 1.3 km) WRF resolutions also successfully resolved the small to mid-scale convective processes, i.e., the small clusters of lower PBL heights indicate the formation of fair-weather cumulus clouds over the land. These clouds are a common feature of lake breeze fronts, as seen in the true color satellite imagery. Quantitative WRF model performance at simulating the lake breeze is discussed in the following sections.

4.3 Observed and Modeled Wind Fields near Lake Michigan and Lake Erie

We compared the WRF model surface wind fields with MADIS observations for the summer months of 2016. The surface winds analysis of the lake breeze convergence zones would indicate if WRF can reproduce these important features that accompany lake breeze frontal movements over the LADCO region.

Both the surface observation and the 1.3 km grid resolution WRF wind fields showed that the surface wind convergence zones were formed for about 40 days[14] in the western shore of Lake Michigan, for about 10 days[15] in the eastern shore of Lake Michigan, and for 20 days[16] in the south shore of Lake Erie in 2016 summer. Evolution of wind shifts over the lakes were carefully examined for lake breeze-induced wind convergence zone formation near the lake shores.

Appendix A.2 contains plots showing the surface wind comparison between observations and WRF modeling results for June 3, July 31, and August 9, 2016. Figure 44 shows a lake breeze convergence zone was formed at 1000 CDT along the western shoreline in Wisconsin, maturated larger in size at 1300 CDT and moved westward at 1600 CDT, and finally disappeared at 1900 CDT. Similarly, Figure 45 show northeasterly winds in the morning hours before 1000 CDT that shifted northerly over the Lake Michigan, and a lake breeze convergence zone was formed along the eastern shoreline of Lake Michigan between 1300 and 1900pm CDT on July 31, 2016. The convergence zone dissipated by 2200 CDT. Again, WRF was successful in reproducing the surface

[14] Wind convergence observed days in the western shore of Lake Michigan: 5/16, 5/30, 6/1, 6/2, 6/3, 6/8, 6/9, 6/10, 6/15, 6/16, 6/19, 6/25, 6/28, 6/29, 7/1, 7/2, 7/4, 7/5, 7/16, 7/18, 7/20, 7/22, 7/23, 7/25, 7/26, 7/27, 8/2, 8/4, 8/5, 8/6, 8/9, 8/14, 8/17, 8/18, 8/22, 8/25, 8/26, 8/31, 9/6, 9/9

[15] Wind convergence observed days in the eastern shore of Lake Michigan: 5/21, 6/17, 6/18, 7/4, 7/31, 8/1, 8/8, 8/18, 9/3, 9/14

[16] Wind convergence observed days in Lake Erie: 5/20, 6/1, 6/2, 6/10, 6/30, 7/3, 7/11, 7/12, 7/22, 7/28, 7/31, 8/4, 8/9, 8/10, 8/19, 8/23, 8/27, 9/9, 9/10, 9/12

flow convergence zone associated with the lake breeze formation along the eastern shoreline of Lake Michigan on this day. The afternoon wind comparisons in Figure 21 and Figure 22, and satellite imagery confirmed that a lake breeze occurred on these days and that the WRF wind fields agreed with observed wind speed and direction. Thus, it confirms that the model successfully reproduced the surface flow convergence zone associated with the lake breeze in Lake Michigan shore on these days.

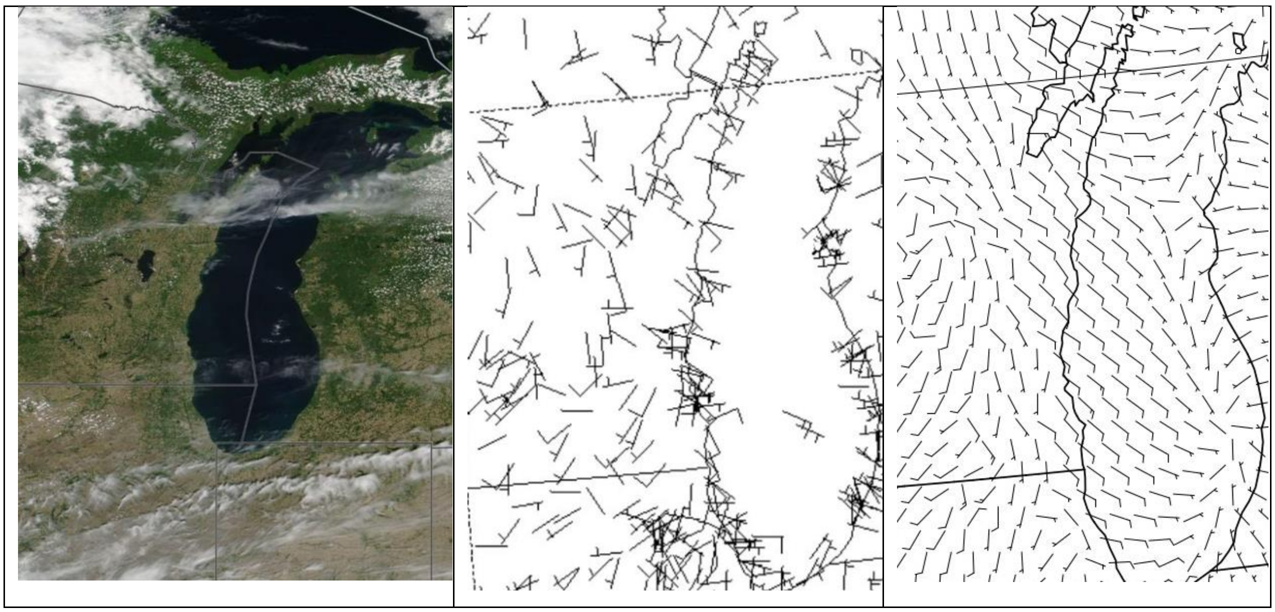

Figure 21. VIIRS true color imagery (left), observed (middle) and 1.33 km WRF (right) surface winds at 4:00 pm CDT on June 3, 2016 over Lake Michigan

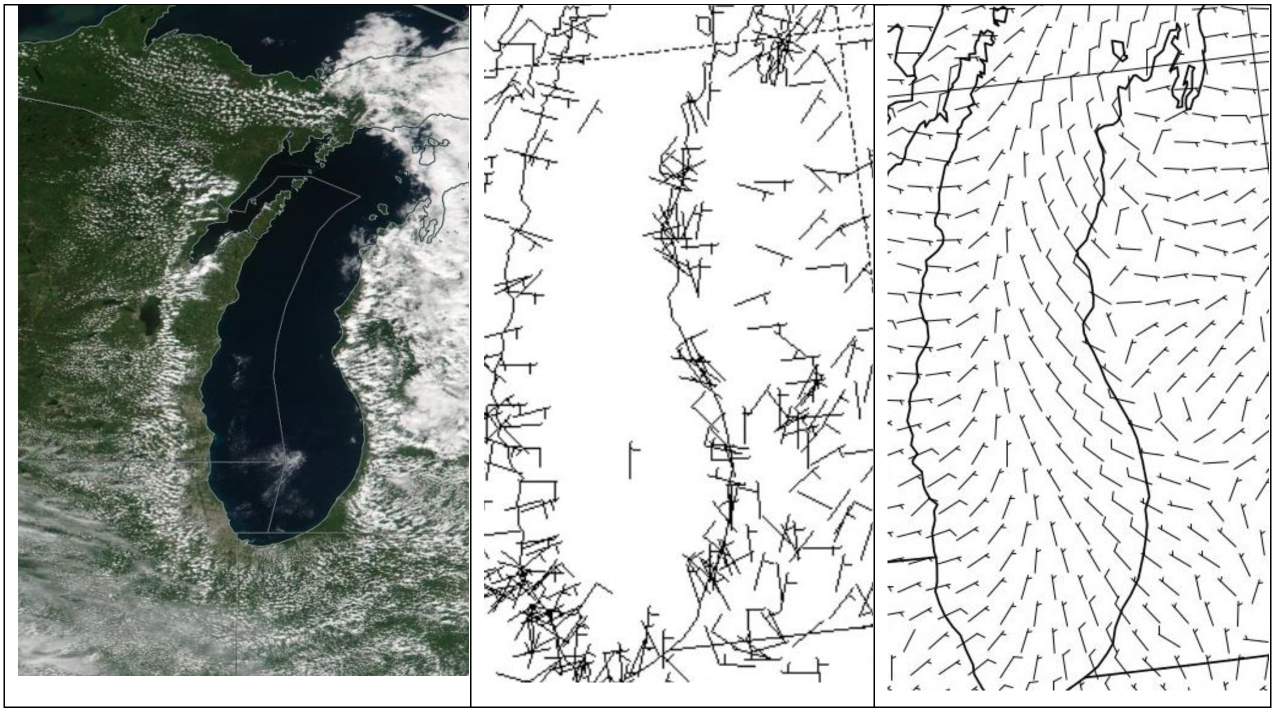

Figure 22. VIIRS true color imagery (left), observed (middle) and 1.33 km WRF (right) surface winds at 4:00 pm CDT on July 31, 2016 over Lake Michigan

Figure 46 and Figure 47 in Appendix A.2 show wind field comparisons along the south shore of Lake Erie on August 9, 2016. The observations indicate southeasterly winds in the morning hours at 1000 CDT. A lake breeze convergence zone developed later along the southern shoreline of Lake Erie between 1300 and 1900 CDT. The convergence zone dissipated by 2200 CDT. These plots illustrate that WRF duplicated the surface flow convergence zone associated with the lake breeze on this day. We also examined the WRF 1.33 km and 4 km resolution simulated winds and confirmed that the model indeed was able to reproduce the surface convergence zones for both domains.

4.4 CART Analysis for Lake Breeze Events

4.4.1 Meteorological conditions of lake breezes in Lake Michigan shoreline

Figure 23 lists the meteorological conditions that CART associated with lake breeze days along the west and east shorelines of Lake Michigan. As ‘lake breeze’ at Lake Michigan shores is a definite variable to indicate air flow from lake to land, CART identifies wind direction as the first branching variable in its classification. The graduated red and blue colored tree nodes (or clusters) at the bottom of the classification tree identify the meteorological conditions associated with lake breeze events (and non-lake breeze events such as land-breezes).

At the Racine, WI (KRAC) station the CART analysis identified two clusters of meteorological conditions associated with the lake breezes:

1. Easterly wind shifts greater than 10° from previous hour (wind direction < 144° and hourly wind direction change >10°) and hot and humid conditions (temperature > 28°C and specific humidity is 14-16 g/kg)
2. Warm and moderate moist air (temperature is 24-28°C and specific humidity is 8-13 g/kg) with north-north-easterly winds (wind direction is 0-24° range)

At the Muskegon, MI (KMKG) station the CART analysis identified a single cluster of meteorological conditions that are associated with the lake breeze: a shifting westerly wind direction and a relatively hot and moist air mass (hourly wind direction shifts slight or greater degree, temperature > 29°C, and specific humidity <16 g/kg).

.

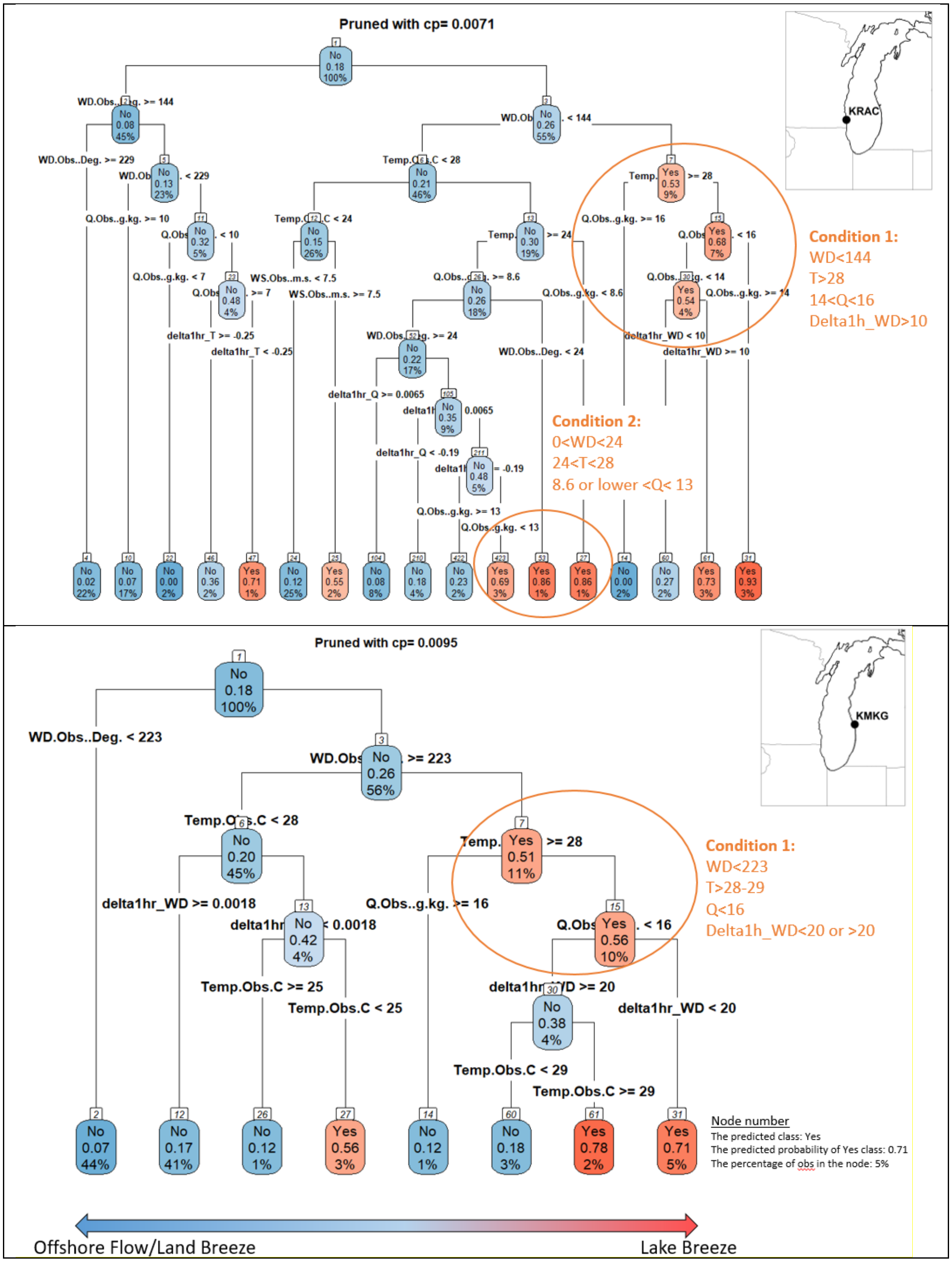

Figure 23. Meteorological conditions classified during the lake breeze periods at western shoreline (KRAC station on the top) and eastern shoreline (KMKG station on the bottom) of Lake Michigan during 12-16 local standard time. Graduated red and blue colored tree nodes indicate strength of predicted probability of the lake breeze events and offshore flows.

.

Table 11 summarizes the typical meteorological conditions and hourly indicators of lake breeze events for the western and eastern shores of Lake Michigan. In the western shore of Lake Michigan, the lake breeze sets in during warm, moderately humid and northeast-to-southeasterly wind conditions. During this condition, wind direction shifts in 10-40 degrees from previous hour record, and wind speed and specific humidity increases by 0.5-1.0 unit during 1200-1600 CDT.

Westerly flow is the dominant meteorological condition for lake breeze events along the eastern shore of the Lake Michigan. Other conditions include hourly wind direction changes in the range of 10-20°, and slight drops in wind speed (0.5-1.0 m/s) during the onset of a lake breeze. The lake breeze occurs in much warmer and more humid conditions in the east shore of Lake Michigan (T>25-28^{o}C and 10g/kg<Q<16 g/kg) as compare to the west shore (18^{o}C<T<25^{o}C and 5g/kg<Q<16 g/kg). There are two METAR stations located on the south end of the lake, however, the CART analysis was only carried out at one station due to extensive missing data at the other station. The lake breeze meteorological condition and hourly indicator at this station is somewhat similar to that of east shore stations.

Table 11. Classified meteorological conditions for lake breeze events in Lake Michigan basin during 12-16 CST, summer of 2016

West shoreline (4 stations)	South (1 station)	East shoreline (5 stations)
Meteorological conditions during the lake breeze events		
18^{o}C< Temp < 25^{o}C	27^{o}C< Temp < 31^{o}C	Temp >25-28^{o}C
5 g/kg<Humidity <16 g/kg	Humidity <10 g/kg	10 g/kg < Humidity <16 g/kg
0/5-2.5 m/s < Wind speed	Wind speed< 5 m/s	3.5 m/s <Wind speed< 4.5 m/s
84 Deg <Wind direction <114-164 Deg	84 Deg <Wind direction <114-164 Deg	223-256 Deg <Wind direction <248-360 Deg
Hourly indicators for onset of lake breeze		
		Very slight temperature drop (0.6 oC per hour)
Moderate humidity increase (0.5-0.8 g/kg per hour)	Slight humidity increase (<0.2 g/kg per hour)	Slight humidity increase (<0.2 g/kg per hour)
Slight wind speed increase (0.5-1.0 m/s per hour)		Slight wind speed decrease (0.5-1.0 m/s per hour)
Slight to greater wind direction shift (10-40 deg per hour)		Slight wind direction shift (10-20 deg per hour)

4.4.2 WRF model performance during lake breeze events along the Lake Michigan shoreline

LADCO calculated model performance statistics using surface observations and WRF modeled values at the shoreline stations on days and locations in which the CART predicted lake breeze probability was greater than 70%. We also calculated performance statistics at the same locations on non-lake breeze days to gain additional insight into WRF performance for lake breeze events. For the non-lake-breeze days we analyzed days with similar temperatures, humidity, and wind speed as the lake breeze days, however, lake breeze wasn't identified from satellite and Doppler imageries and an independent model wind fields that are used and described in the Identifying Lake Breeze Days (Section 4.1).

Table 12 presents the WRF mean absolute errors and mean biases on lake breeze and non-lake breeze days averaged across all three LADCO WRF grid resolution simulations (12/4/1.33 km) near Lake Michigan. WRF performs relatively well at the shoreline stations for days with and without a lake breeze, and under similar meteorological conditions. The model errors and biases are within the WRF performance benchmarks. The model performance is slightly degraded on the lake breeze days compared to the non-lake breeze case, which can partly be explained by a greater sample size for the non-lake breeze days as compare to than for lake breeze days.

Table 12. Average WRF model performance summary for lake breeze and non-lake breeze days along the shoreline of Lake Michigan

Variable	Lake Breeze		Non-Lake Breeze	
	MAE	MB	MAE	MB
Temp2m	1.24	0.50	1.06	0.21
MixingRatio2m	1.30	-0.65	1.06	-0.41
Wind speed10m	1.14	-0.68	1.14	-0.73
Wind direction10m	25.93	1.73	22.29	-2.05

Table 13 presents WRF performance statistics for lake breeze days across different model grid resolutions. Refinement to the model grid resolution does not produce a significant performance improvement. Temperature, specific humidity and wind speed errors for all grid resolutions are in a range of 0.93-1.68; and wind direction errors in a range of 25.7-26.2 degree. The WRF temperature forecasts for the 12km grid have a low bias, while the finer grid simulations tend to overestimate temperatures by 0.7°C on an average during the lake breeze events. Specific humidity and wind speed are underestimated by 0.1-1.0 g/kg and 0.5-0.9 m/s, respectively.

Table 13. Average WRF model performance summary by model grid resolution for the lake breeze events in the shoreline of Lake Michigan

Variable	12 km		4 km		1.3 km	
	MAE	MB	MAE	MB	MAE	MB
Temp2m	1.24	0.01	1.27	0.74	1.22	0.75
MixingRatio2m	1.68	-1.03	1.28	-0.81	0.93	-0.11
Wind speed10m	1.28	-0.90	1.07	-0.62	1.08	-0.52
Wind direction10m	25.70	-0.51	26.22	3.19	25.88	2.52

In addition to these averaged statistics, we analyzed the mean absolute errors and mean biases at specific shoreline stations. Figure 24 and Figure 25 summarize the WRF model errors and biases, respectively, for the lake breeze and non-lake breeze events at each station. The box and whisker plots summarize the performance across all three grids, the dots show the performance statistics for each grid resolution. Light gray lines in each panel represents the Emery et al (2001) model performance benchmark values for each variable.

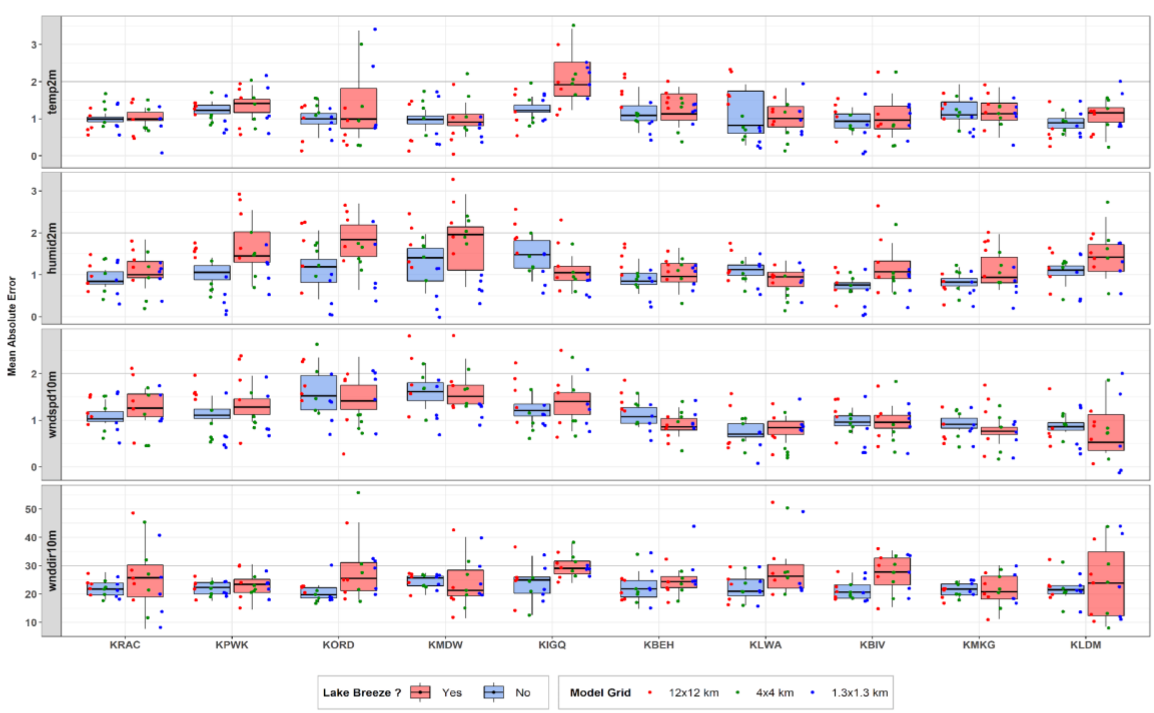

Figure 24. MAEs for temperature, specific humidity, wind speed and direction at METAR stations in Lake Michigan shore.

.

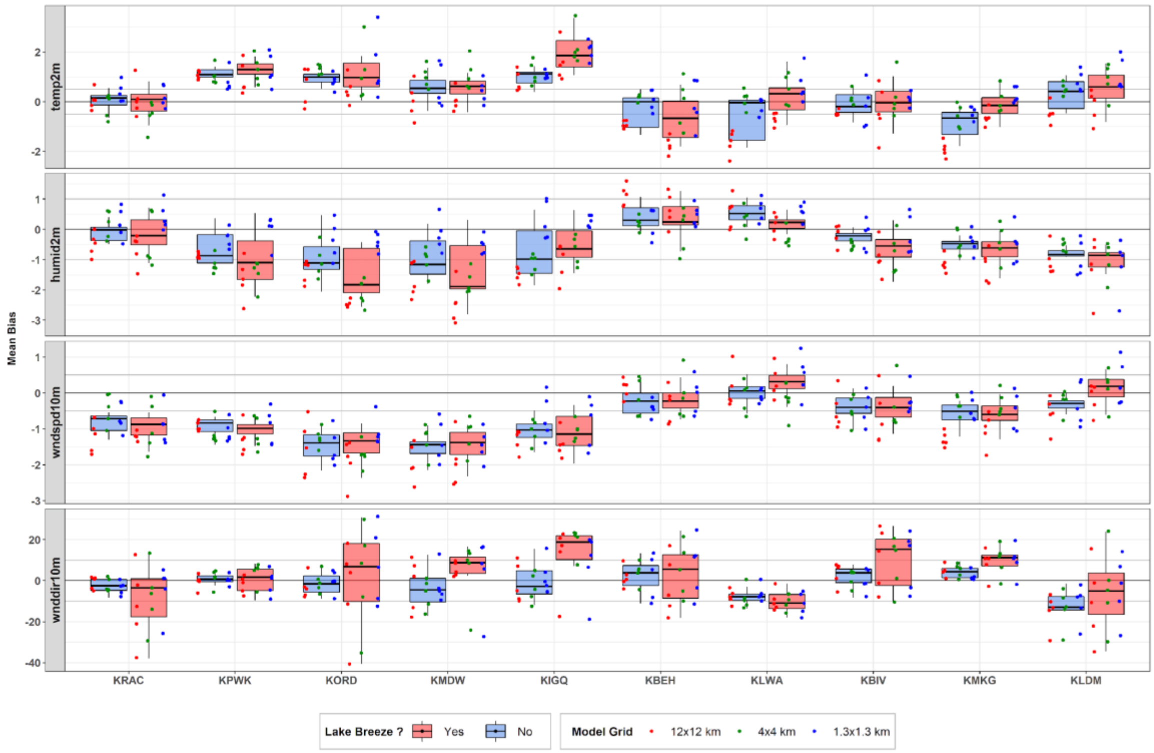

Figure 25. MBs for temperature, specific humidity, wind speed and direction at METAR stations in Lake Michigan shore

WRF generally simulates the temperature, specific humidity and winds at these stations during lake breeze events with error and bias statistics that are within the commonly used performance benchmarks. Model absolute errors for temperature and wind speed are similar for days with and without a lake breeze. Specific humidity and wind direction errors are higher for the lake breeze events than those for similar met conditions without a lake breeze.

At the western Lake Michigan shoreline stations, the MB plot (Figure 25) shows that WRF tends to overestimate temperature, which led to underestimations of specific humidity and wind speed. These underestimations are greater during the lake breeze events. The error and bias plots show that when looking at individual sites the model performance improves at finer grids. At the eastern Lake Michigan shoreline stations, model errors and biases for temperature, specific humidity and wind speed don't differ between the lake breeze and non-lake breeze days. Generally, model performance improves at the finer grids at eastern shoreline stations.

Interquartile range of wind direction biases for the lake breeze events varies from station to station, which could be explained by the lake breeze induced convection formed in lake shore areas.

4.4.3 Meteorological conditions of lake breezes in the south shore of Lake Erie

Common meteorological conditions classified and predicted for lake breeze afternoon hours at the south shore of Lake Erie are shown in Figure 26. CART reveals temperature and wind speed/specific humidity are the top two splitting variables at most of the stations, followed by wind direction and indicator variables designed for identifying the lake breeze conditions such as changes in wind speed, direction, and specific humidity from previous hours. These variables were classified for predicting binary classes of 'Yes' and 'No' for the identified lake breeze day afternoon hours (12:00-16:00 LST). The graduated red and blue colored tree nodes represent the classified meteorological conditions for lake breeze events and non-lake breeze events, such as offshore flow and land-breezes, respectively.

At the KBKL station, the analysis revealed that lake breeze occurs in a combination of three set of meteorological conditions: (1) northerly wind becomes calmer and wind direction shifts in 0-30 degree from previous hour (wind direction ranges in 285-20°; (2) hourly wind direction changes in 0-30°, and hourly wind speed drops in 0-1.3m/s) during relatively hot and humid conditions; and (3) temperature is in 25-30°C and specific humidity is in 12-15 g/kg or greater. At KERI station, lake breeze occurs during the following three set of meteorological conditions: (1) southwest to northerly winds on hot and humid days with slight temperature increases up to 0.75°C from previous hour (wind direction ranges from 249-360° and temperature ranges from 24-29°C, with hourly temperature increase in a range of 0.0-0.75°C/hour); (2) wind speed reduces slightly (hourly wind speed decreases in 0.5-1.0 m/s) on hot and calm days (temperature is in 24-29°C and wind speed is less than 3.6 m/s); and (3) northeasterly winds on hot days (wind direction ranges from 0-44°, air temperature is greater than 29°C).

.

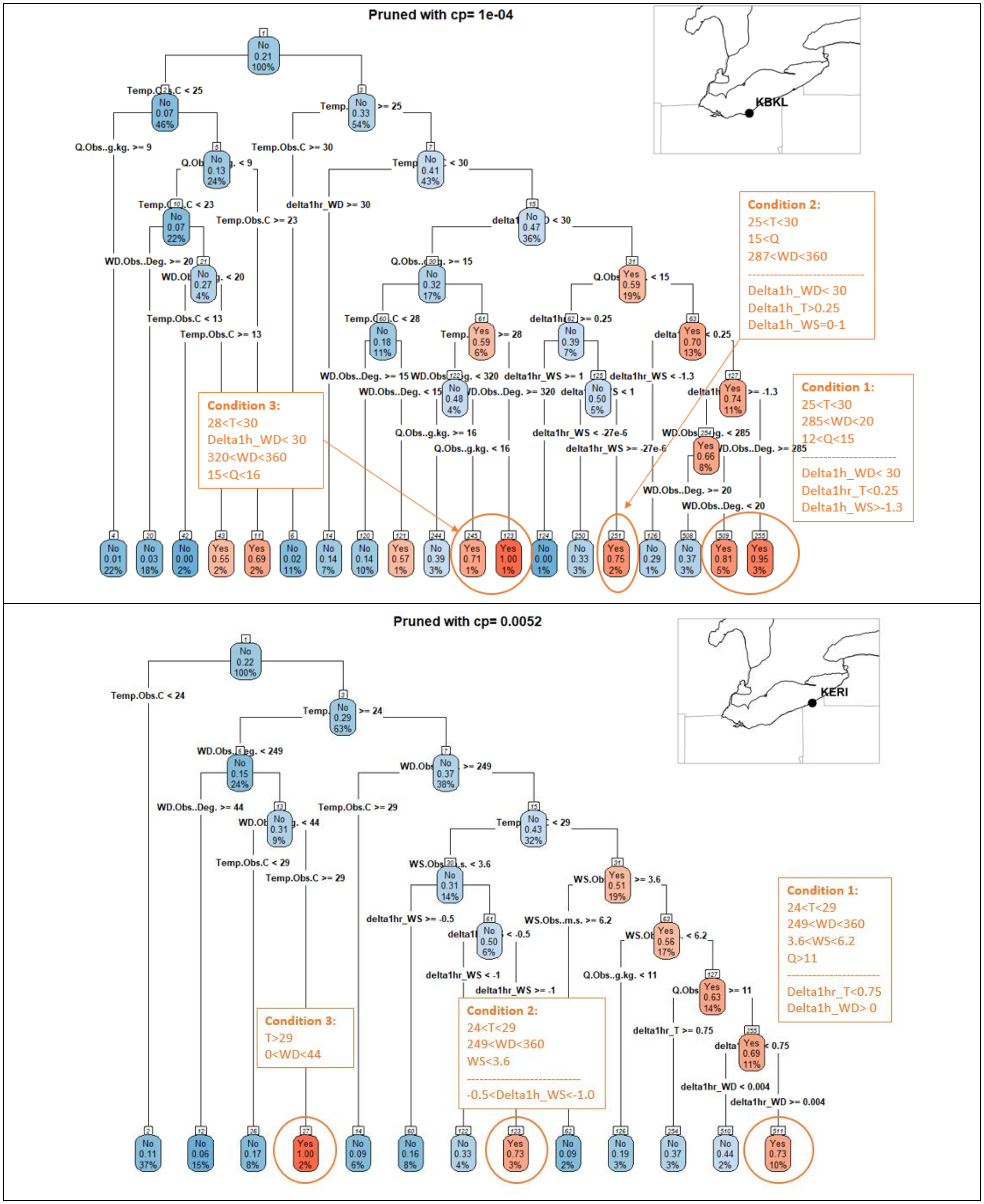

Figure 26. Meteorological conditions classified during the lake breeze periods at KBKL and KERI stations in the south shore of Lake Erie in 2016. Graduated red and blue colored tree nodes

indicate strength of predicted probability of the lake breeze events and offshore flow and non-lake breeze days, respectively.

Our CART analysis found that on the south shore of the Lake Erie the lake breeze sets in during hot and humid conditions with temperatures ranging from 21-31^{o}C and humidity ranging from 10-17 g/kg (Table 14). During these conditions, the wind speeds drop a bit (0.5-1.3 m/s), wind direction shifts slightly (30° as compare to the previous hour recordings), humidity drops slightly (0-0.6 g/kg), and temperature increases (0-0.75°C) during afternoon hours.

Table 14. Typical meteorological conditions during lake breeze in the south shore of Lake Erie, summer of 2016

Meteorological conditions during the lake breeze events
21^{o}C< Temp < 31^{o}C
10 g/kg<Humidity <17 g/kg
0.5-5.0 m/s < Wind speed
280 Deg <Wind direction <20 Deg
Hourly indicators for onset of lake breeze
Slight drop in humidity (0-0.6 g/kg decrease from previous hour)
No change to slight temperature increase (0.0-0.75 oC increase from previous hour)
Slight wind speed decrease (0.5-1.3 m/s decrease from previous hour)
Slight to moderate wind direction shift (<30 deg from previous hour)

4.4.4 WRF model performance during lake breezes in south shore of Lake Erie

Summary of the model errors and biases by lake breeze and non-lake breeze events near the south shore of Lake Erie and by model grid resolution are tabulated in Table 15 and Table 16, respectively. Temperature, specific humidity and wind speed errors for the 12km, 4km and 1.3 km grid resolutions are in a range of 0.95-1.45; and wind direction errors range in 27.6-30.1 degree. Model errors and biases for both lake breeze events and similar met conditions are within the WRF performance benchmarks. The LADCO WRF simulation tends to underestimate these examined variables (Table 15) regardless of different grid resolution (Table 16), however, the errors and biases slightly improve at finer grids.

.

Table 15. Model performance summary for lake breeze and non-lake breeze events in the south shore of Lake Erie

Variable	Lake Breeze		Non-Lake Breeze	
	MAE	MB	MAE	MB
Temp2m	1.09	-0.35	1.28	-0.55
MixingRatio2m	1.19	-0.50	1.24	-0.28
Wind speed10m	1.09	-0.55	1.14	-0.48
Wind direction10m	28.98	-4.27	26.65	0.19

Table 16. Model performance summary by model grid resolution for the lake breeze events in the south shoreline of Lake Erie

Variable	12x12 km		4x4 km		1.3x1.3 km	
	MAE	MB	MAE	MB	MAE	MB
Temp2m	1.16	-0.61	1.02	-0.16	1.07	-0.28
MixingRatio2m	1.45	-1.02	1.15	-0.59	0.95	0.10
Wind speed10m	1.21	-0.91	0.99	-0.48	1.06	-0.27
Wind direction10m	30.73	-5.20	27.55	-4.69	28.66	-2.93

Station specific model performance statistics for sites along the south shore of Lake Erie are shown in Figure 27. The WRF model errors and biases for the lake breeze and non-lake breeze events at each station are summarized by the red and blue boxplots, respectively. The jitter dots show the performance statistics for 12-16 local standard time for the different grid resolutions. Light gray lines in each panel represents the WRF performance benchmark values for errors and biases for each variable.

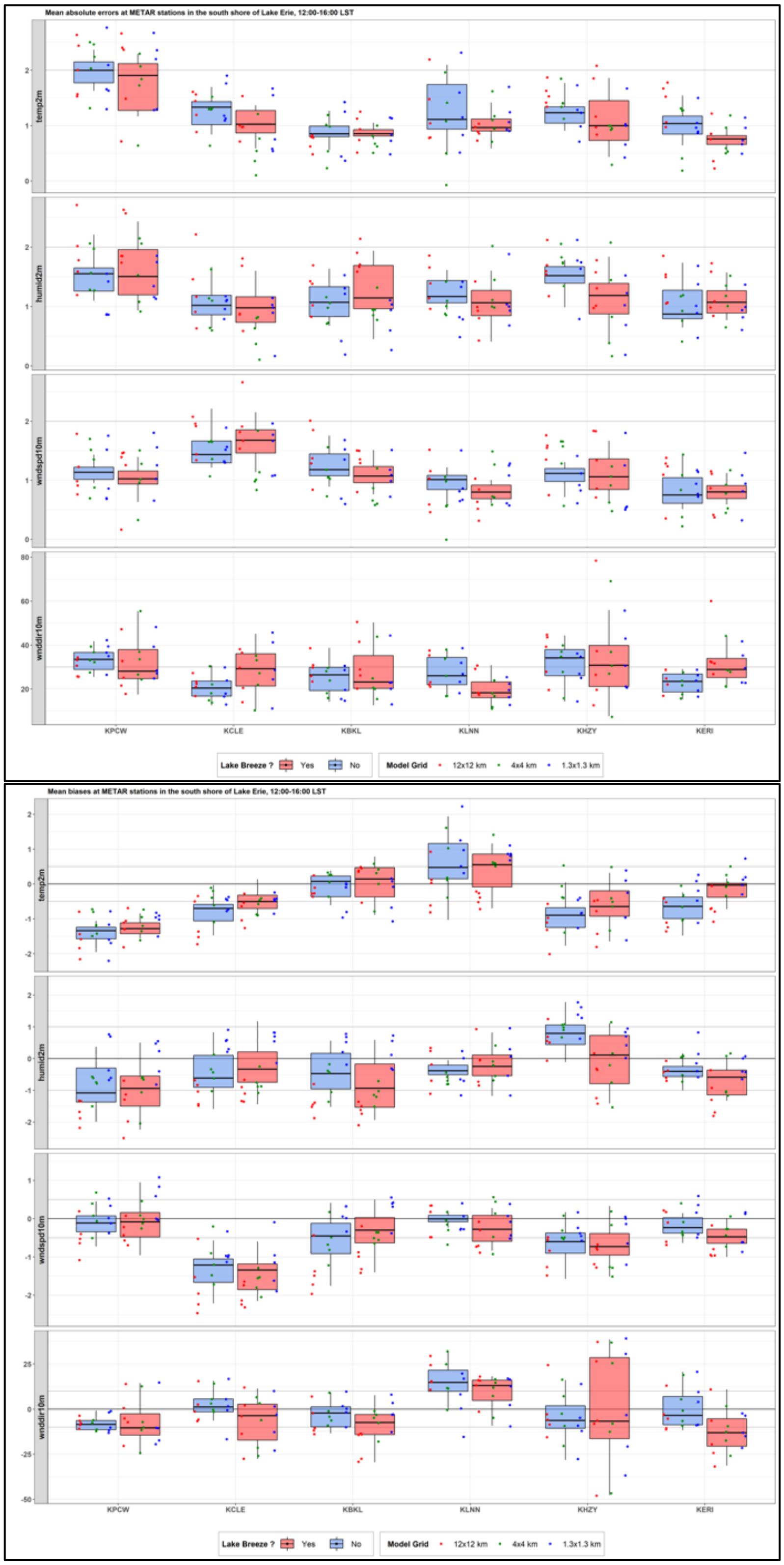

Figure 27. Mean absolute errors (top) and mean biases (bottom) for temperature, specific humidity, wind speed and direction at METAR stations in the south shore of Lake Erie

The CART model for predicting lake breeze periods along the south shore of Lake Erie has a lower accuracy (82% on average) than for the Lake Michigan shoreline (92% accuracy on average). Despite the lower accuracy for predicting Lake Erie lake breeze events with CART, our analysis indicates that WRF performances during lake breeze periods along the south shore of Lake Erie are within the model performance benchmarks. At all of the analyzed Lake Erie stations, except for KPCW, the model performances for lake breeze events are slight better than those for the non-lake breeze conditions, yet the performance statistics vary by hour (not shown).

Specific humidify is the only WRF variable where we see model performance improving from the 12km to 1.33km resolution at all examined stations. We summarized the model performance for meteorological conditions at 1200-1600 LST on CART-identified lake breeze days. In future analyses of the lake breeze, we may consider whether these hours best capture the lake breeze periods in the south shore of the Lake Erie. Sills et al. (2007) indicated that lake breezes occur between 1000 - 20:00pm LST in Lake Erie with durations ranging from 2-13 hours depending on the weather conditions. During the identification process of lake breeze days in Lake Erie, we noted that GFS modeled wind divergence formed over the Lake Erie were relatively weaker than that formed over the Lake Michigan, which could indicate that moderate strength lake breeze forms and lasts for longer hours along the Lake Erie shoreline.

4.5 Lake Breeze Performance Summary

Accurate knowledge of WRF model performance during the lake-breeze events is needed in order to understand and anticipate its impact on simulating surface ozone concentrations in the Great Lakes Basin, especially near the shorelines of the lakes. Qualitative comparison of WRF modeled PBL height and wind fields with the lake-breeze front identified by satellite imagery and observed wind field revealed that WRF successfully reproduced lake-breeze conditions and the associated surface convergence zones formed off of the Lake Michigan and Lake Erie shorelines during selected high ozone days in 2016. Local scale convective processes were better resolved by the 4km and 1.33 km grid resolutions, which likely lead to better simulations of the land and lake circulation near the lake shores.

LADCO identified lake breeze days during summer 2016 by lake-breeze fronts and surface convergence zones as seen in satellite imagery, radar imagery, and NOAA's GFS model wind fields. LADCO developed a CART statistical model using data from selected METAR stations on the shorelines of Lake Michigan and Lake Erie for predicting lake-breeze days. The CART lake breeze model prediction accuracies were 92% for Lake Michigan and 82% for Lake Erie, on average. LADCO used the CART model to determine the typical meteorological conditions and indicators for lake-breeze days along the shores of Lake Michigan and Lake Erie. The model identified wind direction and 2-m temperature as the top two variables for explaining lake breeze vs. non-lake breeze events in the Lake Michigan shore, while 2-m temperature, wind speed, and specific humidity were the variables most associated with the lake breeze along the south shore of Lake Erie.

LADCO calculated WRF model performance for lake-breeze and non-lake breeze days. WRF performed well predicting temperature, moisture, and winds at the shoreline monitors of both lakes. The WRF model errors and biases are within the WRF performance benchmarks for temperature, specific humidity and wind speed, and less than 30 degree errors for wind direction. The model performance is slightly degraded on the lake-breeze days compared to the non-lake breeze days on shoreline of Lake Michigan, while opposite is true on the south shore of Lake Erie. The errors and biases for lake breeze days were slightly improved at finer grids in Lake Michigan and Lake Erie shore.

5 Conclusions and Future Wok

5.1 Cumulative assessment for the 2016 WRF Model Estimates

LADCO simulated meteorology with the WRFv3.9.1.1 model with four nested domains that focus on the Great Lakes Basin. LADCO simulated annual 2016 meteorology for an outer continental U.S. 12-km domain, and the ozone season (April – October) for the inner 4-km and 1.33-km nested domains. LADCO used physics and initialization options identified as the best performing WRF configuration in the LADCO region through a collaboration with the University of Wisconsin through a NASA Health and Air Quality (HAQ) grant-funded project.

The LADCO 2016 WRF simulation is in good agreement with observations of key surface meteorological variables. The WRF performance statistics for all grid resolutions simulated by LADCO are within the acceptable meteorology model performance benchmarks proposed by Emery et al. (2001) and Kemball-Cook et al. (2005) for air quality model applications. It is worth noting that the LADCO 2016 WRF simulation has a cold and dry bias in the summer months across much of the Eastern U.S. The model has a dry bias and underestimates wind direction in the South Central and Southeast in fall and winter seasons.

LADCO compared summer season performance across the different grids that we simulated to evaluate how the model error and bias varies by grid resolution. The errors and biases in temperature and specific humidity predictions are reduced by about 20% in the 4-km resolution simulation compared to the 12-km simulation. There was not an appreciative improvement in model performance for temperature, humidity or winds at 1.33 km resolution. The 1.33 km grid domains did resolve well local scale convective processes and had better performance (specifically, lower errors in wind direction) during the afternoon hours on days when lake breeze conditions were observed.

LADCO applied a novel approach for assessing model performance during lake breeze events. We identified lake breeze days during summer 2016 using satellite and radar imagery of lake-breeze fronts, and with NOAA GFS model wind fields for surface convergence zones. We developed a CART statistical model of lake breeze events using surface observations at stations along the shorelines of Lake Michigan and Lake Erie for predicting lake-breeze and non-lake breeze days. The CART model accuracies were 92% for Lake Michigan and 82% for Lake Erie, on average.

We used the CART results to identify typical meteorological conditions and hourly indicators for lake-breeze days, and then evaluated the model performance during lake breeze conditions. CART identified wind direction and temperature as the top two predictors of lake breeze vs. non-lake breeze days along the Lake Michigan shore, while air temperature and wind speed/humidity were the main predictors along the south shore of Lake Erie. We found that WRF performs relatively well in simulating conditions along the shorelines of the both lakes, model errors and biases are within the commonly used benchmark set by Emery et al. (2001). WRF performance is slightly degraded on the lake-breeze days compared to the non-lake breeze days on shoreline of Lake Michigan, while the opposite is true on the south shore of Lake Erie. The model errors and bias for the lake breeze events are improved at finer grid resolutions at the shoreline sites of Lake Michigan and Lake Erie.

5.2 Lesson Learned and Future Work

LADCO developed a Great Lakes-optimized WRF configuration for simulating air quality. The combination of WRF physical parameterization schemes, soil temperature and moisture initialization, and the nudging scheme used in the LADCO 2016 WRF modeling (LADCO_WRFv39_2016_YNT_GFS_LIS) proved to be the best suited configuration for 12/4/1.33 km grid resolution modeling of the ozone season. While this WRF configuration performed well for sites in the Great Lakes Basin during the ozone season, it did not reproduce the observations as well in other seasons and other parts of the country. Future work is need to further improve model performance for all season and other regions. One idea that LADCO is considering for future WRF applications is to use different physics configurations for the different grid resolutions, for example using one set of the physics options for the CONUS 12-km domain and another set of options for the 4-km and 1.33-km domains.

LADCO used the AMET software to calculate WRF model performance statistics. AMET statistics are derived from collated observation and modeled values at the grid cells in which observation stations are located. For consistency with EPA's attainment test methods for air pollution, which considers modeled advection errors, future work at LADCO may modify, test, and operationalize the core codes of AMET to support the calculation of meteorological performance statistics based on a matrix of grid cells surrounding a monitor, e.g., 3x3 cells surrounding the observation station for the 12km grid resolution regional model.

The model performance evaluation for lake breeze events using CART analysis is a new approach. Our methods will be improved in future applications by increasing the number of predictor variables for lake breeze events to better isolate synoptic scale processes that may have similar characteristics with lake breezes (Laird et al. 2001). We will also attempt to consider varying durations of the lake breeze by identifying lake breeze start and end times (Wagner et al. 2022). We summarized WRF performance for the meteorological conditions that CART identified as lake breeze days during 1200-1600 LST with the goal of having a consistent hour range regardless of the station location. Sills et al. (2007) indicated that lake breeze conditions occurred between 1000-2000 LST along the shores of Lake Erie with durations of 2-13 hours depending on the weather condition. In future applications of the CART lake breeze model LADCO will explore alternative periods during the diel for analyzing lake breeze events.

References

Breiman, L., J. Friedman, R. Olshen, and C. Stone, Classification and Regression Trees, Pacific Grove, CA: Wadsworth (1984).

Brook, J. R., Makar, P. A., Sills, D. M. L., Hayden, K. L., and McLaren, R.: Exploring the nature of air quality over southwestern Ontario: main findings from the Border Air Quality and Meteorology Study, Atmos. Chem. Phys., 13, 10461–10482, https://doi.org/10.5194/acp-13-10461-2013, 2013.

Campbell, P. C., Bash, J. O., and Spero, T. L.: Updates to the Noah land surface model in WRF-CMAQ to improve simulated meteorology, air quality, and deposition. Journal of Advances in Modeling Earth Systems, 11, 231– 256. https://doi.org/10.1029/2018MS001422, 2019.

Case, J. L., Crosson, W. L., Kumar, S. V., Lapenta, W. M., & Peters-Lidard, C. D. (2008). Impacts of High-Resolution Land Surface Initialization on Regional Sensible Weather Forecasts from the WRF Model, *Journal of Hydrometeorology*, *9*(6), 1249-1266. Retrieved May 26, 2022, from https://journals.ametsoc.org/view/journals/hydr/9/6/2008jhm990_1.xml

Case, J. L., Kumar, S. V., Srikishen, J., & Jedlovec, G. J. (2011). Improving Numerical Weather Predictions of Summertime Precipitation over the Southeastern United States through a High-Resolution Initialization of the Surface State, Weather and Forecasting, 26(6), 785-807. Retrieved May 26, 2022, from https://journals.ametsoc.org/view/journals/wefo/26/6/2011waf2222455

Cintineo, R., Otkin, J. A., Kong, F., and Xue, M.: Evaluating the accuracy of planetary boundary layer and cloud microphysical parameterization schemes in a convection-permitting ensemble using synthetic GOES-13 satellite observations, Mon. Wea. Rev., 142, 163-182, 2014.

Chen, F., and Dudhia, J.: Coupling an advanced land-surface/hydrology model with the Penn State/NCAR MM5 modeling system. Part I: Model description and implementation, Mon. Wea. Rev., 129, 569-585, 2001.

Emery, C., E. Tai, and G. Yarwood, 2001. “Enhanced Meteorological Modeling and Performance Evaluation for Two Texas Ozone Episodes.” Prepared for the Texas Natural Resource Conservation Commission, prepared by ENVIRON International Corporation, Novato, CA. 31-August. http://www.tceq.texas.gov/assets/public/implementation/air/am/contracts/reports/mm/EnhancedMetModelingAndPerformanceEvaluati on.pdf

Ek, M. B., and Coauthors: Implementation of Noah land surface model advances in the National Centers for Environmental Prediction operational mesoscale Eta model, J. Geophys. Res., 108, 8851, doi:10.1029/2002JD003296, 2003.

Harkey, M., and Holloway, T.: Constrained dynamical downscaling for assessment of climate impacts, J. Geophys. Res. Atmos., 118, 2316-2148, doi: 10.1002/jgrd.50223, 2013.

Hong, S-Y., Y. Noh, Y., and J. Dudhia, J.: A new vertical diffusion package with explicit treatment of entrainment processes. Mon. Wea. Rev., 134, 2318–2341, doi: 10.1175/MWR3199.1, 2006.

Hong, S.-Y.: A new stable boundary-layer mixing scheme and its impact on the simulated East Asian summer monsoon, Quart. J. Roy. Meteor. Soc., 136, 1481–1496, 2010.

Griffin, S. M., and Coauthors: Evaluating the impact of planetary boundary layer, land surface model, and microphysics parameterization schemes on upper-level cloud objects in simulated GOES-16 brightness temperatures. J. Geophys. Res. - Atmos, 126, e2021JD034709. https://doi.org/10.1029/2021JD034709, 2021.

Kain, J.S.: The Kain-Fritsch convective parameterization: An update, J. Appl. Meteorol. Climatol., 43(1), 170-181, doi: 10.1175/1520-0450(2004)043<0170:TKCPAU>2.0.CO;2, 2004.

Kemball-Cook, S., Y. Jia, C. Emery, and R. Morris, 2005. Alaska MM5 Modeling for the 2002 Annual Period to Support Visibility Modeling. Prepared for the Western Regional Air Partnership, by ENVIRON International Corp., Nov

Morrison, H., Curry, J. A., and Khvorostyanov, V. I.: A new double-moment microphysics parameterization for application in cloud and climate models. Part 1: Description, J. Atmos. Sci., 62, 1665-1677, doi: 10.1175/JAS3446.1, 2005.

McNally, D. E., 2009. "12km MM5 Performance Goals." Presentation to the Ad-hoc Meteorology Group. 25-June. http://www.epa.gov/scram001/adhoc/mcnally2009.pdf

Pleim, J. E.: A combined local and nonlocal closure model for the atmospheric boundary layer. Part 1: Model description and testing, J. Appl. Meteorol. Climatol., 46, 1383-1395, doi: 10.1175/JAM2539.1, 2007.

Pleim, J. E. and Gilliam, R.: An indirect data assimilation scheme for deep soil temperature in the Pleim-Xiu land surface model. J. Appl. Meteorol. Climatol., 48, 1362-1376, doi: 10.1175/2009JAMC2053.1, 2009.

Pleim, J. E., and Xiu, A.: Development of a land surface model. Part II: data assimilation, J. Appl. Meteorol. 42, 1811–1822. https://doi.org/10.1175/1520-0450(2003)042<1811:DOALSM>2.0.CO;2, 2003.

Schwab, D. J., Leshkevich, G. A., and Muhr, G. C.: Satellite measurements of surface water temperature in the Great Lakes: Great Lakes Coast Watch, Journal of Great Lakes Research, 18, 247– 258, 1992.

Skamarock, W.C., J.B. Klemp, J. Dudhia, D.O. Gill, M. Barker, M.G. Duda, X.-Y. Huang, W. Wang, and J.G. Powers, 2008: A description of the Advanced Research WRF version 3. NCAR Technical Note NCAR/TN475+STR

Sills, D. M. L., Brook, J. R., Levy, I., Makar, P. A., Zhang, J., and Taylor, P. A.: Lake breezes in the southern Great Lakes region and their influence during BAQS-Met 2007, Atmos. Chem. Phys., 11, 7955–7973, https://doi.org/10.5194/acp-11-7955-2011, 2011.

Sutton, C., Hamill T. M., and Warner T. T.: Will perturbing soil moisture improve warm-season ensemble forecasts? A proof of concept, Mon. Wea. Rev., 134, 3174–3189, 2006.

Thompson, G., Field, P. R., Rasmussen, R. M., and Hall, W. D.: Explicit forecasts of winter precipitation using an improved bulk microphysics scheme. Part II: Implementation of a new snow parameterization, Mon. Wea. Rev., 136, 5095–5115, 2008.

Thompson, G., Tewari, M., Ikeda, K., Tessendorf, S., Weeks, C., Otkin, J., Kong, F.: Explicitly-coupled cloud physics and radiation parameterizations and subsequent evaluation in WRF high-resolution convective forecasts. Atmos. Res., 168, 92-104, doi:10.1016/j.atmosres.2015.09.005, 2016.

US EPA. 2019. Technical Support Document for EPA's Updated Regional Haze Modeling. Research Triangle Park, NC. https://www.epa.gov/sites/production/files/2019-10/documents/updated_2028_regional_haze_modeling-tsd-2019_0.pdf

US EPA, 2019b. Meteorological Model Performance for Annual 2016 Simulation WRF v3.8. (EPA-454/R-19-010) United States Environmental Protection Agency.

U.S. EPA, 2019c. 2016 Hemispheric Modeling Platform Version 1: Implementation, Evaluation, and Attribution. Research Triangle Park, NC. U.S. Environmental Protection Agency. U.S. EPA

Appendix A: Additional Materials

Additional LADCO WRF 2016 simulation MPE plots are available on the LADCO website:

https://www.ladco.org/technical/modeling-results/

A.1 CONUS 12 WRF MPE Plots

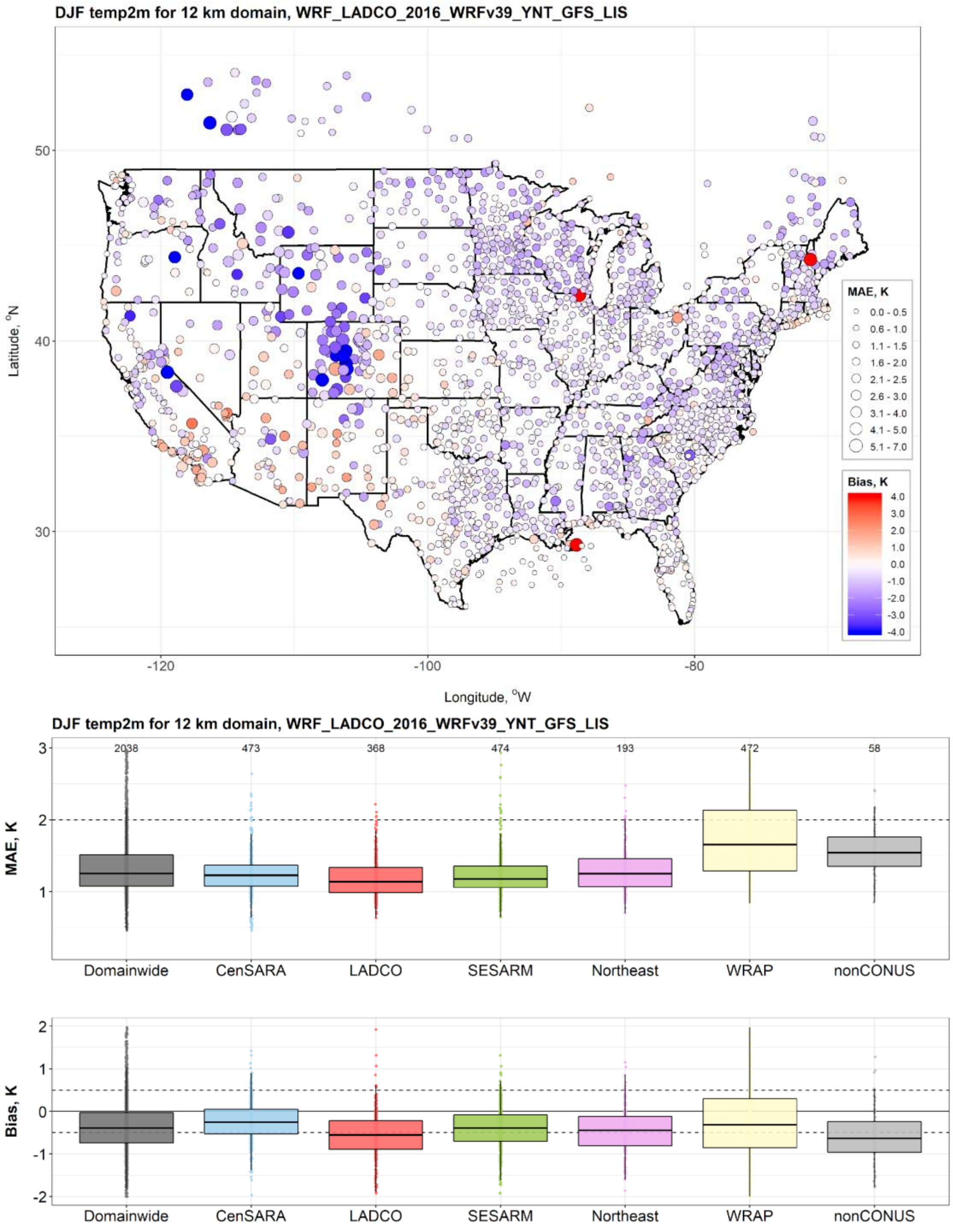

Figure 28. Mean Absolute Errors and Biases for Temperature, the 12 km Domain, Winter 2016

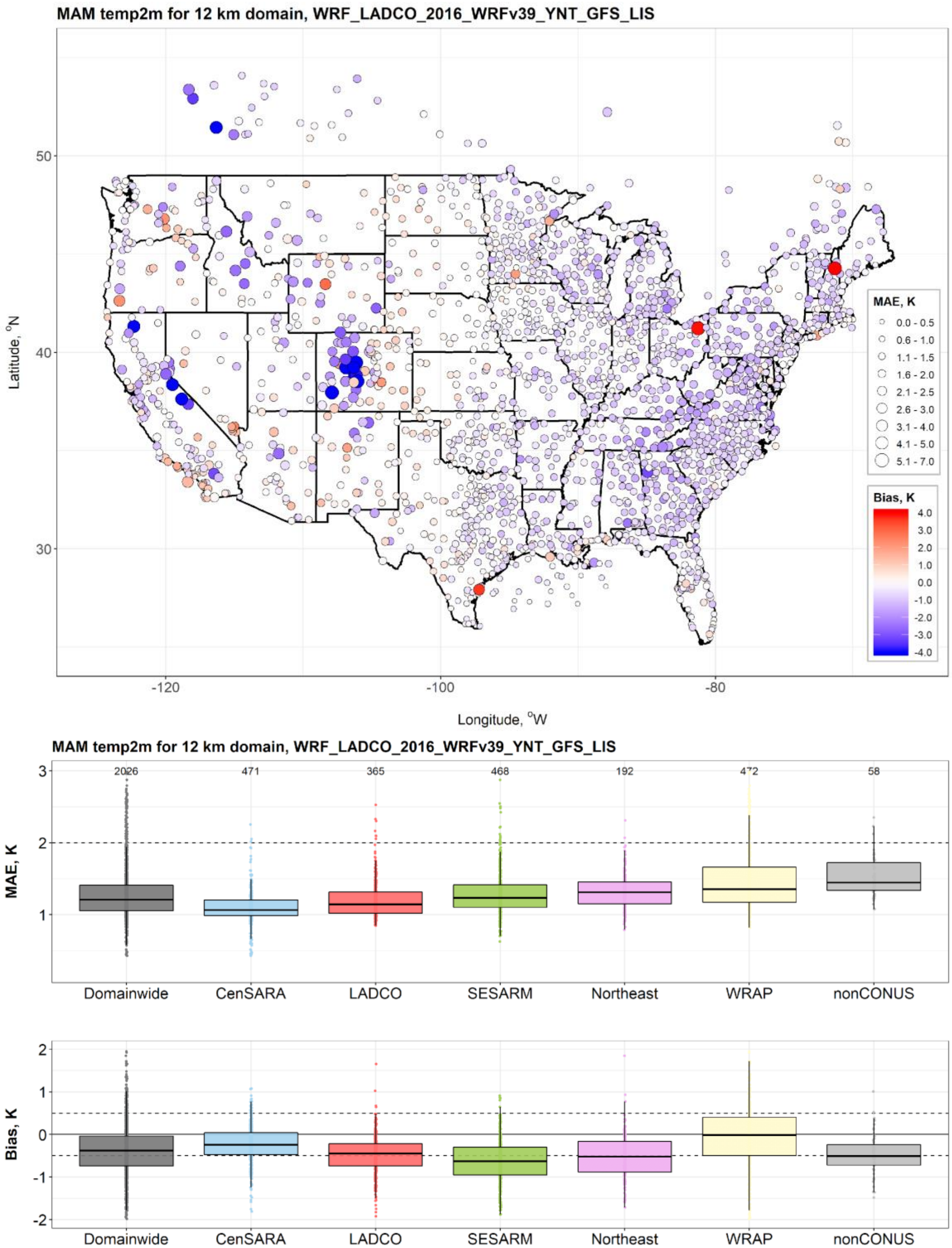

Figure 29. Mean Absolute Errors and Biases for Temperature, the 12 km Domain, Spring 2016

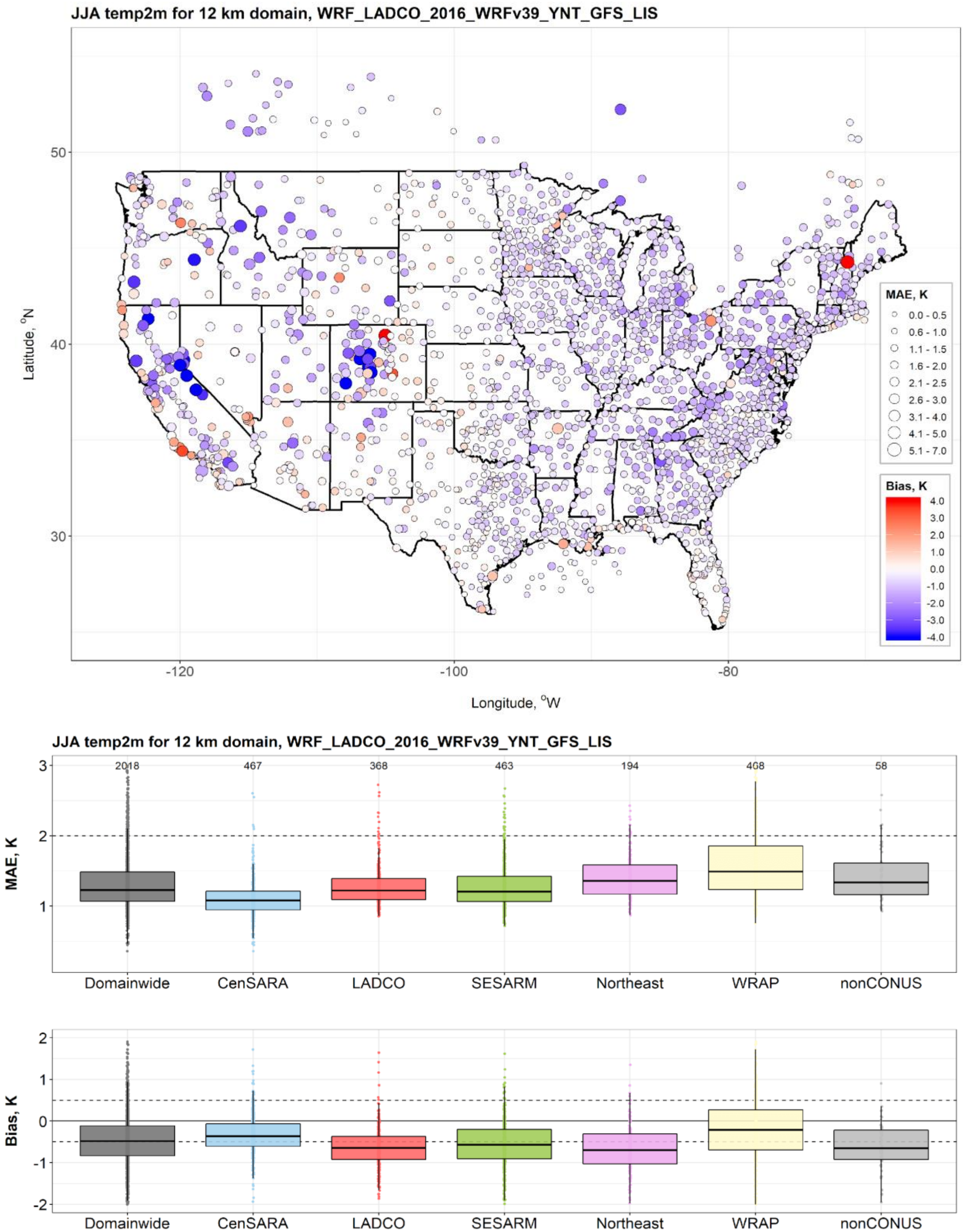

Figure 30. Mean Absolute Errors and Biases for Temperature, the 12 km Domain, Summer 2016

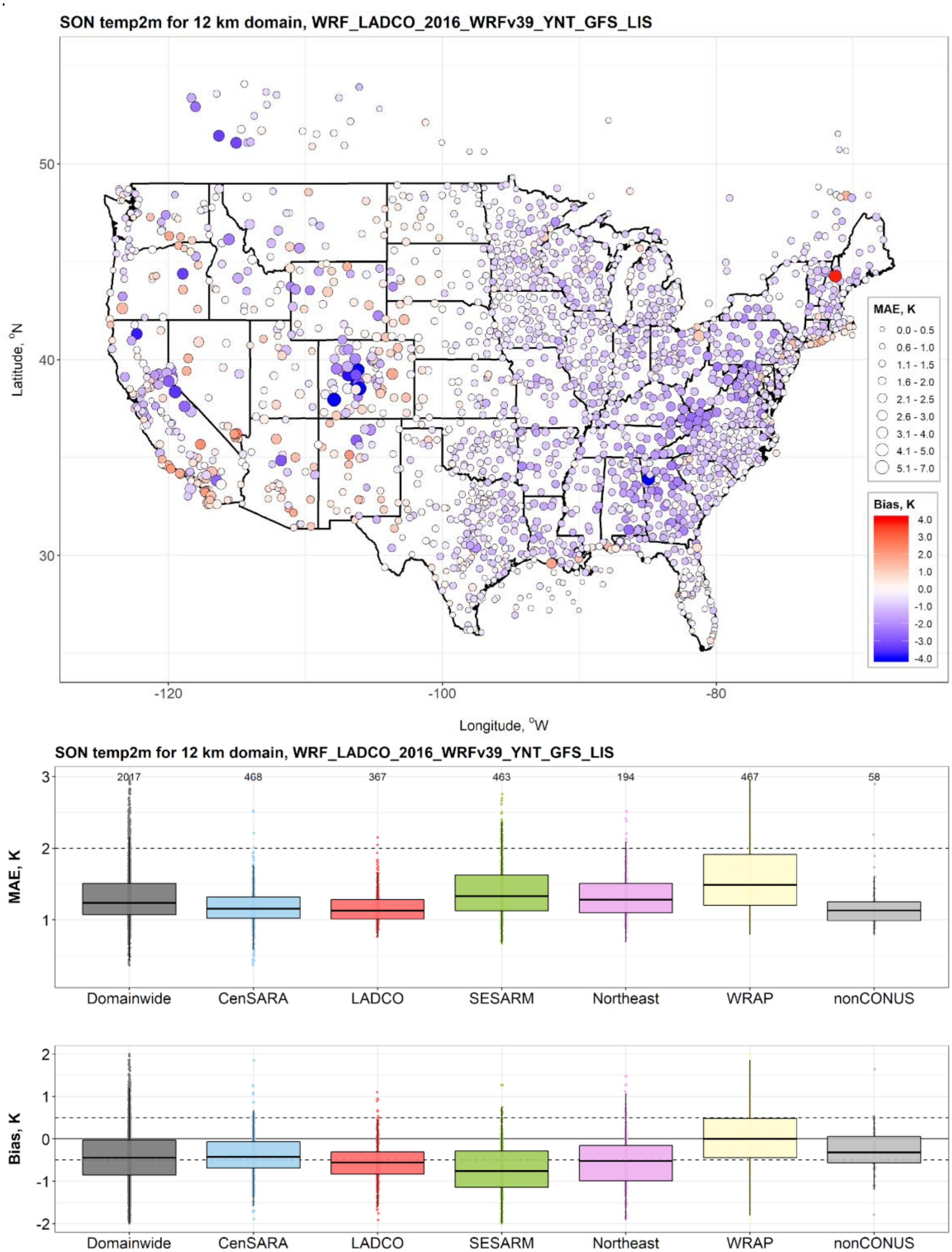

Figure 31. Mean Absolute Errors and Biases for Temperature, the 12 km Domain, Fall 2016

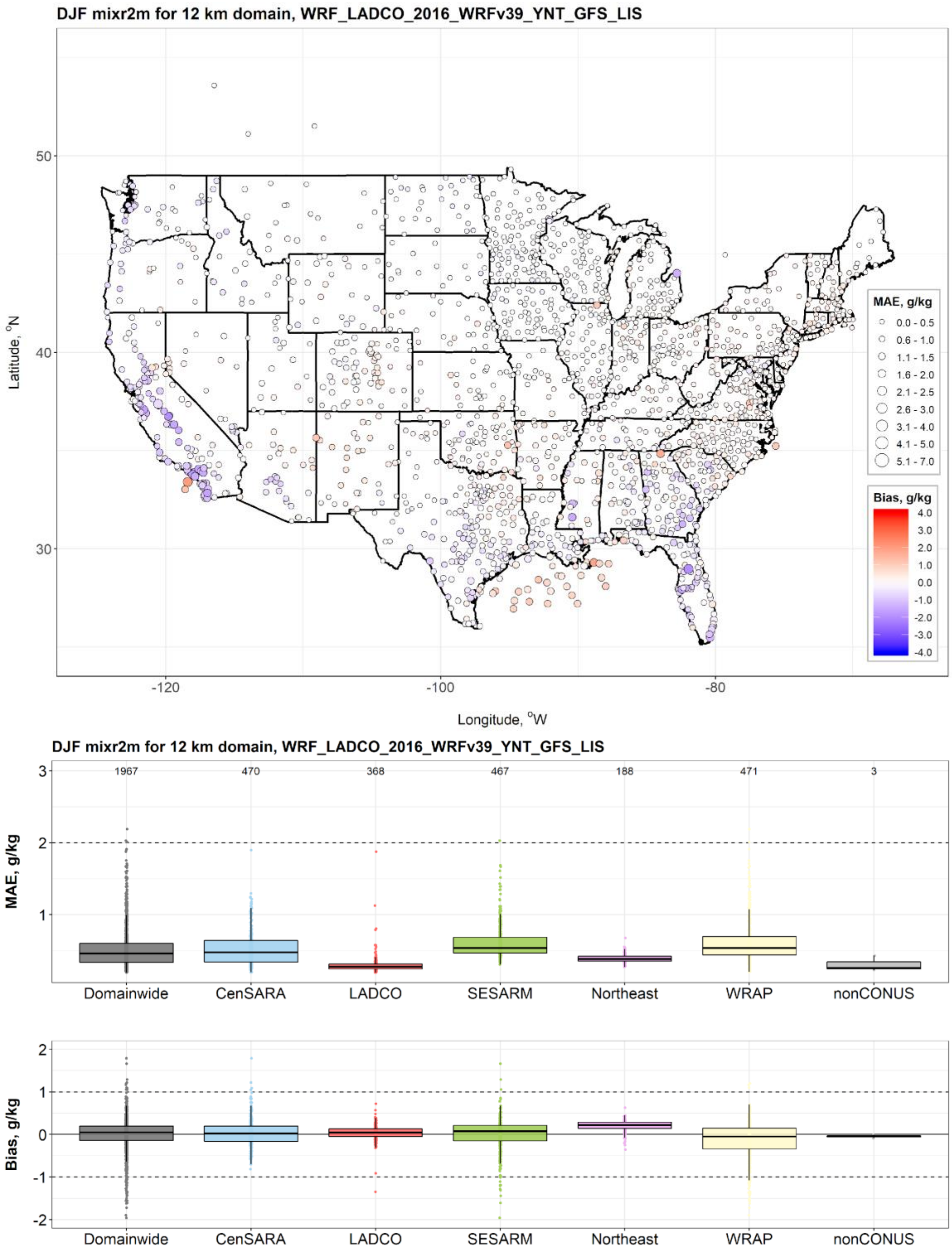

Figure 32. Mean Absolute Errors and Biases for Specific Humidity, the 12 km Domain, Winter 2016

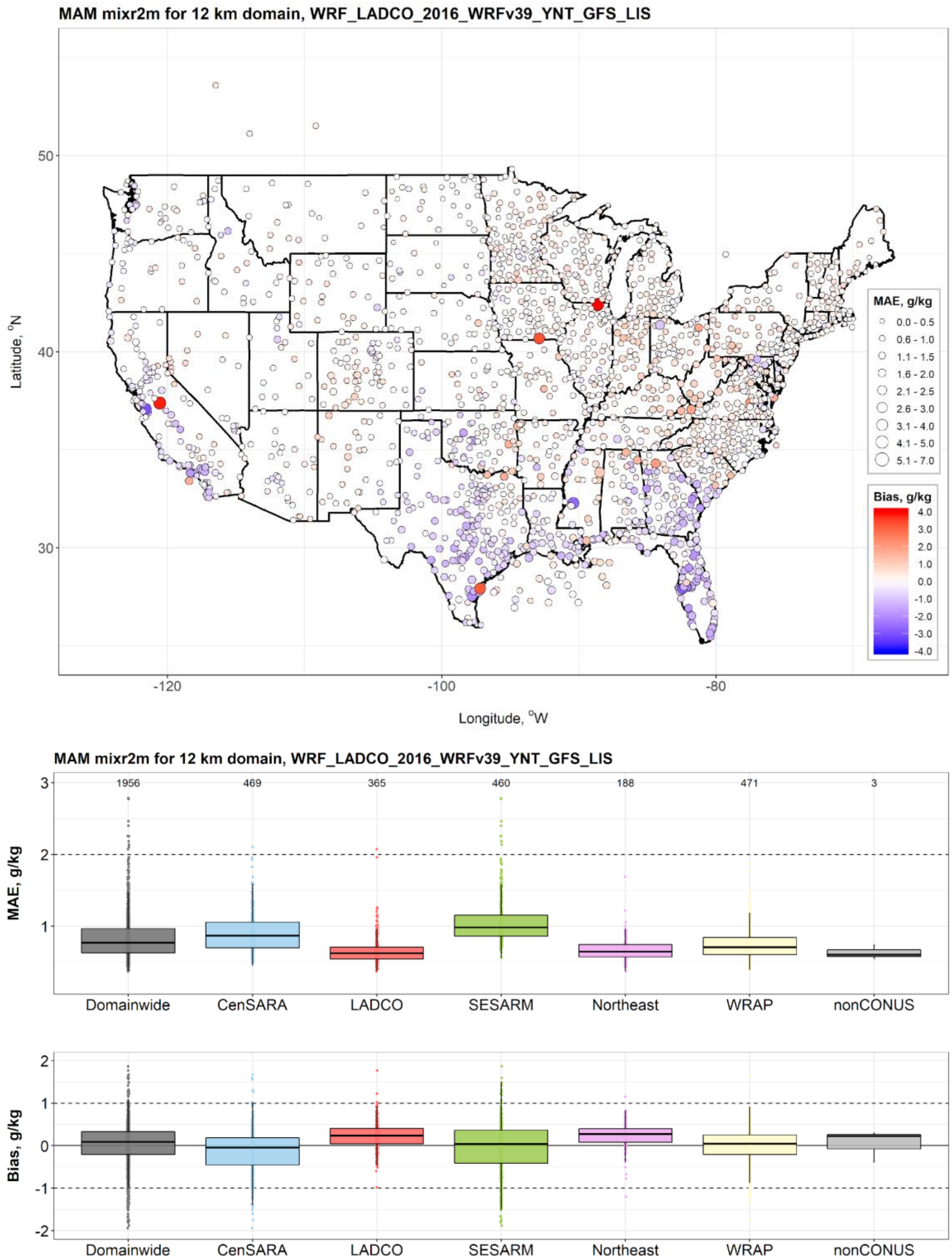

Figure 33. Mean Absolute Errors and Biases for Specific Humidity, the 12 km Domain, Spring 2016

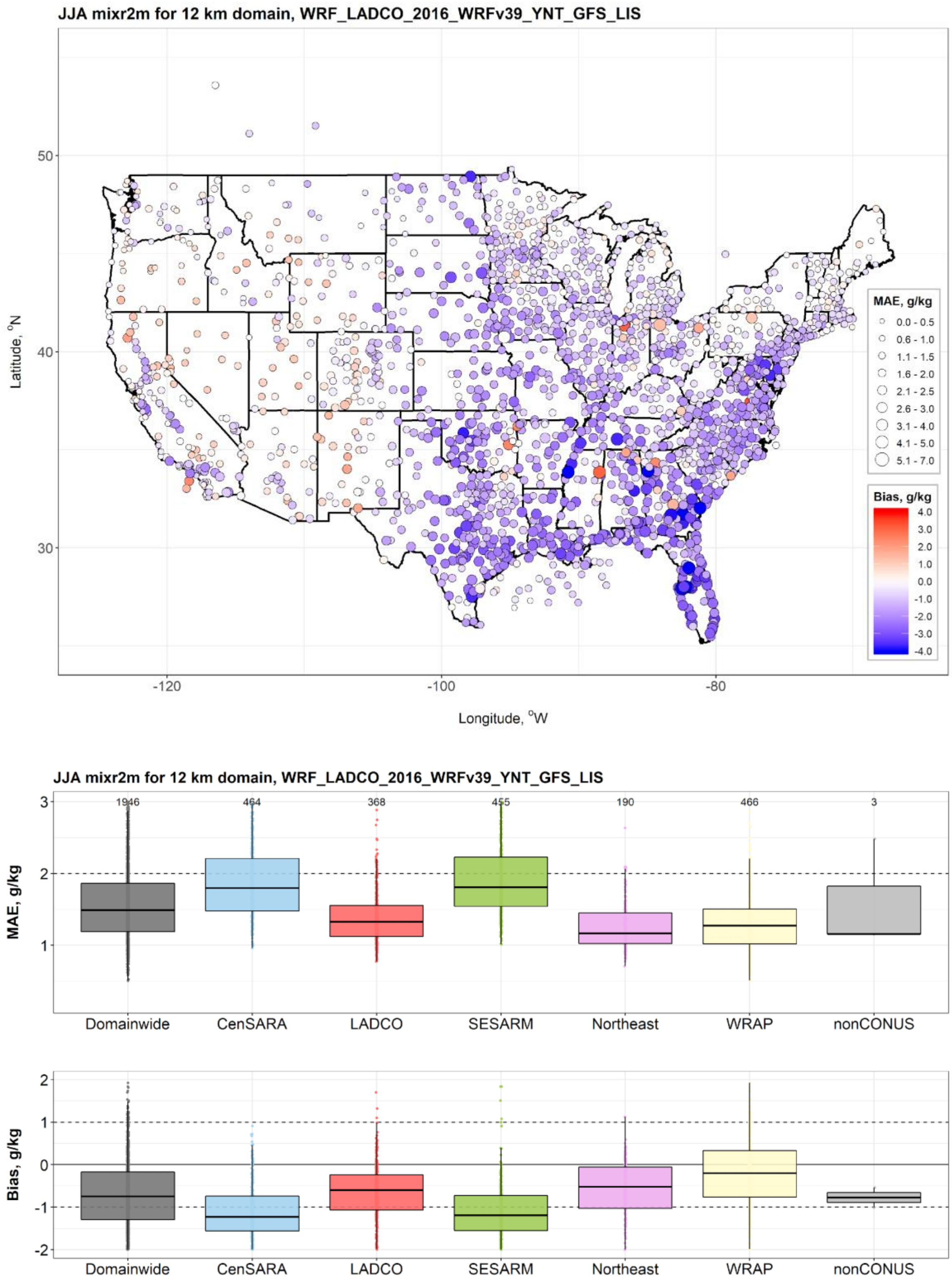

Figure 34. Mean absolute errors and biases for Specific Humidity, the 12 km Domain, Summer 2016

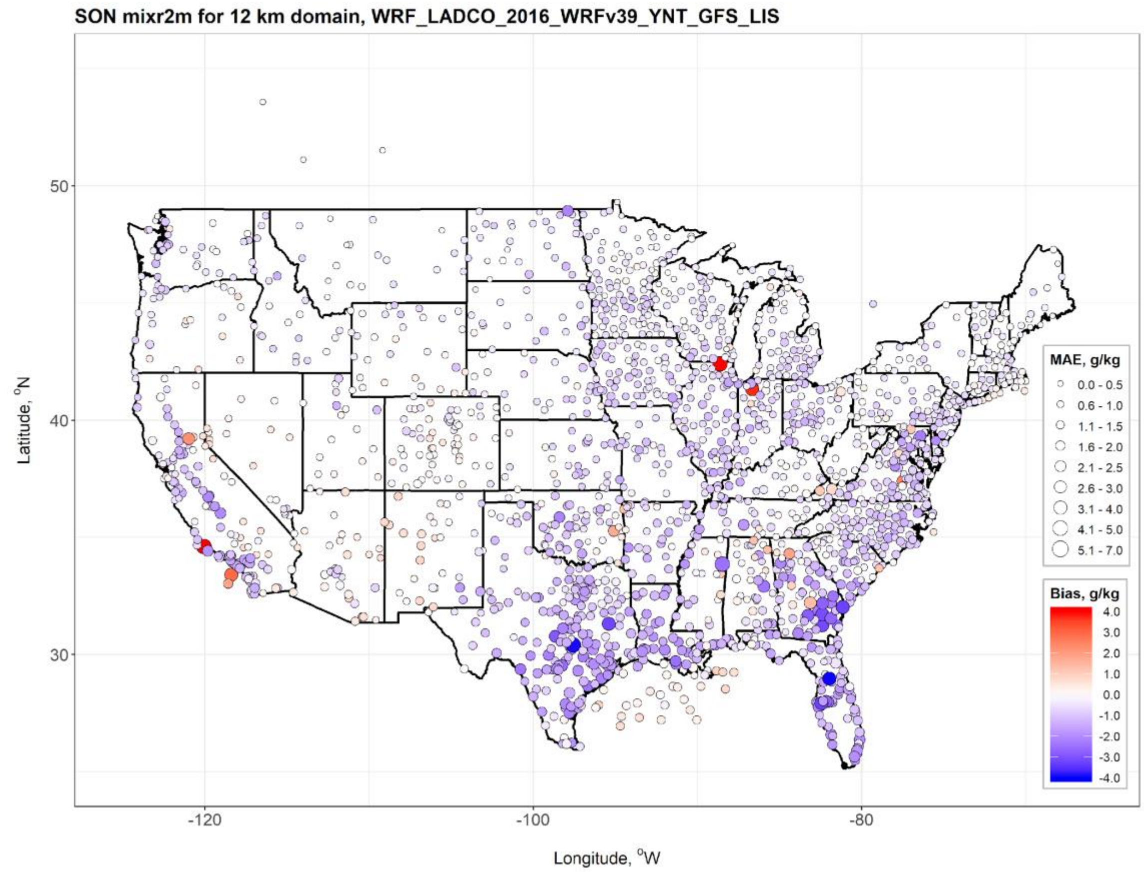

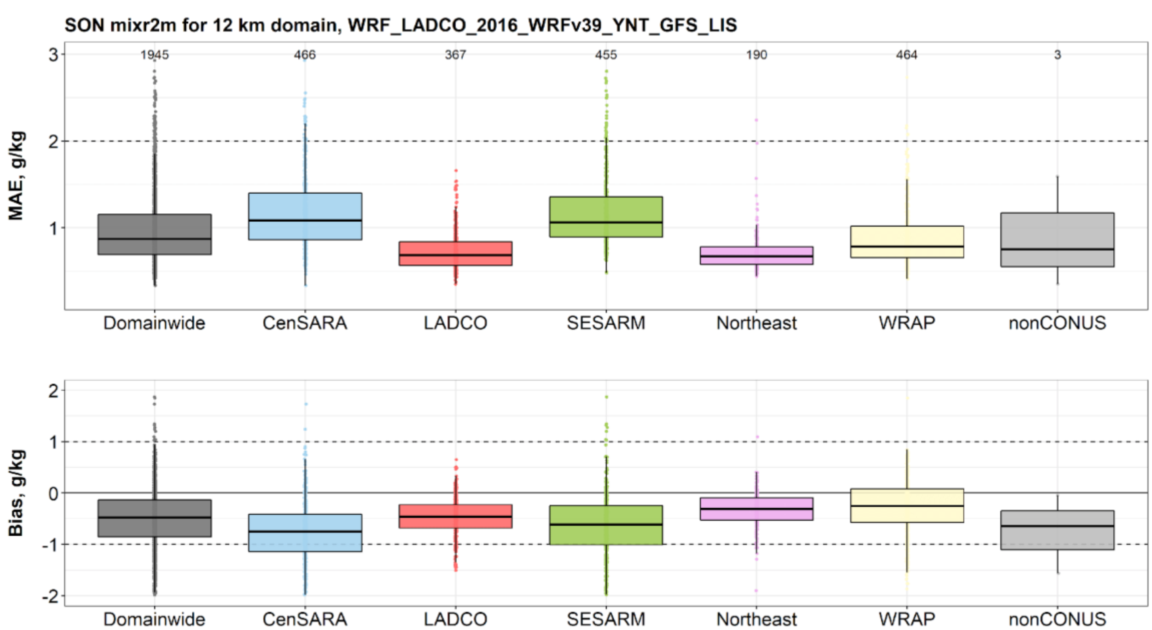

Figure 35. Mean Absolute Errors and Biases for Specific Humidity, the 12 km Domain, Fall 2016

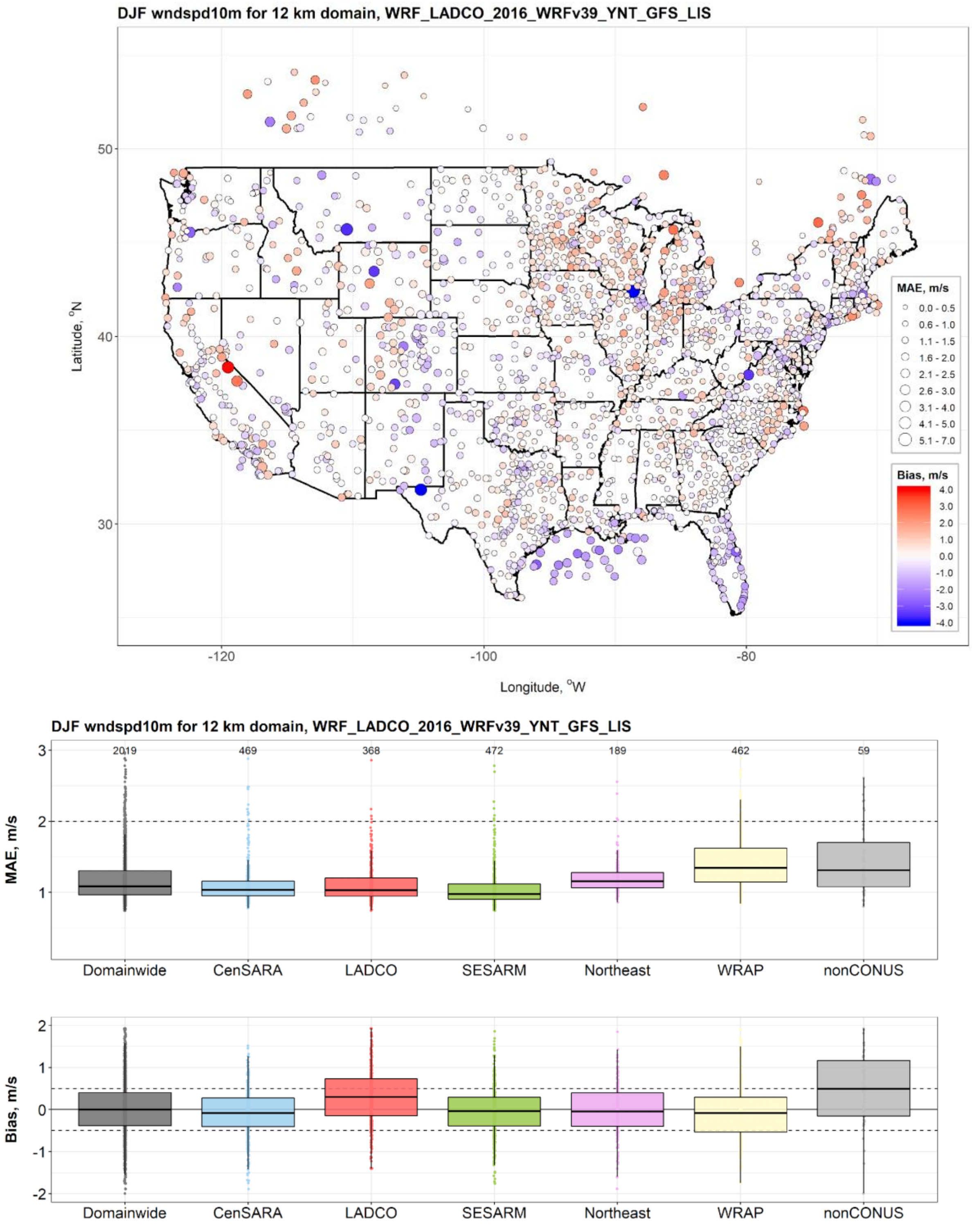

Figure 36. Mean Absolute Errors and Biases for Wind Speed, the 12 km Domain, Winter 2016

.

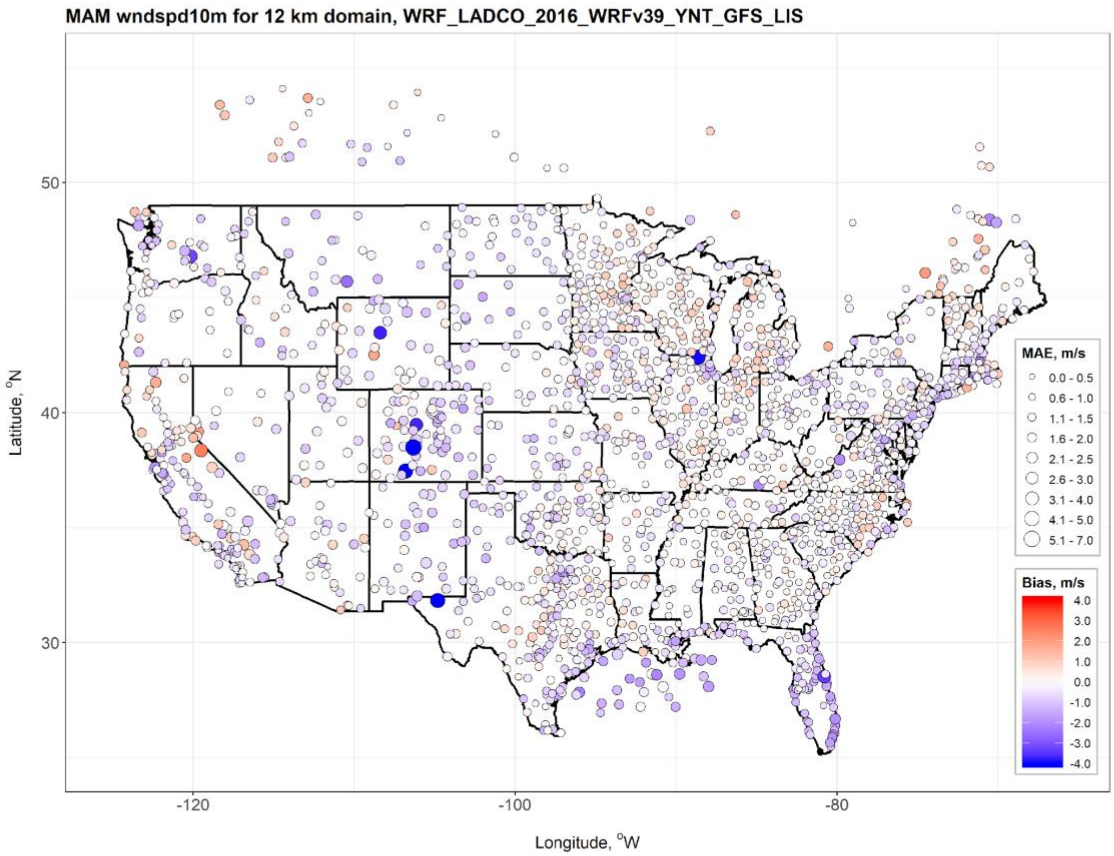

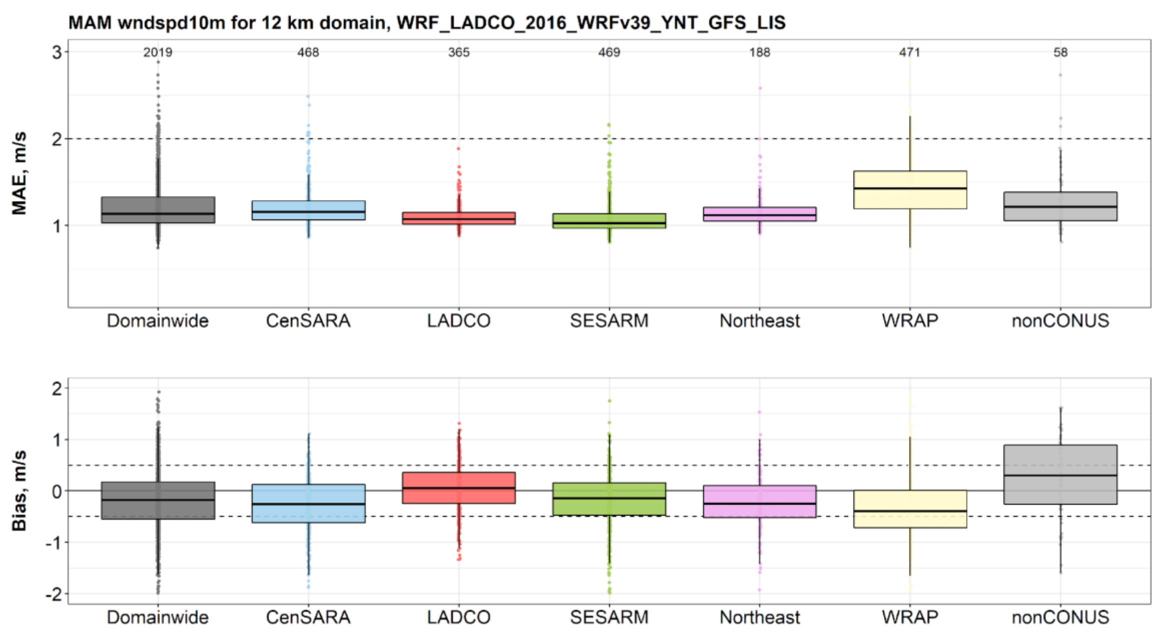

Figure 37. Mean Absolute Errors and Biases for Wind Speed, the 12 km Domain, Spring 2016

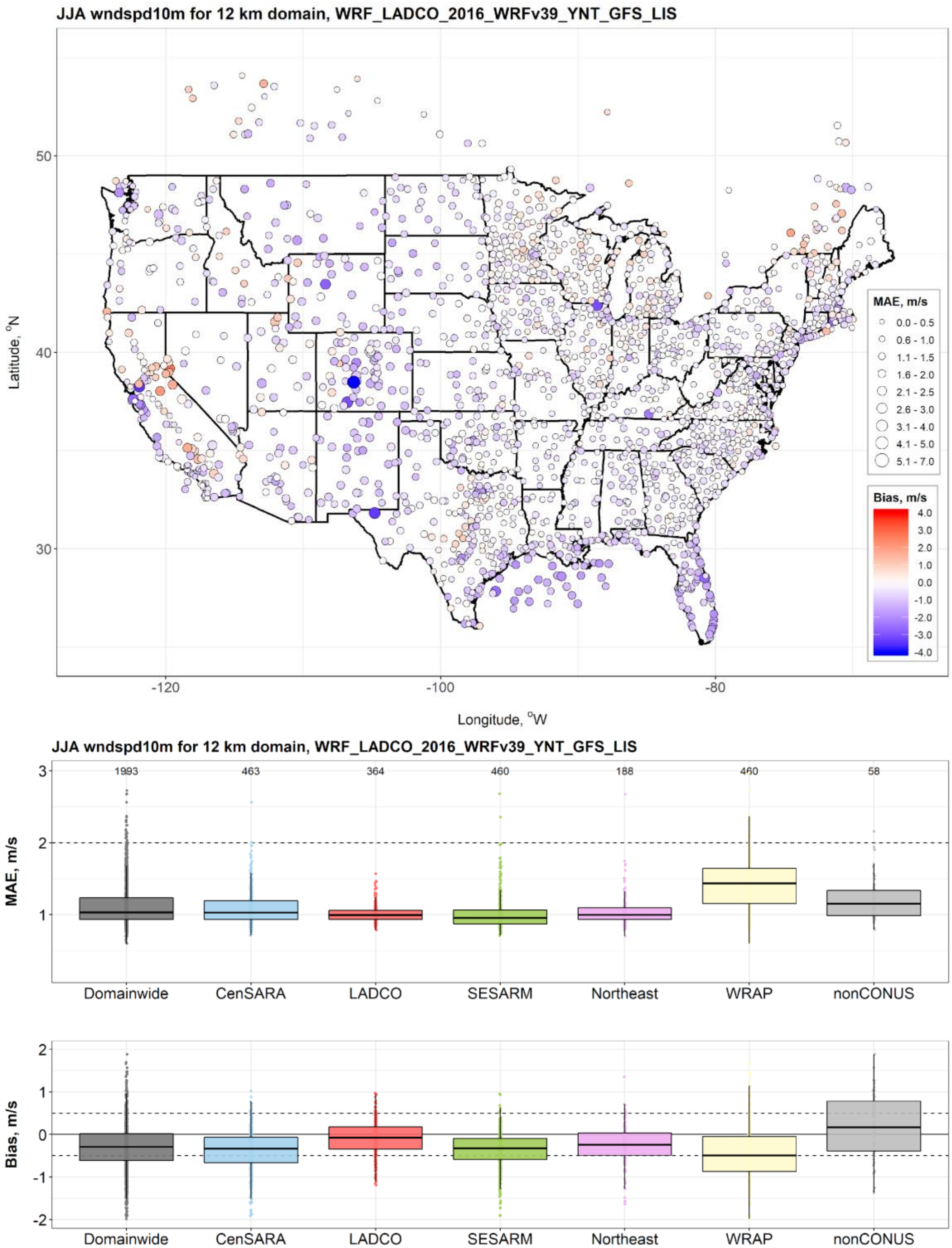

Figure 38. Mean Absolute Errors and Biases for Wind Speed, the 12 km Domain, Summer 2016

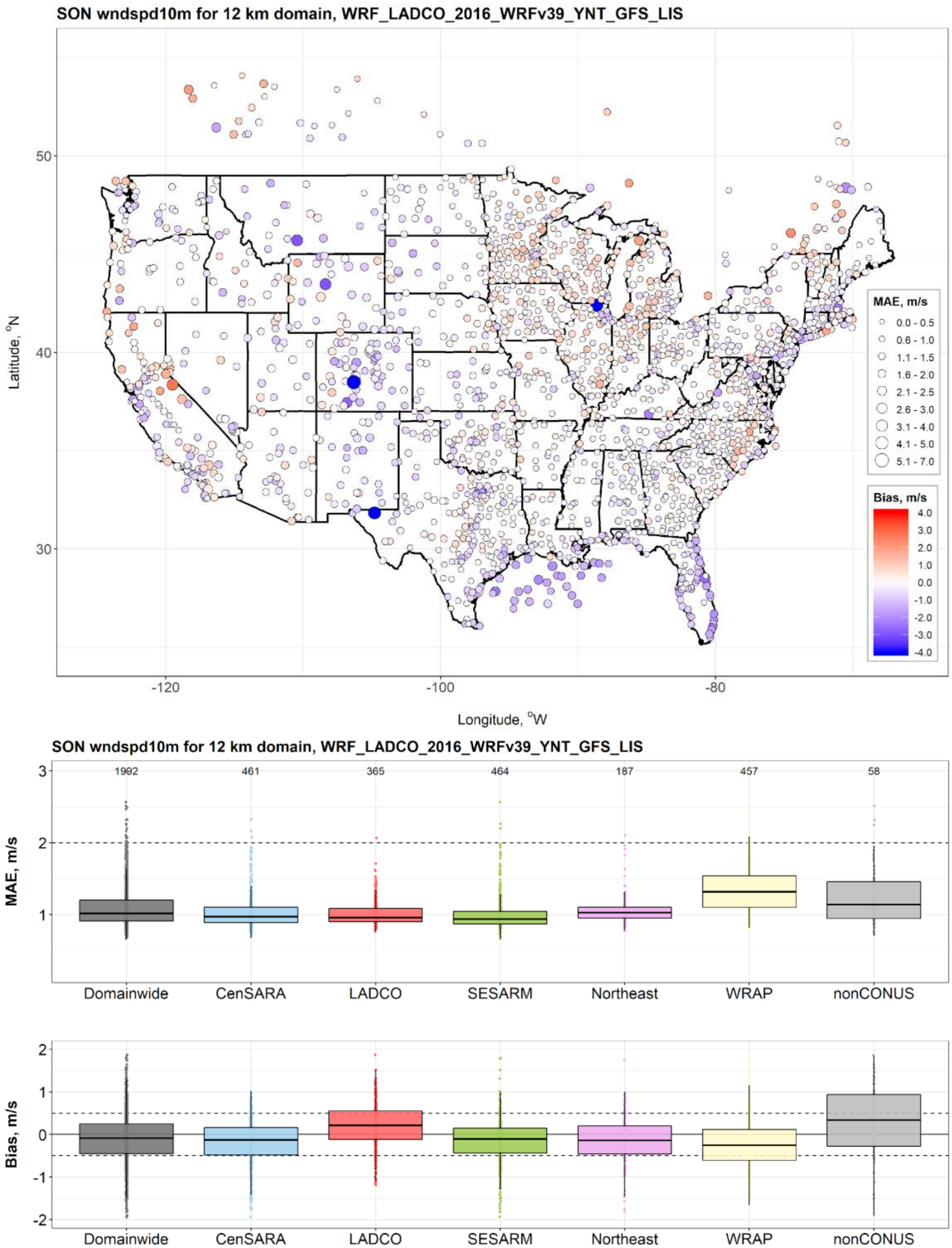

Figure 39. Mean Absolute Errors and Biases for Wind Speed, the 12 km Domain, Fall 2016

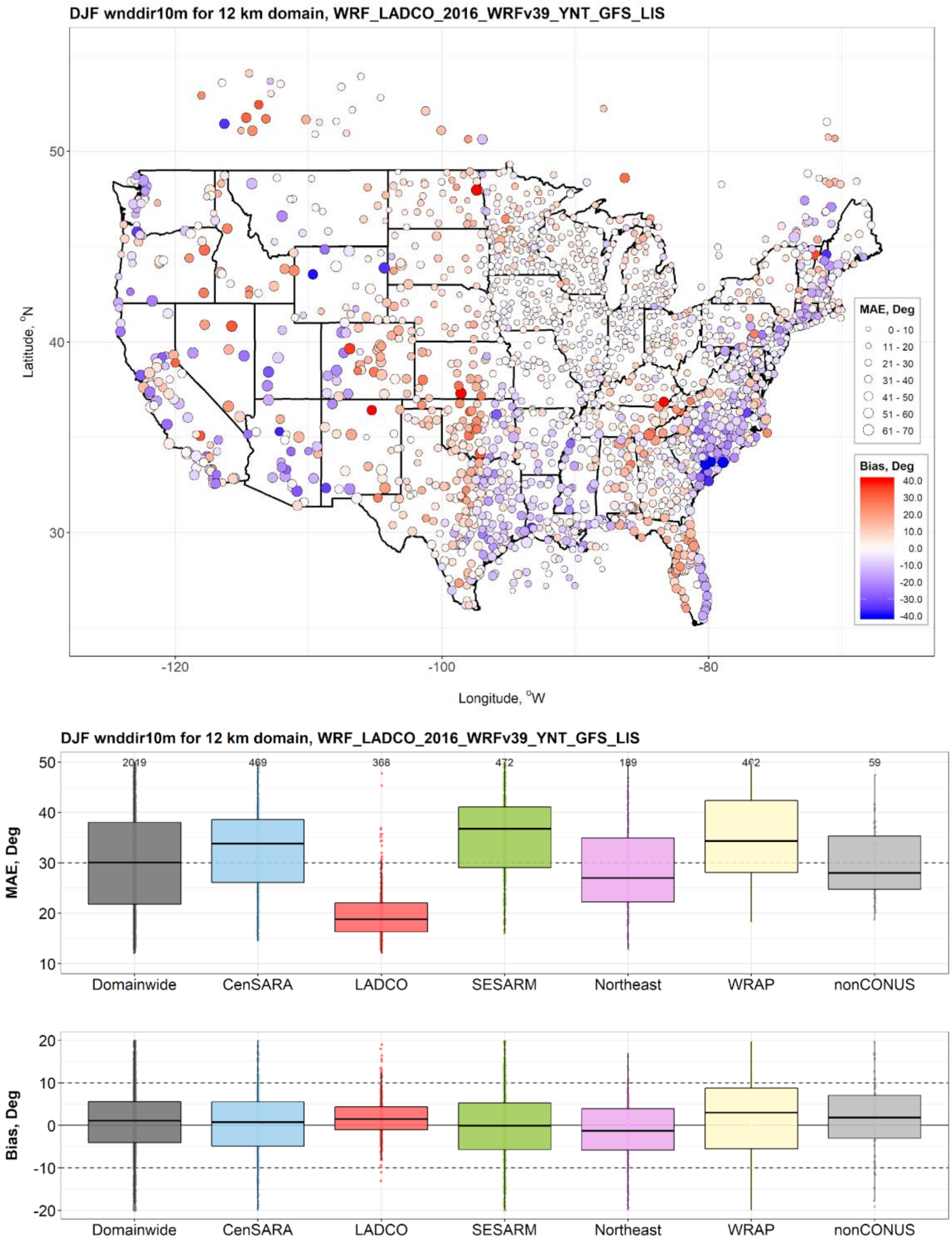

Figure 40. Mean Absolute Errors and Biases for Wind Direction, the 12 km Domain, Winter 2016

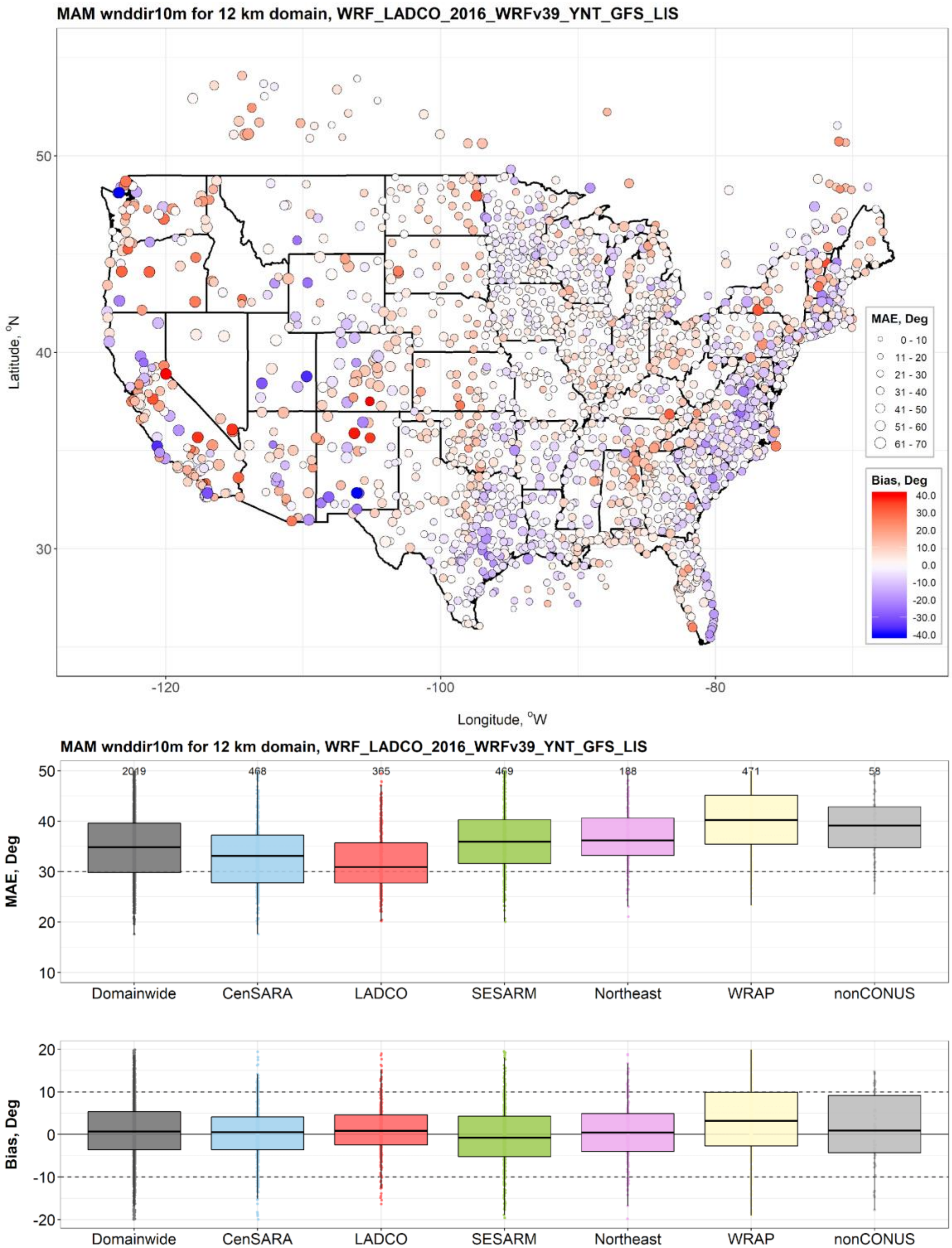

Figure 41. Mean Absolute Errors and Biases for Wind Direction, the 12 km Domain, Spring 2016

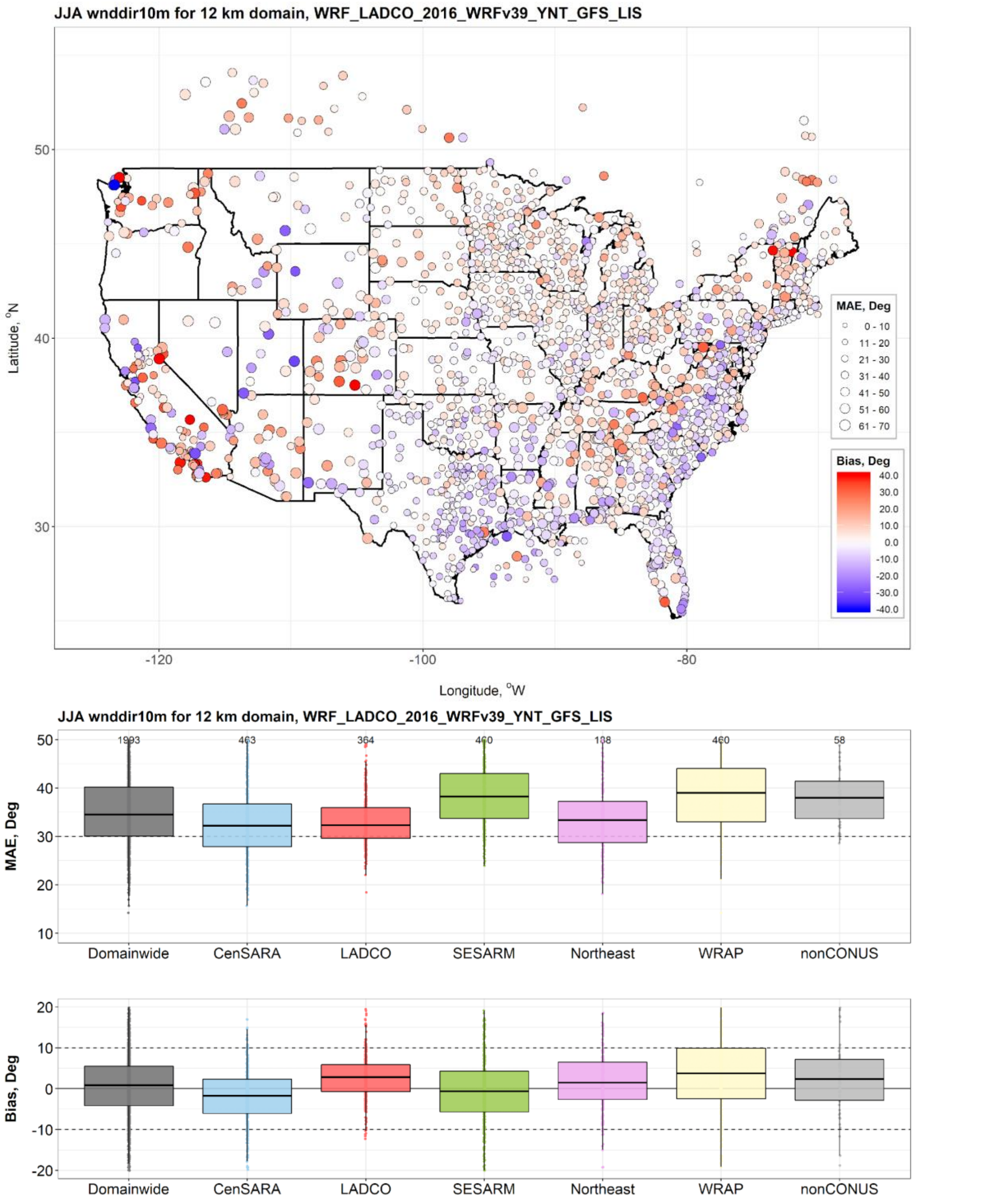

Figure 42. Mean Absolute Errors and Biases for Wind Direction, the 12 km Domain, Summer 2016

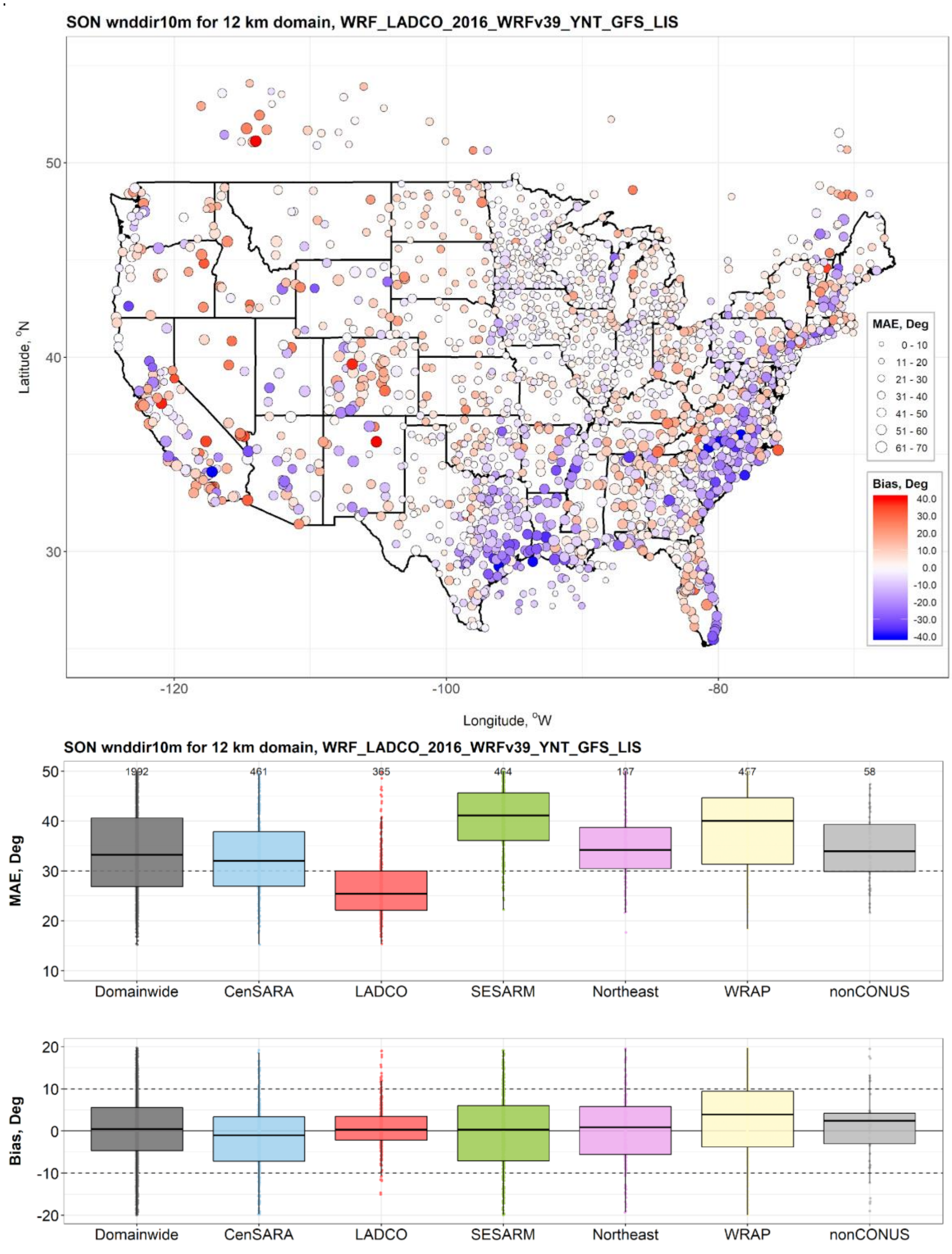

Figure 43. Mean Absolute Errors and Biases for Wind Direction in the 12US2 Domain, Fall 2016

A.2 Lake Breeze Analysis Plots

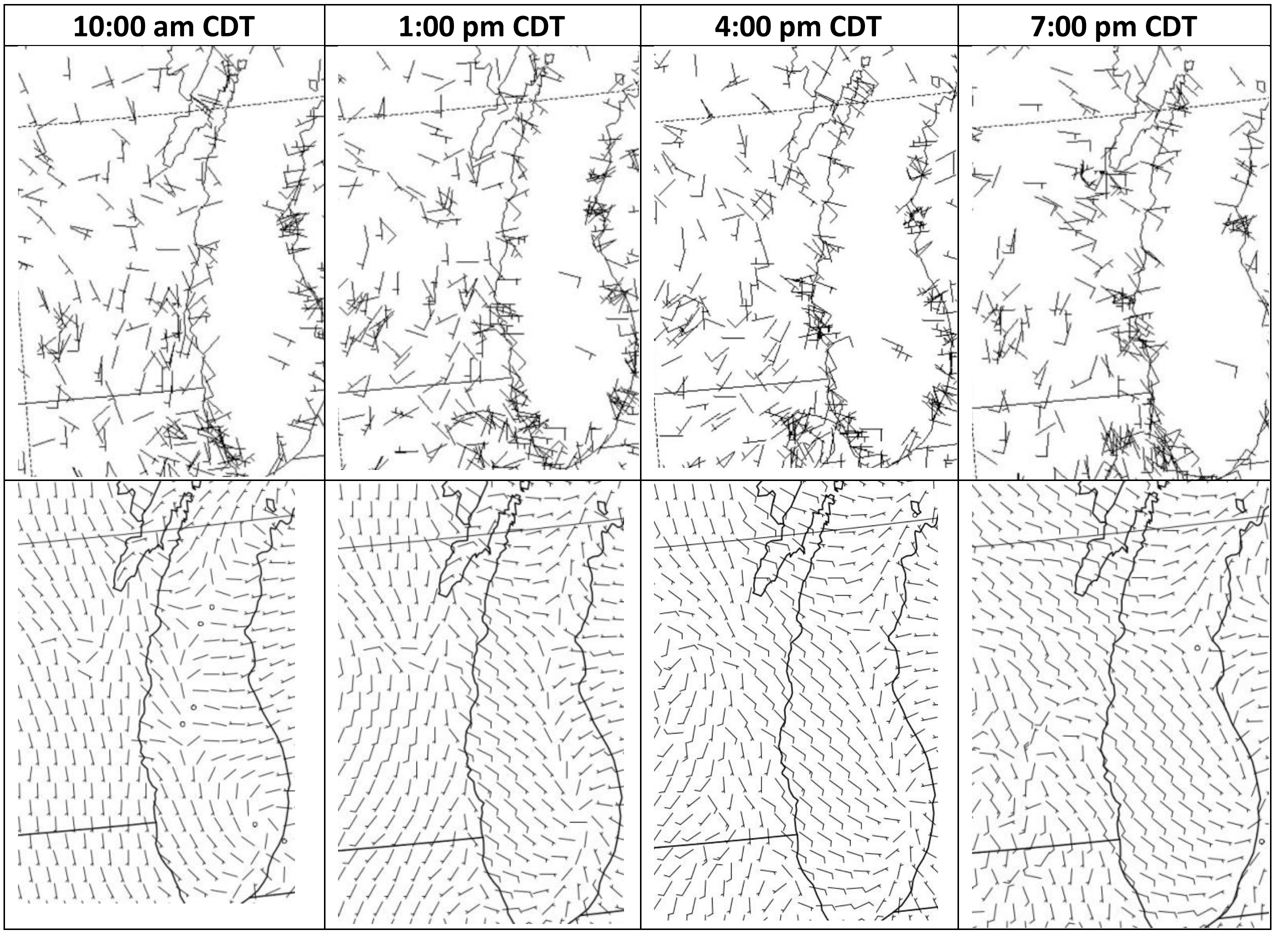

Figure 44. Observed (top) and 1.33 km WRF (bottom) surface wind barbs in the western shore of Lake Michigan, 10:00am - 7:00pm CDT on June 3, 2016

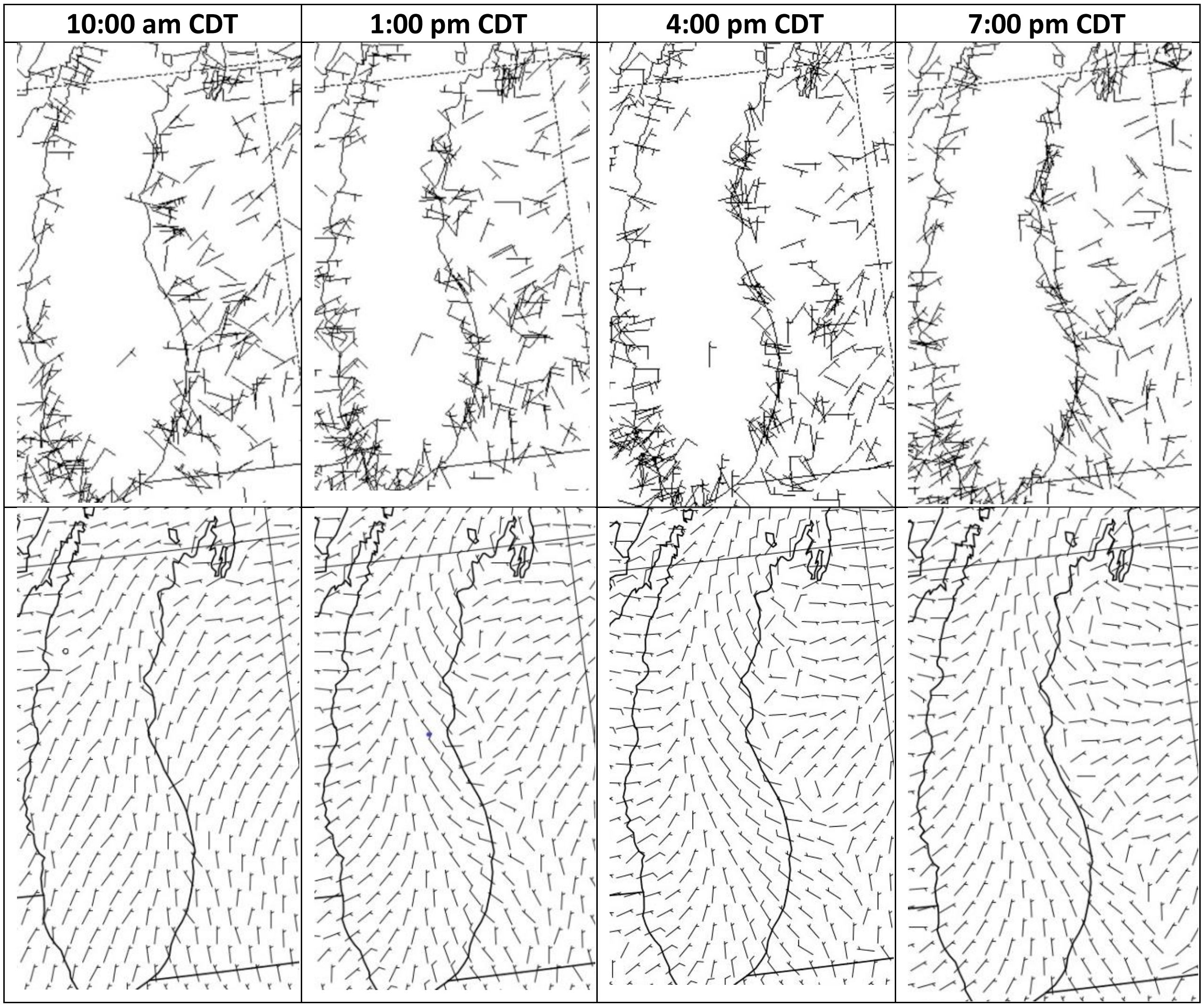

Figure 45. Observed (top) and 1.33 km WRF (bottom) surface winds in the eastern shore of Lake Michigan, 10:00am - 7:00pm CDT on July 31, 2016

10:00am CDT	1:00pm CDT

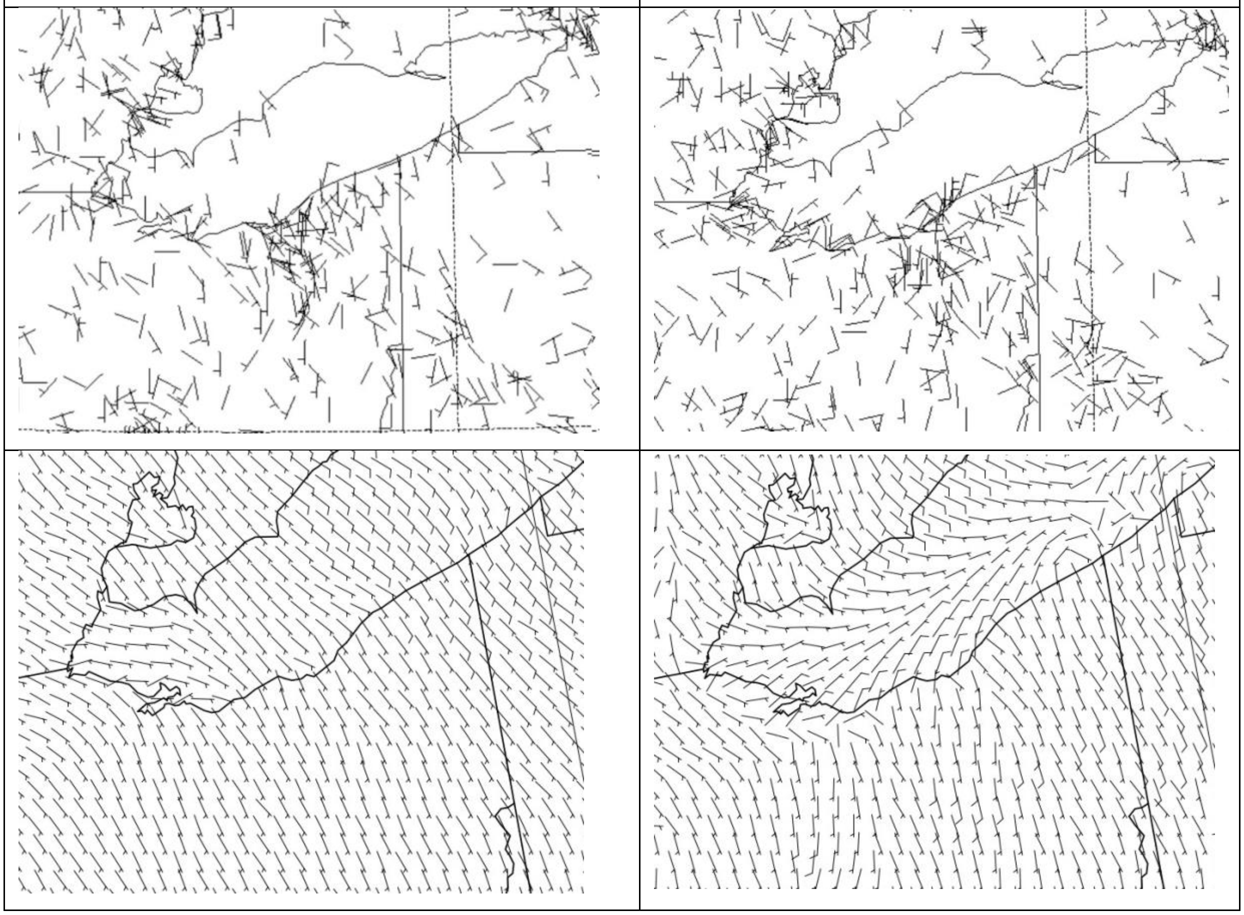

Figure 46. Observed (top) and 1.33 km WRF (bottom) surface winds surface winds in Lake Erie, 10:00am and 1:00pm CDT on August 9, 2016

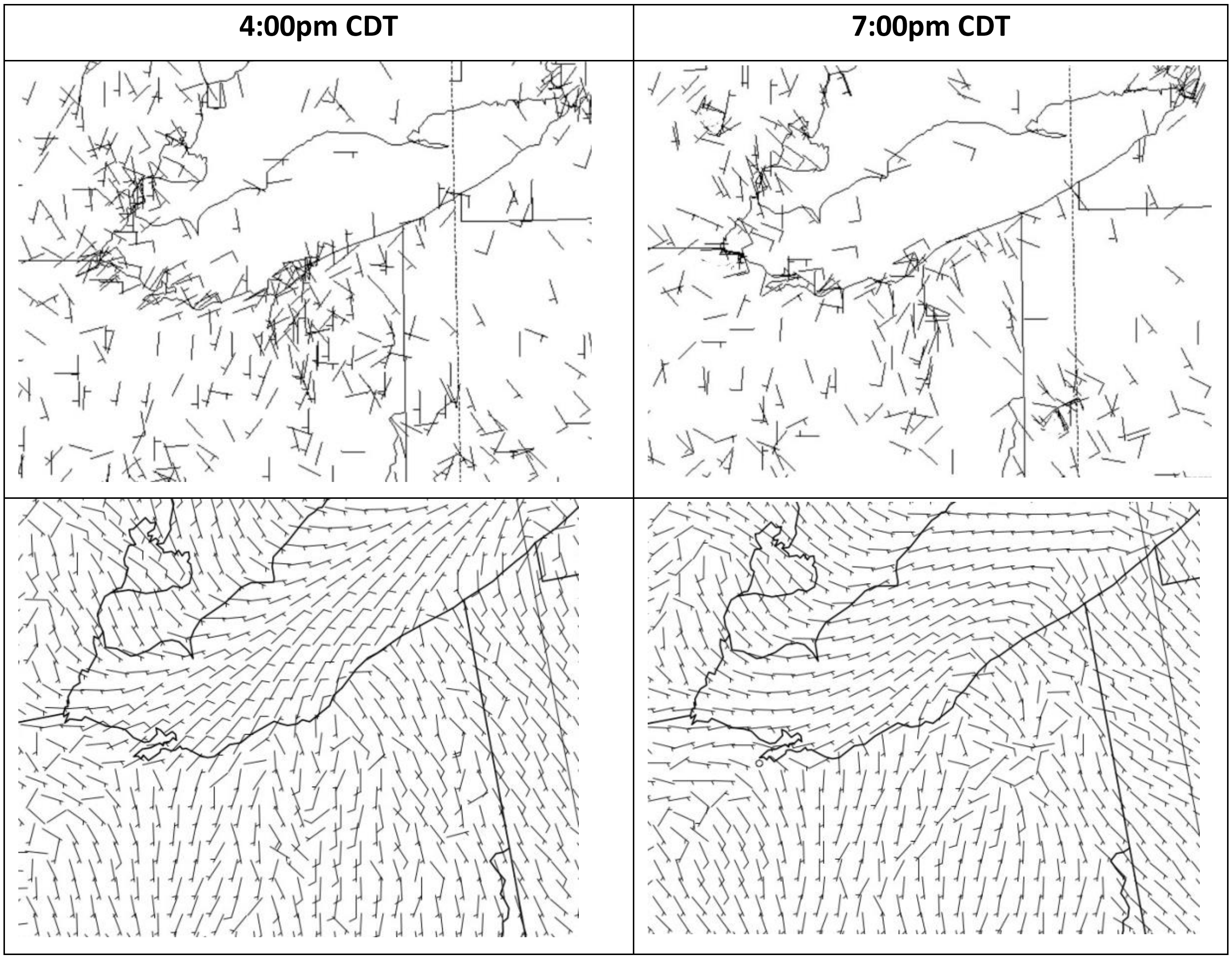

Figure 47. Observed (top) and 1.33 km WRF (bottom) surface winds in Lake Erie, 4:00pm and 7:00pm CDT on August 9, 2016